JOURNAL OF

CHROMATOGRAPHY

INTERNATIONAL JOURNAL ON CHROMATOGRAPHY, ELECTROPHORESIS AND RELATED METHODS

ELSEVIER

JOURNAL OF CHROMATOGRAPHY

CONTENTS

CHROM. 22 656

Renaissance of gas chromatography–time-of-flight mass spectrometry

Meeting the challenge of capillary columns with a beam deflection instrument and time array detection

J. T. WATSON*

Departments of Chemistry and Biochemistry, Michigan State University, East Lansing, MI 48824 (U.S.A.)

G. A. SCHULTZ

Department of Chemistry, Michigan State University, East Lansing, MI 48824 (U.S.A.)

R. E. TECKLENBURG, Jr.

Department of Biochemistry, Michigan State University, East Lansing, MI 48824 (U.S.A.)

and

J. ALLISON

Department of Chemistry, Michigan State University, East Lansing, MI 48824 (U.S.A.)

(First received November 5th, 1989; revised manuscript received June 26th, 1990)

ABSTRACT

This report describes the use of a unique beam deflection time-of-flight mass spectrometer to address some of the demands made on mass spectrometry by new developments in high-resolution capillary column gas chromatography. An integrating transient recorder is used in combination with this beam deflection time-of-flight instrument to apply the concept of time array detection in capturing all of the mass spectral information available from the ion source, thereby greatly enhancing the signal-to-noise ratio quality of the mass spectral data. The applicability of the time array detection approach to gas chromatography–mass spectrometry is demonstrated in the context of an analysis of the standard Grob mixture for assessing performance of capillary column chromatography. During analysis of the Grob mixture by gas chromatography–mass spectrometry, mass spectra were recorded at a rate of 20 scan files per second. The data indicate that this rate of mass spectral scan file generation is adequate to provide a suitable data base for reconstruction of the chromatographic profile. In addition, the effective scan rate is high enough that there is no distortion in the relative peak intensities throughout the individual mass spectra of components regardless of the relatively high dynamic changes in partial pressure of the analyte as reflected by the sharp peaks in the chromatographic profile. The experimental results indicate that the beam deflection time-of-flight mass spectrometer can provide mass spectra at a scan file generation rate much higher than that possible with the conventional quadrupole or magnetic sector mass spectrometer, but at comparable detection limits.

INTRODUCTION

Gas chromatography (GC)–mass spectrometry (MS) is a powerful technique because it combines a separation technique with an identification technique. The separation power of modern high-performance gas–liquid chromatography helps

CASE A

Sample introduced from reservoir

partial
pressure
of
analyte
in
ion source

constant

time →

m/z →   m/z →   m/z →
scan file 1   scan file 2   scan file 3

CASE B

Sample introduction by gas chromatograph

partial
pressure
of
analyte
in
ion source

time →

m/z→   m/z→   m/z→
scan file 1   scan file 2   scan file 3
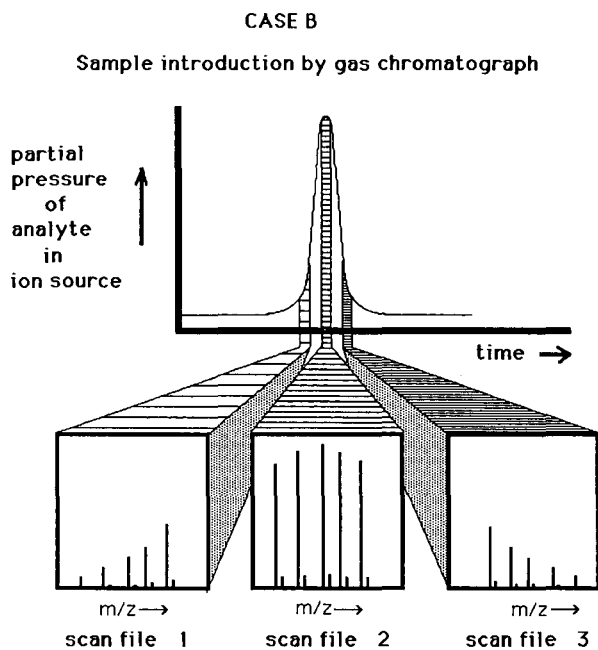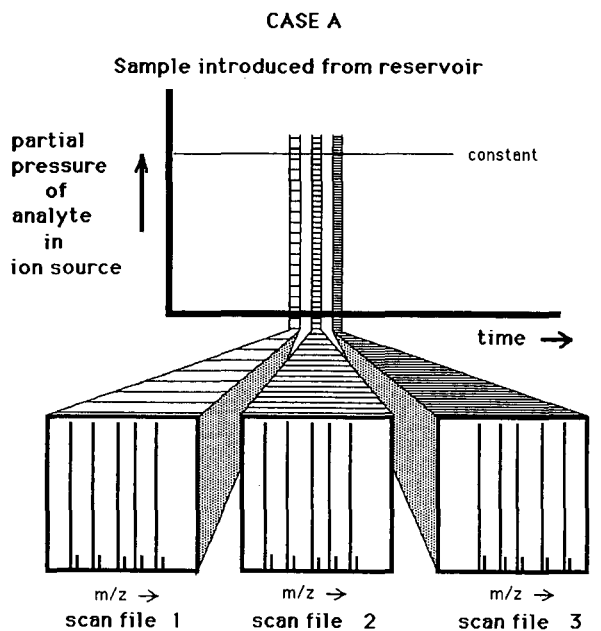
Fig. 1. Graphical illustration of the influence of analyte partial pressure in the ion source of a mass spectrometer on the resulting bar graph mass spectra. Case A: When analyte partial pressure is constant, spectra in scans 1, 2 and 3 are identical in the relative intensities of the peaks representing this hypothetical compound. Case B: When the partial pressure of the hypothetical compound changes in the ion source during scans 1, 2 and 3, the spectra are skewed as described in the text.

make available at least partially purified mixture components for analysis by mass spectrometry for identification purposes. Paradoxically, the dynamic nature of sample concentrations at the outlet of a gas chromatograph, especially in capillary column chromatography, tends to violate one of the cardinal rules in MS [1]. That is, it is important for the partial pressure of the analyte in the ionization chamber to remain constant during the time interval in which the mass spectrometer is scanned to acquire a mass spectrum; this condition ensures that the relative peak intensities represented in the mass spectrum are related to structural features of the molecule, and not distorted due to changes in partial pressure of the analyte during acquisition of that mass spectrum.

The influence of a dynamic partial pressure of an analyte in a mass spectrometer's ion source on the appearance of the acquired mass spectra is illustrated in Fig. 1. Case A in Fig. 1 represents the acquisition of three mass spectra of a hypothetical analyte maintained at constant pressure in the ion source. Case B in Fig. 1 represents analysis of the same hypothetical analyte when introduced to the mass spectrometer ion source via a gas chromatograph. The partial pressure of analyte in the ion source of the mass spectrometer rises and then falls as the analyte emerges from the gas chromatographic column. Scans 1 and 3 were acquired as the analyte concentration (partial pressure) was changing most rapidly in the ion source during mass spectral acquisition, and these mass spectra show a distortion or skewing of relative peak intensities. The relative peak intensities in each mass spectrum are indicative of the partial pressure of the analyte in the ion source, as well as the inherent fragmentation pattern of the compound. This situation complicates mass spectral interpretation, and limits compound identification based on mass spectral matching approaches.

Problems in capilary GC–MS

Problem 1: The acquisition of true mass spectra. The very definition of a gas chromatogram is, in fact, the temporal profile of partial pressures of analytes as they emerge from the chromatographic column. Improvements in the resolving power of capillary columns during the last decade, as reflected by the very sharp peaks (2–3 s in duration) in the chromatograms [2,3], have placed severe demands on the mass spectrometer to scan quickly enough to avoid distorting the mass spectra without sacrificing other important mass spectral features such as resolving power and the signal-to-noise ratio associated with the data. This problem is exacerbated during the common occurrence of poorly resolved components; in this case, the ion source may contain the vapor of one component or the other for only a few milliseconds, and it is imperative to capture an undistorted "pure" spectrum during this brief interval. An assessment [4] of the capacity for various mass analyzers to scan rapidly during analyses by GC–MS indicates that present demands for high scan rates (approaching ten scans per second over the mass range 50 to 500 daltons) made by high-resolution GC has forced many of the common mass analyzers to their very limit of performance as established by the physics underlying their operating principles. On the other hand, the time-of-flight mass spectrometer, by virtue of its rapid cycle time, has the capacity for generating complete mass spectra at a rate even higher than that presently demanded by GC–MS instruments that utilize the most efficient high-resolution GC capillary columns.

Problem 2: The satisfactory reconstruction of the chromatographic profile from mass spectral data. The problem resulting from the great disparity between the rate of change in sample partial pressure in capillary GC and the data acquisition rate of complete mass spectra is illustrated in Fig. 2. In each of the three panels in Fig. 2, the true chromatographic profile is illustrated by the dashed line; the solid line in each of the three panels is an attempt to reconstruct the chromatographic profile from data points available from a data base consisting of consecutively-recorded mass spectra. Each point represents the reconstructed total ion current (TIC) obtained by summing the measured intensities of all of the mass spectral peaks in one mass spectrum. In panels A and B, the rate of data acquisition yielded one scan file per second; thus, in these two panels there is available only one TIC point per second for purposes of reconstructing the chromatographic profile. The only difference between panels A and B is the synchrony between the repetitive scanning of the mass spectrometer and initialization of the chromatographic process. As can be seen in panels A and B, such utilization of mass spectral data for reconstruction of the true chromatographic profile is severely limited. However, as shown in panel C, if three points per second are available (due to scanning the mass spectrometer three times per second) from which to reconstruct the chromatographic profile as indicated by the solid line in panel C, the true chromatographic profile is more correctly described.

Problem 3: Limitations of "scanning" mass analyzers. Another major problem in GC–MS is the sacrifice of considerable ion counting statistical information when the technique of scanning of the mass spectrometer is used. As in most spectroscopic
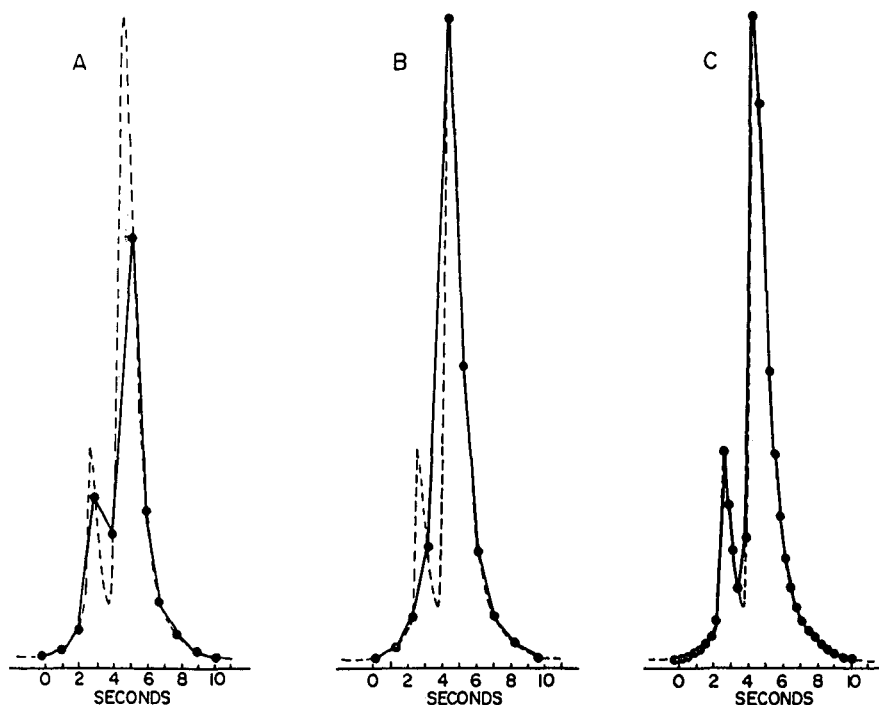
Fig. 2. Comparison of the true chromatographic profile (---) and attempts to reconstruct the chromatographic profile (—) from 10 data points for cases A and B, and 30 data points for case C, as described in the text (adapted from ref. 4 with permission of the American Chemical Society).

instruments which use the exclusive process of scanning, considerable information is lost as some parameter is varied to allow resolution elements of the mass spectrum to consecutively pass across the detector slits. Sweeley *et al.* [5], Hammar *et al.* [6] and other pioneers as reviewed by Falkner [7] solved this problem with selected-ion monitoring (SIM) which dedicates the instrument to monitoring ion current at only a selected resolution element (*m/z* value). Whereas the excellent sensitivity of SIM (femtomoles) is achieved by integrating all of the ion current from the ion source at a particular resolution element or *m/z* value of the mass spectrum, such good sensitivity could be achieved, in principle, while acquiring complete mass spectra if it were possible to integrate all ion current at all resolution elements or all *m/z* values across the mass spectrum all of the time. Such a process is possible only through array detection which measures all ion currents over a range of *m/z* values simultaneously. It would be desirable to acquire the complete mass spectrum in consecutive scans at the same high sensitivity otherwise available only by selected-ion monitoring. The key features of repetitive scanning and its advantages and disadvantages are presented in Fig. 3 in parallel with the key features of SIM together with its advantages and disadvantages.

A solution

As indicated in the conclusion of Fig. 3, the beneficial aspects of repetitive acquisition of mass spectra in the generation of a complete data field for a GC–MS

Repetitive Complete Scans   Selected Ion Monitoring

a.) 10–50ng required   a.) 10–50pg detected
b.) acquire and store com-   b.) dedicated to mon-
    prehensive data base   itoring only selected
    of complete mass   ion currents
    spectra   c.) nearly continuous out-
                                     put; cycle time 10 to
                                     100Hz

                     time
                     (scan#)

100   400 500 600
      m/z ⟶

c.) reconstruct mass chro-   d.) real-time out put
    matograms

            m/z 423   m/z 423
            m/z 513   m/z 513
time (scan#)⟶   time⟶

d.) also have data base to   e.) limited (if any) other
    reconstruct other mass   data
    chromatograms

    FLEXIBLE   SENSITIVE

            BOTH FEATURES AVAILABLE
               IF ALL ION CURRENTS
            RECORDED ALL THE TIME

Fig. 3. Summary of operational features and mutually exclusive advantages of the technique of repetitive scanning and selected ion monitoring (reprinted from ref. 1 with permission from Raven Press).

analysis can be combined with the high sensitivity of SIM only if array detection is used to record the mass spectrum. The approach of using array detectors in mass spectrometry was pioneered by Giffen et al. [8] at the Jet Propulsion Laboratory in the 1970s. This resulted in the development of a device called an electro-optical ion detector which was evaluated subsequently in GC–MS by Hedfjall and Ryhage [9]. The technique of Fourier transform (FT) MS also provides array detection in that all ions present in the device are detected simultaneously [10], although the application of this instrument in GC–MS has not been extensively pursued to date. While FT-MS can obtain an impressive number of mass spectra per second, there are acquisition rate/resolution trade-offs. To avoid problems with limited dynamic range and other potential mechanical difficulties with these and other approaches to array detection, the research effort in the Michigan State University (MSU) Mass Spectrometry Facility has pursued developments in time-of-flight MS to conduct array detection in time.

Time-of-flight (TOF) MS, because of its pulsed nature and the very short time required for producing any given transient mass spectrum, i.e., an ion sampling time ranging from 3 to 100 μs, makes this technique an ideal method for sampling rapidly changing partial pressures of analytes in the ion source. As explained in early reports on this work [4,11], time array detection is achieved in TOF-MS by digitizing the output from the detector such that all information in all resolution elements of the transient time-of-flight mass spectrum are collected following each extraction pulse from the ion source. For this purpose, an integrating transient recorder (ITR) has been designed and implemented, as described elsewhere [12]. Briefly the ITR digitizes the ion detector output at 200 MHz, is capable of producing up to 50 complete mass spectra per second, and can sustain high data collection rates continuously for up to one hour without loss of data. Another major requirement for proper utilization of time array detection is the necessity of providing optimum ion focus for ions of all m/z values from each ion packet so that each of the 5000–10 000 transient mass spectra reaching the detector per second have properly resolved mass spectral peaks. Conventional techniques in TOF-MS such as time-lag focusing are mass-dependent and are not generally useful in conjunction with time array detection, although we have obtained preliminary results [13] using time array detection with mass collection over narrow mass ranges which fall within the limits of acceptable focus by a fixed value of the time-lag parameter. The MSU group also has pursued techniques of beam deflection TOF-MS for purposes of achieving mass-independent ion focus and for improving the resolving power, in general, of TOF-MS by eliminating the aberration in resolution caused by the "turn around time" problem [14]. The technical details of a most recent version of a beam deflection TOF-MS system will be described elsewhere [15]. This report provides a preliminary assessment of the beam deflection TOF-MS system developed at MSU with time array detection for purposes of gathering complete mass spectra from a standard test mixture introduced via capillary column GC.

EXPERIMENTAL

Preliminary results from the GC–TOF-MS system based on beam deflection as represented schematically in Fig. 4 are presented here. In brief, the gas chromatograph used is a Hitachi 663-30, fitted with an 18 m (DB-1, 0.18 mm I.D.) capillary column; the test sample described herein is the Grob mixture (Supelco catalog No.
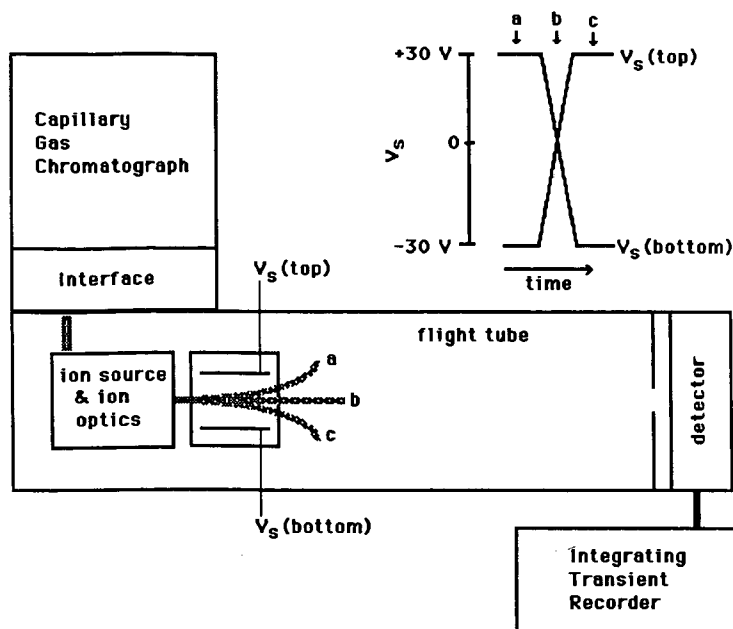
Fig. 4. Schematic diagram of the beam deflection TOF-MS system showing the gas chromatograph, continuous ion source, beam deflection assembly, CEMA detector, and ITR.

4-7304). The GC–MS interface is a heated block design from JEOL. The time-of-flight mass spectrometer is a highly modified Bendix 12-101 instrument. The source and source housing from a double-focusing mass spectrometer, a DuPont 21-491, is used to provide a continuous, narrow, focussed beam of ions produced by electron or chemical ionization. Ions formed in the source are accelerated to a kinetic energy of approximately 3000 eV. Ion packets are formed by beam deflection [14]. To obtain a rapidly changing electric field in the beam deflector for good mass spectral resolution, dynamic voltages ("pulses") of equal magnitude, but of opposite sign (designated as V_s in Fig. 4), are applied to each deflection plate yielding temporally narrow ion packets. The time-dependent voltages used are generated from pulsing circuitry that was developed in-house. Typically, the voltages V_s applied are modulated between + 30 V and − 30 V. The circuitry provides a rise time of < 10 ns and a fall time of < 20 ns. Ion packets traverse a 2.0-m flight tube, and transient mass spectra are generated at a rate of 5000 s^{-1}. This beam deflection TOF-MS system provides better than unit resolution for all ions in the m/z 2–1000 range, with all ions in optimal focus for each ion packet. A resolving power of > 1400 has been demonstrated for this instrument [15].

An in-house designed and built integrating transient recorder [12] was used to continuously collect full mass range, mass spectra throughout the entire duration of the GC–MS run (20 min). Data collection with the ITR is accomplished by a 200 MHz flash analog-to-digital converter. The digitized data are passed to 16 high speed ECL (emitter coupled logic) summer cards where 5 to 5000 transients are summed to form a mass spectral scan file. If 5000 transients are produced each second by the

TOF-MS system, summation of 5 to 5000 transients corresponds to mass spectral generation rates of 1000 scan files per second to 1 scan file per second, respectively. The integrated scan files are passed across a VME bus to three Motorola 68020 parallel processors whereby time/mass calibration, and/or conversion to reconstructed mass chromatograms and/or real-time conversion to mass, intensity pairs occurs. Finally, the processed scan files are written to a 300 Mbyte Priam disk drive (typical scan file sizes = 500–2000 bytes).

RESULTS AND DISCUSSION

The principal goals of this paper are to demonstrate that beam deflection TOF-MS is capable of producing good quality mass spectra and that these mass spectra are well focussed and resolved over the complete mass range so that time array detection can be implemented by means of an ITR. The importance of acquiring complete mass spectra at a rate of 20 scan files per second in deconvoluting unresolved chromatographic components is illustrated in the analysis of a capillary column test mixture. As described elsewhere, the ITR is capable of generating up to 1000 complete summed spectra per second [4,11,12]. This scan file generation rate would provide 1000 data points per second from which a chromatographic profile could be reconstructed from a data base of consecutively-recorded mass spectra. However, such a high frequency of scan file generation is not necessary to reconstruct the profiles available from most high-resolution gas chromatographs at this time. In the preliminary assessment of time array detection described here, a scan file generation rate of 20 scan files per second has been found adequate to provide 20 data points per second from which to reconstruct chromatographic profiles having peak widths on the order of two seconds.

Representation of the chromatographic profile
Fig. 5 shows the reconstructed total ion current (RTIC) chromatogram of a standard test mixture [16] analyzed using GC–beam deflection TOF-MS–ITR, repre-
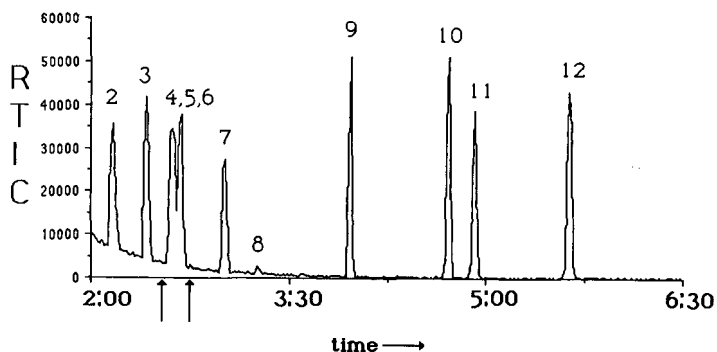
Fig. 5. Reconstructed TIC chromatogram (RTIC) of standard Grob test mixture as separated on a 20 m × 0.18 mm I.D. column containing DB-1, 0–0.4 μm film thickness at a flow-rate of 1.5 ml/min with a temperature program of 20°C/min from 120 to 200°C. Components (approx. 50 ng each) in the mixture: 1 = 2,3-butanediol; 2 = decane; 3 = 1-octanol; 4 = nonanal; 5 = 2,6-dimethylphenol; 6 = undecane; 7 = 2,6-dimethylaniline; 8 = 2-ethylhexanoic acid; 9 = C_{10} acid methyl ester; 10 = C_{11} acid methyl ester; 11 = dicyclohexylamine; 12 = C_{12} acid methyl ester. Time in min:s.

senting approximately 50 ng of each component. A scan file generation rate of one scan file per second offers one TIC point per second to reconstruct the chromatographic profile. Generation of one TIC point per second is typical of most available GC–MS instruments (*e.g.*, quadrupoles and magnetic sector instruments) in use today.

Several questions must be addressed concerning the results in Fig. 5. Does the RTIC, reconstructed from the one-scan-file-per-second data base, adequately represent the chromatography? Also, it was known that the mixture contained 12 components, but only 10 peaks are shown in the RTIC. The portion of the chromatogram containing the solvent peak and 2,3-butanediol is not shown here (Fig. 5), so there should be 11 components represented by the RTIC. To answer these questions, another aliquot of the test mixture was analyzed by GC–beam deflection TOF-MS–ITR, summing every 250 transient mass spectra, thereby generating 20 scan files per second. The RTIC chromatogram, resulting from the 20-scan-files-per-second data base at approximately 2.5 min into the run, is shown in Fig. 6b; for comparison, the corresponding segment of the RTIC in Fig. 5 (between the vertical arrows), obtained from the one-scan-file-per-second data base is reproduced as Fig. 6a. There are two obvious advantages to the greater scan file generation rate that can be seen upon comparing Fig. 6a and b. Because the 20-scan-files-per-second data base offers 20 points per second to reconstruct the waveform (Fig. 6b), the chromatographic profile is more accurately represented in terms of peak shapes, relative heights, and relative
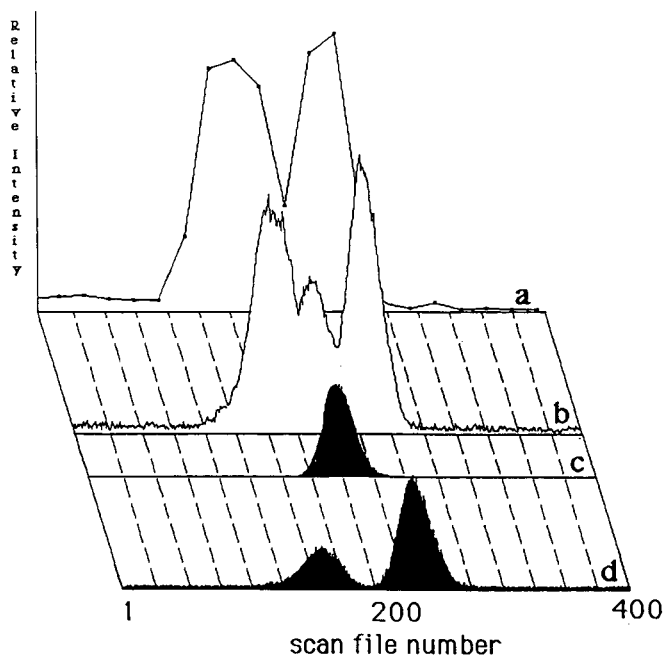
Fig. 6. (a–d) Data over a region of the chromatogram representing coeluting components. (a) RTIC obtained from spectra collected at 1 scan file/s; it only shows evidence for two components. (b) RTIC obtained from spectra collected at 20 scan files/s; it shows evidence for three components. (c) Mass chromatogram at m/z 122 representing the molecular ion of 2,6-dimethylphenol. (d) Mass chromatogram at m/z 57 representing an alkyl cation, a characteristic ion of both nonanal and undecane.

areas. This feature of the data provides better quantification of the components in the mixture. The other advantage is that the RTIC generated from higher scan file generation rates more accurately represents the true chromatographic profile. It is obvious from the RTIC presented in Fig. 6b that this region of the chromatogram contains three components.

Chester and Cram [17] have investigated the relationship between the number of data points required to represent the profile of a given chromatographic peak and the characteristic features of that peak shape as described by σ, where σ^2 is the variance that can be related to the mathematical function describing the profile. It has been previously estimated that 10 data points (scan files) per standard deviation unit are necessary to obtain an accurate representation of the chromatographic peak height, area, and position assuming a Gaussian peak [18]. The minimum number of data points which can accurately represent this profile is 10 scan files per second. Most scanning mass analyzers would not be able to represent the chromatography in this situation due to their scan file generation rate limitations.

The high scan file generation rates allow the presence of three components to be recognized in this unresolved region of the reconstructed chromatogram in Fig. 6b. Can the three components be identified from the mass spectral data base even though the components are coeluting? Because the components in the test mixture are known, as well as the type of column used for analysis, we were able to determine which components were expected to be in this region of the chromatogram. One of the expected components is 2,6-dimethylphenol. Instead of searching through the 200 scan files which contain mass spectral data for a match of the data to a library mass spectrum of this compound, we can display the mass chromatogram of one of the dominant ions in the mass spectrum of 2,6-dimethylphenol. A mass chromatogram is a graphic display of the peak intensity at a specified mass-to-charge value *versus* scan file number [19]. The library mass spectrum of 2,6-dimethylphenol indicates that the molecular ion is represented by the base peak at m/z 122. Fig. 6c is the mass chromatogram of m/z 122 and identifies the middle component as 2,6-dimethylphenol. Another component expected to be in this region of the RTIC is undecane; the alkyl cation $C_4H_9^+$, m/z 57, was selected as a designate ion for this hydrocarbon. The mass chromatogram at m/z 57 displayed in Fig. 6d shows that the mass spectra of both of the other two components contain this alkyl cation. The mass chromatograms at m/z 57 and 122 (Fig. 6d and c, respectively) provide information on the chromatographic peak shapes of the three components. By choosing a scan file which does not contain both m/z 122 and m/z 57, one can obtain a pure mass spectrum for each of the three components represented here. A visual inspection of the mass chromatogram represented in Fig. 6d shows a region (scan files 190–200) where the ion current at m/z 57 is minimal. Because the mass spectra of the other two components have an intense peak at m/z 57, this is a region of the data base that should provide a reasonably pure mass spectrum of the middle component. The mass spectrum contained in scan file 192 is shown in Fig. 7a. A similar procedure was used to obtain pure mass spectra of the other two components by choosing scan files which do not contain ion current at m/z 122. Ion current at m/z 122 is observed in scan files 160–232. Fig. 7b shows the mass spectrum in scan file 159 which is identical with the library spectrum of nonanal. Fig. 7c shows the mass spectrum in scan file 240 which is identical with that of undecane.

a

b

c
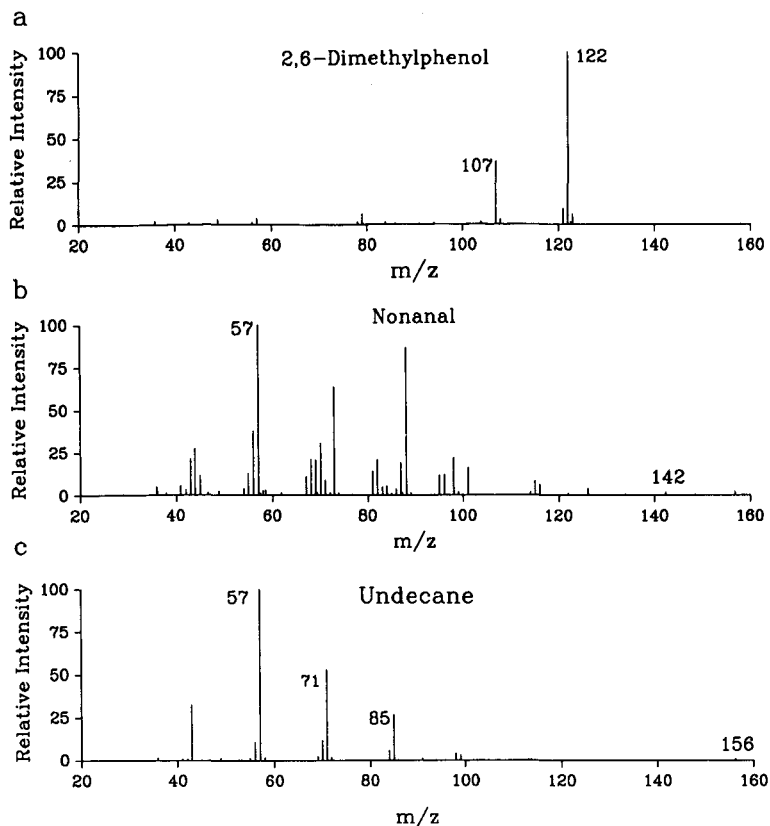
Fig. 7. Mass spectra selected from the several hundred scan files collected at 20 scan files/s as represented in Figs. 5 and 6. (a) Mass spectrum of 2,6-dimethylphenol obtained from scan file 192. (b) Mass spectrum of nonanal obtained from scan file 159. (c) Mass spectrum of undecane obtained from scan file 240. These spectra represent components 5, 4 and 6 in Fig. 5.

Limits of detection

The detection limit of the GC–beam deflection TOF-MS–ITR at 20 scan files per second was compared to that of the JEOL JMS-AX505H MS system which is a commercially available double-focusing sector instrument routinely used for GC–MS analyses. The fastest scan rate available with the JEOL instrument is 0.9 s per decade (*e.g.*, m/z 50-500) which generates 1.1 scan files per second.

Complete mass spectra were collected during the analysis of the standard test mixture at various concentrations at the scan file generation rate described above for each mass spectrometer. Mass chromatograms were reconstructed from the corresponding data bases. The area of the peak in the mass chromatogram at m/z 122 (corresponding to the base peak in the mass spectrum of 2,6-dimethylphenol) was plotted *versus* the amount of analyte injected. The limit of detection was calculated using the method of regression analysis [20] on each data set. The y-intercept of each regression line was used as an estimate of the blank signal, y_b. The signal, $y = y_b + 3s_b$, determines the limit of detection. The limit of detection calculated for both the

JEOL instrument and the GC–beam deflection TOF-MS–ITR system was 0.6 ± 0.2 ng of 2,6-dimethylphenol.

Quality of mass spectra

An important feature of the data obtained with GC–beam deflection TOF-MS–ITR is the absence of mass spectral skew, due to the high sampling rate (5000 s^{-1}) of the continuous ion beam. Thus, the mass spectra of individual components obtained at different scan file generation rates are identical, each having the same relative peak intensities throughout the mass range. This feature of the data would have allowed identification of the three components by use of available mass spectral deconvolution routines [21] to distinguish the coeluting components based on their characteristic contributions to peak intensities among the adjacent scan files.

CONCLUSIONS

We have shown that the GC–beam deflection TOF-MS–ITR combination is capable of providing good-quality GC–MS data. The GC–beam deflection TOF-MS–ITR system can generate data files at a rate greater than those commonly available from quadrupole and magnetic sector instruments. The importance of the high scan file generation rate was illustrated by comparison of reconstructed total ion current chromatograms from data bases collected at 20 scan files per second and at one scan file per second, the latter being representative of the performance of most magnetic or quadrupole instruments (even though, in principle, these instruments can generate data at higher rates, but at the expense of performance and data quality). Here we have shown an example where one scan file per second is insufficient to reproduce the chromatographic profile; in this case, we reanalyzed the mixture by GC–MS generating 20 scan files per second. Each mass spectral transient is free of any skewing due to the changing partial pressure of the analyte in the ion source, thus the summed spectra are free of the types of skew that would be imposed by other scanning instruments.

This report describes one approach by which the MSU research group is attempting to respond to the fact that developments (*e.g.*, scan speeds) in MS have not progressed in a timely fashion commensurate with improvements in GC resolving power. Chromatograms are now being reported with peak widths on the order of tens of milliseconds [2]; further improvements in GC could make contemporary MS of little use as a GC detector. While these preliminary results with the GC–beam deflection TOF-MS–ITR system are not competitive from the standpoint of sensitivity (because the source is designed for a magnetic sector instrument), they do illustrate that developments in TOF-MS and its use with the ITR provide a mass spectrometer that can "keep up" with the demands imposed by high-resolution GC on MS. These developments provide the basis for sustaining the use of MS as a GC detector, the data from which can be used to both adequately represent the chromatography and identify eluting components of complex mixtures.

REFERENCES

1 J. T. Watson, *Introduction to Mass Spectrometry*, Raven Press, New York, 2nd ed., 1985.
2 L. A. Lanning, R. D. Sacks, R. F. Mouradian, S. P. Levine and J. A. Foulke, *Anal. Chem.*, 60 (1988) 194-196.
3 P. A. Leclercq and C. A. Cramers, *J. High Resolut. Chromatogr. Chromatogr. Commun.*, 11 (1988) 845-848.
4 J. F. Holland, C. G. Enke, J. T. Stults, J. D. Pinkston, B. Newcome, J. Allison and J. T. Watson, *Anal. Chem.*, 55 (1983) 997A.
5 C. C. Sweeley, W. H. Elliott, I. Fries and R. Ryhage, *Anal. Chem.*, 38 (1966) 1549-1553.
6 C.-G. Hammar, B. Holmstedt and R. Ryhage, *Anal. Biochem.*, 25 (1968) 532-548.
7 F. C. Falkner, *Biomed. Mass Spectrom.*, 4 (1977) 66-67.
8 C. E. Giffen, H. G. Boettger and D. D. Norris, *Int. J. Mass Spectrom. Ion Phys.*, 15 (1974) 437-449.
9 B. Hedfjall and R. Ryhage, *Anal. Chem.*, 53 (1981) 1641-1644.
10 M. L. Gross and D. L. Rempel, *Science (Washington, D.C.)*, 226 (1984) 261.
11 J. Allison, J. F. Holland, C. G. Enke and J. T. Watson, *Anal. Instr.*, 16 (1987) 207.
12 R. Tecklenburg, B. Newcome and J. F. Holland, *Rev. Sci. Instrum.*, (1990) in press.
13 E. Erickson, G. C. Enke, J. F. Holland and J. T. Watson, *Anal. Chem.*, 62 (1990) 1079–1084.
14 J. D. Pinkston, M. Rabb, J. T. Watson, and J. Allison, *Rev. Sci. Instrum.*, 57 (1986) 583.
15 G. E. Yefchak, G. A. Schultz, J. Allison and C. G. Enke, *J. Am. Soc. Mass Spectrom.*, (1990) in press.
16 K. Grob, Jr., G. Grob and K. Grob, *J. Chromatogr.*, 156 (1978) 1–20.
17 S. N. Chesler and S. P. Cram, *Anal. Chem.*, 43 (1971) 1922.
18 C. G. Enke, J. T. Watson, J. Allison and J. F. Holland, presented at the *37th ASMS Conference on Mass Spectrometry and Allied Topics, Miami Beach, FL, May 1989*, Abstract No. MOA 1130, p. 32.
19 R. A. Hites and K. Biemann, *Anal. Chem.*, 42 (1970) 855-860.
20 J. C. Miller and J. N. Miller, *Statistics for Analytical Chemistry*, Wiley, New York, 1984.
21 J. W. Biller and K. Biemann, *Anal. Lett.*, 7 (1974) 515-528.

Sheathed-flow hydrogen atmosphere flame ionization detector for gas chromatography

M. M. GALLAGHER, D. G. McMINN and H. H. HILL, Jr.*

Department of Chemistry, Washington State University, Pullman, WA 99164-4630 (U.S.A.)

(First received October 17th, 1989; revised manuscript received June 28th, 1990)

ABSTRACT

A new design of the hydrogen atmosphere flame ionization detector is presented that involves a sheathed flow of gases. Consumption of hydrogen is reduced by an order of magnitude compared to earlier designs without compromising significantly the sensitivity and selectivity. Linear dynamic range calibrations and molar response factors as a function of hydrogen flow are presented for iron, carbon, lead and tin. Analysis of fish tissue spiked with 135 ppb (10^9) (as tin) each of tetra-*n*-propyl tin, tri-*n*-butyl tin hydride and tetra-*n*-butyl tin demonstrates analytical utility.

INTRODUCTION

Analysis of environmental samples contaminated with organometallic compounds is an on-going concern. Extensive use of organotin compounds as stabilizers in the plastic industry, as antifouling agents in marine paints and as topical insecticides, as well as combustion and spillage of organolead compounds used in the gasoline industry allows easy access of these compounds to the environment [1]. Emphasis recently has been placed on the analysis of fish and shellfish tissues, marine sediments, and seawater for organotin residues derived from land based biocides and marine antifouling agents [2]. Although the use of alkyllead modifiers in gasoline is being phased out, analysis of these compounds continues to be of interest [3].

The majority of the analytical procedures developed to date require significant sample workup prior to analysis or provide incomplete information as to speciation of the metal contaminant. Few techniques allow for speciation and quantification of both tin and lead compounds and those that do require expensive instrumentation. A wide variety of detectors has been utilized, ranging from some having selective response to more universal detectors [4–7].

The hydrogen atmosphere flame ionization detector (HAFID), introduced in 1972, is a simple yet highly sensitive and selective detector for certain organometallic compounds [8]. It has been shown to be on the order of 10 000 times more sensitive to organometallics than to carbon, with detection limits as low as the subpicogram range and has potential for the determination of organometallic components in complex hydrocarbon mixtures [9]. Recent work has extended its utility to detection after supercritical fluid chromatography [10].

Modification of a conventional FID to produce a HAFID requires three basic

changes. First, the hydrogen and air inlets are interchanged. Second, the hydrogen is doped with small quantities of SiH_4. Third, the collecting electrode is raised to approximately 7 cm above the jet tip.

There are two basic operating modes of the HAFID. The first is termed the negative mode since organometallic compounds cause a reduction in the current which is collected, producing a negative peak. The second is a positive mode where all compounds entering the flame yield an increase in ion current. In both situations, hydrocarbons respond by an increase in ion current, although the response is several orders of magnitude less than that of the organometallic species. Nevertheless, in the positive mode a large concentration of hydrocarbon entering the flame is difficult to distinguish from an organometallic response. Operation in the negative mode thus offers a distinct advantage since only organometallics yield negative peaks. Mechanisms accounting for these repsonse characteristics have not yet been delineated.

Previous designs of the HAFID have required hydrogen flows of up to 4 l/min. This large flow necessitated special venting and work procedures. Simply miniaturizing the detector in an attempt to lower the hydrogen requirements has proven unsuccessful.

In this paper a new detector design is presented which incorporates a third gas line that supplies a sheath of nitrogen gas to surround the active atmosphere of hydrogen and SiH_4. The gas streams are kept separated by a concentric collar attached to the base of the detector.

EXPERIMENTAL

Reagents

Tetra-*n*-propyltin ($SnPr_4$), tetra-*n*-butyl tin ($SnBu_4$), tri-*n*-butyl tin hydride ($SnBu_3H$), tetra-*n*-butyl lead ($PbBu_4$) and bis-cyclopentadienyl iron (ferrocene) were purchased from Aldrich (Milwaukee, WI, U.S.A.) and used without further purification. Tetradecane (C_{14}) was purchased from Sigma (St. Louis, MO, U.S.A.). Gases were purchased from Liquid Air (Spokane, WA, U.S.A.), except for SiH_4 (1020 ppm) in H_2 which was purchased from Airco Specialty Gases (Santa Cruz, CA, U.S.A.).

Detectors

The sheathed-flow HAFID used in this study is depicted in Fig. 1. Unlike previous designs, it was not a modification of an existing FID. The complete detector was machined from type 304 stainless steel. The jet tip, bored to No. 72 drill size (0.635 mm) was smaller than the 1.5 mm bore used in earlier designs where much higher gas flows were used. The addition of the modular baffle plate, concentric with the flame jet, provided approximate laminar flow. A collar 29.7 mm in length, inserted into the baffle plate, maintained separation of the N_2 sheath gas from the active atmosphere of H_2 and SiH_4. Flame ignition was provided by a model airplane glow plug. The collecting electrode was constructed using the terminal pin of coaxial bulkhead fitting, friction fitted to a length of stainless steel tubing. This configuration allowed the electrode height to be varied above the jet tip by means of spacers and adjustment of a tubing setscrew. The electrode was centered above the jet tip and biased to -90 V using an Eveready 490 battery connected in series with the input
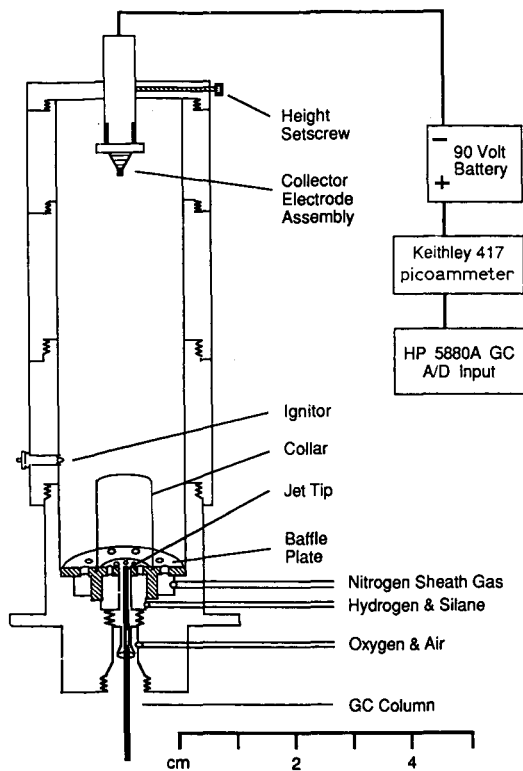
Fig. 1. Sheathed-flow hydrogen atmosphere flame ionization detector. A = Analog; D = digital; GC = gas chromatograph.

head of a Keithley 417 picoammeter. The amplified output of the picoammeter was reduced by a voltage divider and connected to the analog input board of the supporting Hewlett-Packard (HP) 5880A gas chromatograph where it was processed and displayed. The FID supplied with the chromatograph was operated as recommended by the manufacturer.

Chromatigraphic conditions

All chromatography was performed on a Hewlett-Packard Model 5880A gas chromatograph equipped with a 30 m × 0.25 mm DB-1 column (J & W Scientific, Folsom, CA, U.S.A.). The carrier gas was hydrogen at a flow rate of 1.7 ml/min with a split ratio of 1:10. The injection port was held at 275°C with the detector temperature at 300°C for both the FID and HAFID. The external walls of the HAFID were heated to 210–225°C by resistance heat tape to prevent condensation of water. For both the calibration curves and molar response factor studies the oven was operated isothermally at a temperature that produced retention times resulting in a partition ratio (k') of approximately 2. Oven temperatures used were 145°C for iron (ferrocene), 165°C for carbon (C_{14}), 210°C for lead ($PbBu_4$), and 195°C for tin ($SnBu_4$).

The spiked fish tissue analysis used a temperature program with an initial temperature of 70°C, held for 1 minute, ramped at 5°C/min to 300°C and ended with a 5-min isothermal period. The amount of tissue extract injected for each chromatogram was adjusted to produce roughly equal peak heights in the HAFID ($-$ mode, 2 μl; $+$ mode, 3 μl) with the FID receiving a standard 1-μl injection.

Detector conditions

Gas flows to the HAFID, concentration of the SiH_4, and height of the electrode above the jet tip are all of prime consideration for optimal response to organometallic compounds [11]. The values used here are not optimized, but prior work has established these as working well on a day-to-day basis. In a given response mode, all factors were held constant for each metal throughout both the calibration curve and molar response study, excepting total hydrogen flow which was the variable in the molar response study. Gas flows are listed in Table I.

TABLE I

DETECTOR GAS FLOWS

	Total hydrogen flow (ml/min)	Silane doping concentration (ppm)	Oxygen flow (ml/min)	Nitrogen flow (ml/min)	Nitrogen sheath gas flow (ml/min)	Electrode height above jet tip (mm)
Positive mode						
Iron	370	130	22	89	500	70
Carbon	380	140	22	35	500	70
Lead	360	140	18	73	500	70
Tin	380	130	27	70	500	70
Negative mode						
Iron	370	240	18	74	100	75
Carbon	360	240	18	33	320	75
Lead	470	420	40	93	500	65
Tin	410	190	12	47	660	70

Calibration curves and molar response as a function of hydrogen flow

To determine the linear dynamic range of the sheathed-flow HAFID, a series of standards was injected under both positive and negative mode operating conditions. To determine the optimal reduced hydrogen flow, studies were conducted using the same SiH_4 doping concentration and flame conditions as the calibration studies, but allowing variation in the total hydrogen flow. Both positive and negative mode studies used the same mass of each organometallic compound injected. The value was selected from the center of the compound's linear range.

Analysis of fish tissue

A 37-g sample of orange roughy fish fillet was spiked with a solution containing 5 μg tin per component from $SnPr_4$, $SnBu_3H$ and $SnBu_4$ resulting in a concentration of 135 ppb each as Sn. The sample was homogenized and extracted using the modified Bligh and Dyer procedure outlined by Sullivan *et al.* [12]. No attempt was made to clean up the extract, although concentration was required.

RESULTS AND DISCUSSION

By adding the external sheath of N_2 and separating the active core of H_2 and SiH_4, the response of the HAFID could be maintained at hydrogen flow-rates an order of magnitude less than previous designs without sacrificing selectivity and sensitivity. The sheathed-flow HAFID appears to need somewhat higher SiH_4 doping concentrations, at least in the positive mode. High-flow designs operating in the positive mode had optimal SiH_4 concentrations of 10–35 ppm, while this design required 125–150 ppm. In the negative mode, both detector designs respond well at SiH_4 concentrations in the range of 250–400 ppm. At this time, no explanation is available for this phenomenon. This higher SiH_4 requirement caused increased deposition of SiO_2, requiring occasional maintenance to remove deposits. The optimal flow-rate of the N_2 sheath gas depended on the total flow of O_2 and air, requiring higher flow of N_2 as the total flow increased. A higher than optimal flow of the N_2 sheath gas was required in order to sweep out the detector volume and maintain peak sharpness. The modular construction of this design allowed jet tip, collar and baffle plate replacement without major disassembly of the detector.

The positive response curves (Fig. 2) showed a linear range spanning approximately two orders of magnitude for each compound tested. In these initial studies it appears that the sheathed-flow HAFID has a reduced dynamic range over that avail-
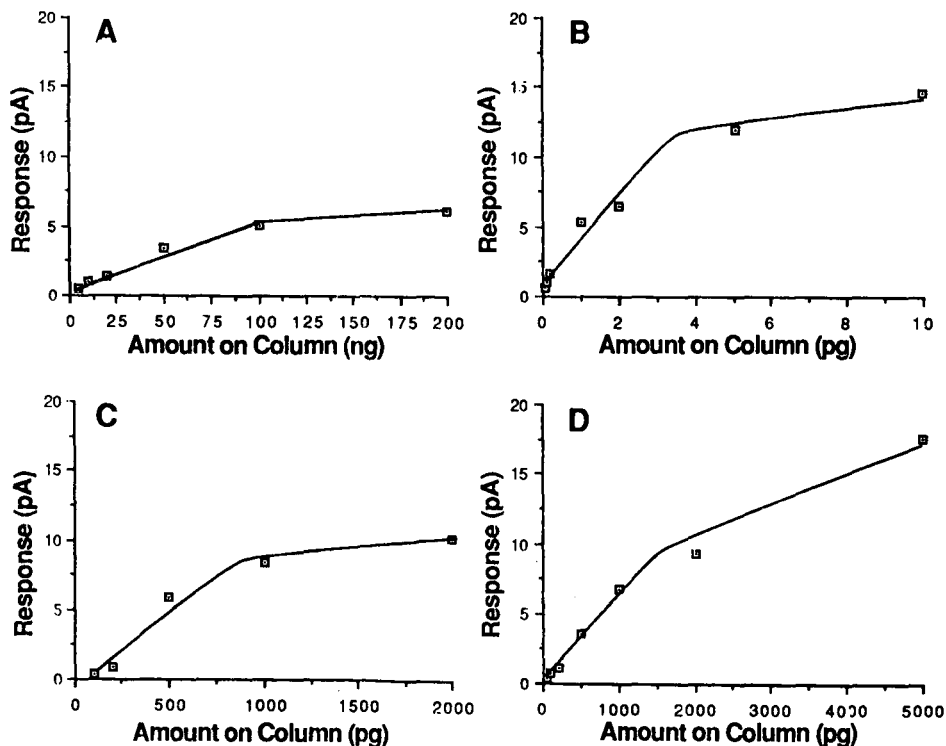
Fig. 2. Positive mode response curves. Detector conditions are listed in Table I. (A) Carbon; (B) iron; (C) lead; (D) tin.

able with earlier designs. At higher amounts injected, saturation of the flame was observed. Iron, injected as ferrocene, gave the lowest detection limit of approximately 20 fg (measured at twice the average noise level). The selective response for iron *versus* carbon, calculated at the $1 \cdot 10^{-12}$ A response level, is nearly 10^5. Tin and lead, injected as the tetrabutyl compound, showed a similar linear range with the calculated detection limit for tin being approximately 20 pg and for lead, 60 pg. At high levels of tin injected, the effect of swamping the detector appeared as split peaks, while response to the other compounds leveled off when the detector was overloaded. Carbon response was also linear for approximately two orders of magnitude, but the detection limit was much higher, in the low nanogram range.

The negative mode calibration curve, shown in Fig. 3, was similar to the positive mode curves, but the organometallic compounds responded by quenching the ion current, yielding a negative peak. The carbon response was always an increase in ion current, regardless of the doping conditions used. Although displayed on the same scale as the organometallic compounds, the carbon response is actually of opposite polarity. Combining the opposing peak direction and organometallic response enhancement, negative mode operation permitted rapid identification of organometallic components. Detection limits in the negative mode were normally equal to, or an order of magnitude lower than, those obtained under positive mode conditions. This
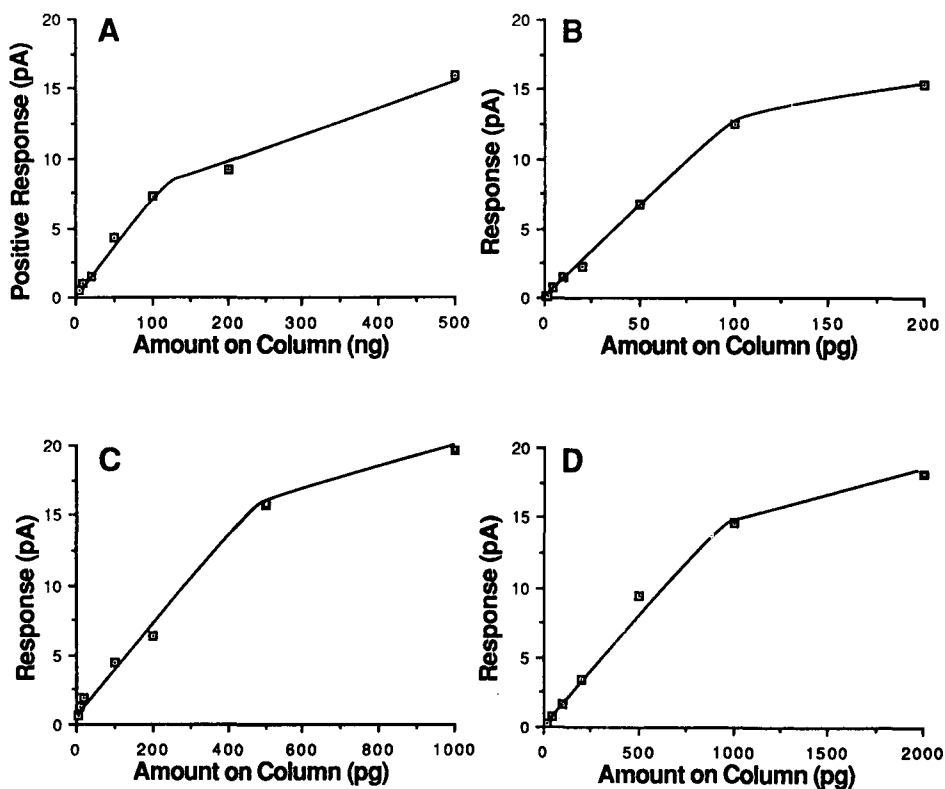
Fig. 3. Negative mode response curves. Detector conditions are listed in Table I. (A) Carbon; (B) iron; (C) lead; (D) tin.
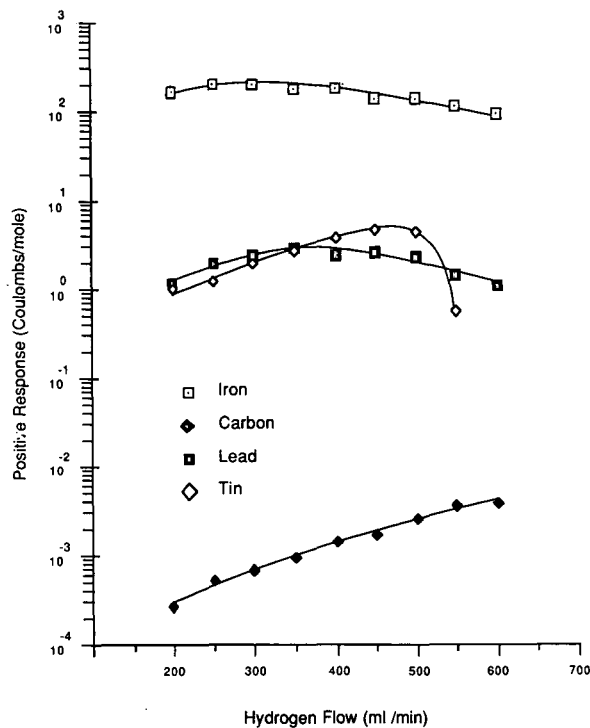
Fig. 4. Positive mode molar response study. Detector conditions are listed in Table I, SiH_4 concentration held constant while hydrogen flow varied.

behavior was seen for tin and lead, but the detection limit for iron was raised by a factor of 100. At this time, no explanation is available.

Response factors (coulomb/mole) were calculated from peak areas. The positive mode molar response factor study (Fig. 4) shows the enhancement of the sheathed-flow HAFID response for organometallics as compared to carbon response. At optimal hydrogen flow of 300 ml/min, the molar response for iron is 208.5 C/mole, while carbon response is $7.0 \cdot 10^{-4}$ C/mole. Thus, ionization efficiencies (ions/molecule) of the flame under these conditions were $2.16 \cdot 10^{-3}$ and $7.26 \cdot 10^{-9}$, respectively. Selectivity (molar response of iron/molar response of carbon) calculated from those data was $3 \cdot 10^5$.

In general, organometallic response increased to a maximum, followed by a drop in response factor as the hydrogen flow was increased to a maximum of 600 ml/min. Molar response for carbon was seen to rise continually with increased hydrogen gas flow. Note that the value for tin at 600 ml/min is not plotted, as this value changed response polarity from positive to negative.

Fig. 5, negative mode molar response, depicts all the organometallic compounds studied exhibiting this type of polarity inversion at one or another extreme of hydrogen flow. As in the negative mode calibration curve, the response to carbon was an increase in the ion current, while the organometallic compounds showed quenching of background current, resulting in negative peaks. In a given analysis, this rever-
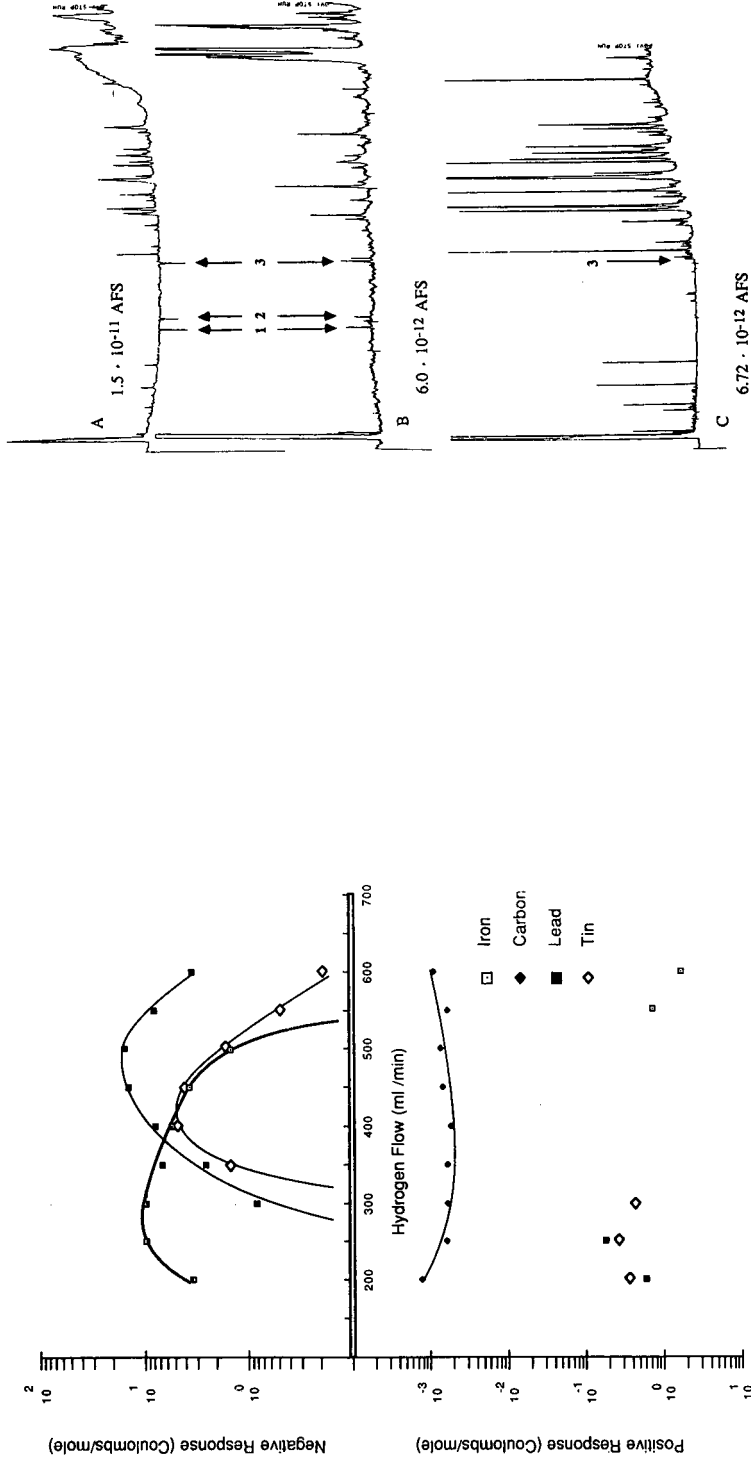
Fig. 5. Negative mode molar response study. Detector conditions are listed in Table I, SiH$_4$ concentration held constant while hydrogen flow varied.

Fig. 6. Chromatograms of an extract from fish. (A) Sheathed-flow HAFID negative mode response; (B) sheathed-flow HAFID positive mode response; (C) FID response. Column 30 m × 0.25 mm DB-1, 1:10 split of 2 µl (− mode), 3 µl (− mode), 1 µl (FID). Column temperature program: 70°C initial, ramping 5°C/min to 300°C, hold for 5 min. HAFID and FID operated at 300°C. 1 = SnPr$_4$; 2 = SnBu$_3$H; 3 = SnBu$_4$.
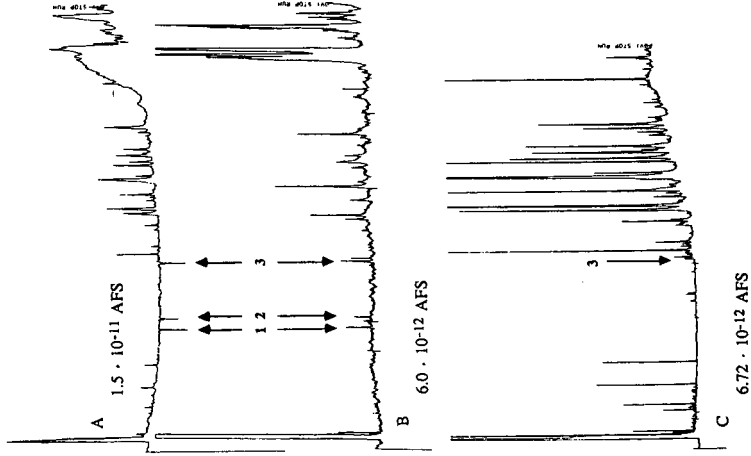
sal of polarity would aid visualization of the peak, but would be difficult to quantify for closely eluting peaks. For purposes of comparison, we use the term absolute molar selectivity, here defined as the absolute molar response of the metal containing compound divided by the response of the carbon containing compound. The maximum absolute molar selectivity (molar response ratio) obtained in this study was $1.2 \cdot 10^4$ obtained for lead and carbon at a hydrogen flow of 500 ml/min. From the rapid changes in molar response factor as hydrogen flow is varied, it is evident that the organometallic compound under consideration will dictate the detector conditions employed.

The chromatograms of the extract from the spiked fish sample are depicted in Fig. 6, with the elution order being $SnPr_4$, $SnBu_3H$ and $SnBu_4$. The top two tracings are of the sheathed-flow HAFID response from the negative and positive mode respectively, while the bottom tracing shows the response obtained with the commercial FID. Note that the negative mode sheathed-flow HAFID chromatogram is easy to interpret with the peaks of interest being inverted. The FID analysis, run at an attenuation of 2^2, does not provide sufficient sensitivity to identify and quantify the organometallic components of the sample. Further concentration and increase of the sample size, along with a possible clean-up step would be necessary for use with the FID.

ACKNOWLEDGEMENT

REFERENCES

1 J. A. J. Thompson, M. G. Sheffer, R. C. Pierce, Y. K. Chau, J. J. Cooney, W. R. Cullen and R. J. Maguire, *Organotin Compounds in the Aquatic Environment National Research Council Canada, 22494*, Ottawa, 1985.
2 M. D. Stephenson and D. R. Smit, *Anal. Chem.*, 60 (1988) 696.
3 A. M. Bond and N. M. McLachlan, *Anal. Chem.*, 58 (1986) 756.
4 K. S. Epler, T. C. O'Haver, G. C. Turk and W. A. MacCrehan, *Anal. Chem.*, 60 (1988) 2062.
5 S. H. Vien and R. C. Fry, *Anal. Chem.*, 60 (1988) 465.
6 M. D. Muller, *Anal. Chem.*, 59 (1987) 617.
7 J. W. McLaren, D. Beauchemin and S. S. Berman, *Anal. Chem.*, 59 (1987) 610.
8 W. A. Aue and H. H. Hill, Jr., *J. Chromatogr.*, 74 (1972) 319.
9 D. R. Hansen, T. J. Gilfoil and H. H. Hill, Jr., *Anal. Chem.*, 53 (1981) 837.
10 M. A. Morrissey and H. H. Hill, Jr., HRC CC, *J. High Resolut. Chromatogr. Chromatogr. Commun.*, 11 (1988) 375.
11 D. G. McMinn, R. L. Eatherton and H. H. Hill, Jr., *Anal. Chem.*, 56 (1984) 1293.
12 J. J. Sullivan, J. D. Torkelson, M. M. Wekell, T. A. Hollingworth, W. L. Saxton, G. A. Miller, K. W. Panaro and A. D. Uhler, *Anal. Chem.*, 60 (1988) 626.

CHROM. 22 668

Effects of the pre-column in automated on-column injection capillary gas chromatography

R. F. ARRENDALE and J. T. STEWART*

Department of Medicinal Chemistry and Pharmacognosy, University of Georgia, College of Pharmacy, Athens, GA 30602 (U.S.A.)

and

R. M. MARTIN

Tobacco Safety Research Unit, Agricultural Research Service, United·States Department of Agriculture, P.O. Box 5677, Athens, GA 30613 (U.S.A.)

(First received March 6th, 1989; revised manuscript received June 25th, 1990)

ABSTRACT

In this work, we investigated the effects of pre-columns and press-fit connectors on automated cold on-column injection capillary gas chromatography. Verapamil, a calcium channel blocking vasodilator used in the treatment of angina, arrhythmias and hypertension, and norverapamil, an active metabolite, were used as model compounds in these investigations. Wide-bore fused-silica tubing deactivated with OV-1701-vinyl was also studied with respect to its suitability as pre-column material. The detector response of verapamil *versus* an internal standard was consistent at μg/ml and ng/ml levels, while that of norverapamil decreased with the amount injected. However, the decrease in response of norverapamil appeared to be unrelated to the presence of a pre-column or press-fit connector in the chromatographic system.

INTRODUCTION

Cold on-column injection using traditional narrow-bore (0.2–0.32 mm I.D.) fused-silica (FS) capillary columns with modern automatic injection systems requires the attachment of a pre-column consisting of short section of wide-bore (0.52 mm I.D.) FS tubing. In a recent article Grob and Schilling [1] reviewed the current literature on these uncoated pre-columns or retention gaps and listed three additional purposes which included: (1) analysis of dirty samples; (2) reconcentration of bands broadened in space; and (3) high-oven-temperature on-column injection. In 1986, Rohwer *et al.* [2] introduced the press-fit connector. The introduction of the press-fit type connectors has revolutionized the attachment of pre-columns to coated capillary columns [1,2]. This is especially true when the I.D. of the pre-column differs from the I.D. of the coated capillary column. Recent reports suggest that the press-fitt connector may soon replace the previously used butt connectors and fused connectors [1,3].

Verapamil (Fig. 1), a calcium channel blocking vasodilator used in the treatment of angina, arrhythmias and hypertension, undergoes significant first-pass hepatic metabolism [4]. The N-demethylated metabolite, norverapamil (Fig. 1), retains pharmacological activity and may reach levels in serum equal to or greater than the parent compound. Determination of verapamil in human serum has been accom-
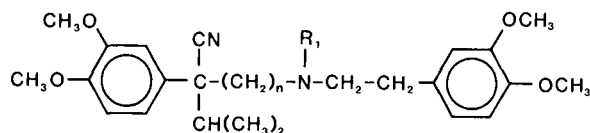
Fig. 1. Structures of verapamil, norverapamil and D-517.

plished using a variety of techniques including gas chromatography (GC) with nitro-
gen–phosphorus detection (NPD) [5–8]. The determination of norverapamil by GC
using NPD has been relatively unsuccessful. However, the reasons for this failure
have not been thoroughly investigated.

Capillary GC using cold-on column injection is the preferred GC methodology
in terms of reproducibility and linearity of response [9]. In addition, cold on-column
injection places the least stress on sensitive solutes of any injection mode. Sample
components are restricted exclusively to the environment of the column itself until
they reach the detection system [9]. However, as discussed above, automation of
on-column injection requires the addition of a pre-column when narrow-bore (0.2–
0.32 mm I.D.) columns are used. In this work, we investigated the effects of the
pre-column and the press-fit connectors on the analysis of verapamil and norverapa-
mil using D-517 {Fig. 1, α-isopropyl-α-[(N-methyl-N-homoveratryl)-β-aminoethyl]-
3,4-dimethoxyphenylacetonitrile} as an internal standard (IS). The difference in the
reactivity of verapamil and its active metabolite, norverapamil, toward the GC sys-
tem was also studied. The FS pre-column (0.52 mm I.D.) used in this work was
deactivated with OV-1701-vinyl (7% phenyl, 7% cyanopropyl, 86% methyl silicone
with 1% of these groups replaced by vinyl groups) using the method of Arrendale and
Martin [10]. To our knowledge, deactivated pre-columns of this type have not been
investigated previously.

EXPERIMENTAL

Materials
        Verapamil, norverapamil and D-517 (hydrochlorides, Fig. 1) for use as stan-
dards were kindly provided by Knoll (Whippany, NJ, U.S.A.). Fused-silica (FS) capil-
lary tubing (0.32–0.52 mm I.D.) was obtained from Polymicro (Phoenix, AZ,
U.S.A.); OV-1701-vinyl from Alltech (Arlington Heights, IL, U.S.A.); and isooctane
(2,2,4-trimethylpentane), distilled-in-glass grade, from Burdick and Jackson (Musk-
egon, MI, U.S.A.). Press-fitt connectors were obtained from Hewlett-Packard (Avon-
dale, PA, U.S.A.) and from Restek (Press-Tight™ Connectors, Bellefonte, PA,
U.S.A.). The wide-bore, thick-film, FS capillary column (Megabore™, DB-5, 30 m ×
0.52 mm I.D., 1.5 μm film thickness) was obtained from J & W (Rancho Cordova,
CA, U.S.A.); and the narrow-bore, thin-film, FS capillary column (HP-1, cross-link-
ed methyl silicone, 12 m × 0.2 mm I.D., 0.33 μm film thickness) from Hewlett-

Packard. All other FS capillary columns and the OV-1701-vinyl deactivated pre-columns used in this work were laboratory prepared as previously described [10].

Sample preparation

	Standards of D-517, verapamil and norverapamil (hydrochlorides) were prepared in methanol at 40–200 parts per million (μg/ml) and 40–200 parts per billion (ng/ml). The free bases for GC analysis were obtained by placing 2 ml of standard into clean 150 × 16 mm Pyrex screw-cap culture tubes with PTFE cap liners. The methanol was removed with a stream of dry nitrogen under mild heat (43°C), and 2 ml of double-distilled water, 100 μl of concentrated ammonium hydroxide (29.3% NH_3) and 5 ml of isooctane were added. The mixture was vortexed for 2 min, allowed to stand for 10 min, vortexed again and centrifuged for 5 min at 540 g. The organic layer (isooctane) was transferred to a 100 × 13 mm Pyrex screw-cap culture tube which had been tapered in a flame. The isooctane was evaporated with a stream of dry nitrogen under mild heat (43°C) and the standards were re-dissolved in 100 ml of isooctane. A portion of this solution was transferred to a 0.1-ml automatic injector vial for analysis by cold on-column injection capillary GC using the automatic sampler.

Gas chromatography

	Capillary GC was performed with a Hewlett-Packard 5890A gas chromatograph equipped with a dedicated on-column capillary inlet, a flame ionization detection (FID) system, a NPD system and a 7693A automatic sampler. The GC and automatic sampler were controlled with a Hewlett-Packard 3393A computing integrator. The FS capillary GC columns and their dimensions used in this work included the following: (1) SE-54, 30 m × 0.32 mm I.D., 0.1 μm film thickness; (2) SE-54, 20 m × 0.52 mm I.D., 0.33 μm film thickness; (3) SE-54, 30 m × 0.32 mm I.D., 0.2 μm film thickness; (4) HP-1 (cross-linked methyl silicone), 12 m × 0.2 mm I.D., 0.33 μm film thickness; (5) DB-5, 30 m × 0.52 mm I.D., 1.5 μm film thickness. The temperature programs varied depending on which column was used, but always began at 90°C with a 1 min hold followed by a temperature ramp to the final temperature. The final temperature also varied with the column used (see legends of individual figures for more details). All sample injections were 1 μl of isooctane using the Hewlett-Packard 7693 automatic sampler in the on-column injection mode. In the on-column mode, the automatic sampler uses a syringe equipped with a 26-gauge needle to allow insertion of the needle into 0.52 mm I.D. or larger columns. All attachment of pre-columns to the various FS capillary columns were done with the press-fit connectors. When using NPD, the detector attenuation was initially set at low sensitivity (attenuation = 5–8) and automatically changed to high sensitivity (attenuation = 0–1) just before elution of the standard components.

RESULTS AND DISCUSSION

	Evaluation of the press-fit connectors at high sample (μg/ml) levels was accomplished by analysis of our standard mixture (Fig. 2A) using a wide-bore FS capillary column, then removing a 1-m section of the column and re-connecting it as a pre-column using a press-fit connector, and again analyzing the standard mixture

Fig. 2. Cold on-column injection capillary GC separation of a standard mixture of (1) D-517 (IS), (2) verapamil and (3) norverapamil using a wide-bore FS SE-54 column. Conditions: column dimensions, 20 m × 0.52 mm I.D.; film thickness, 0.3 μm; temperature program, 90°C for 1 min, 90–280°C at 10°C/min; column flow, 60 cm/s helium; detection, FID; FID temperature, 330°C. (A) Column only, (B) column with 1 m removed and reconnected as a pre-column using a press-fit connector, and (C) column only with 0.01% TEA added to the sample.

(Fig. 2C). We also evaluated a basic chemical modifier, triethylamine (TEA, 0.01%), added to the solvent (isooctane), to change and/or improve the results (Fig. 2B) [8]. The precision (% relative standard deviation) of the response factors [K = (areas x/amount x)/(area IS/amount IS)] for verapamil and norverapamil were 0.2 and 1.7%, respectively, for the three analyses in Fig. 2 based on the IS, D-517. Thus, at these levels (μg/ml), the press-fit connector appears to have no effect upon the analysis of verapamil and norverapamil, nor does the addition of TEA.

We also found that the attachment of a 1-m pre-column of 0.52 mm I.D. FS tubing deactivated with OV-1701-vinyl [10] had no effect on the analysis at μg/ml levels. The effect of the length of the pre-column was studied for several lengths between 0.07 and 3.00 m. Analysis of our three components at μg/ml levels using a 0.07-m pre-column (Fig. 3A) and a 3.00-m pre-column (Fig. 3B) showed no effect from the difference in pre-column length.

The classic works on pre-columns or '"retention gaps" [1] showed that these initial column sections of very low retention efficiently eliminated band broadening in space. We also looked at the effects of the film thickness of the pre-columns (Fig. 4). The differences in chemical reactivity of verapamil and its active metabolite, norvera-pamil, are clearly illustrated by the chromatogram obtained using the column with a blank (undeactivated) FS pre-column (Fig. 4A). Although the verapamil peak is broadened, its response relative to the IS (D-517) was unaffected, while norverapamil was completely absorbed by the blank FS pre-column. As expected, a pre-column deactivated with OV-1701-vinyl (Fig. 4B) gave good results, but a pre-column with a 0.33-μm film of SE-54 resulted in peak broadening and splitting (Fig. 4C). A pre-column with higher retention power than the capillary column need not be very long to produce these peak distortions. A 0.07-m FS pre-column with a 0.33-μm film of
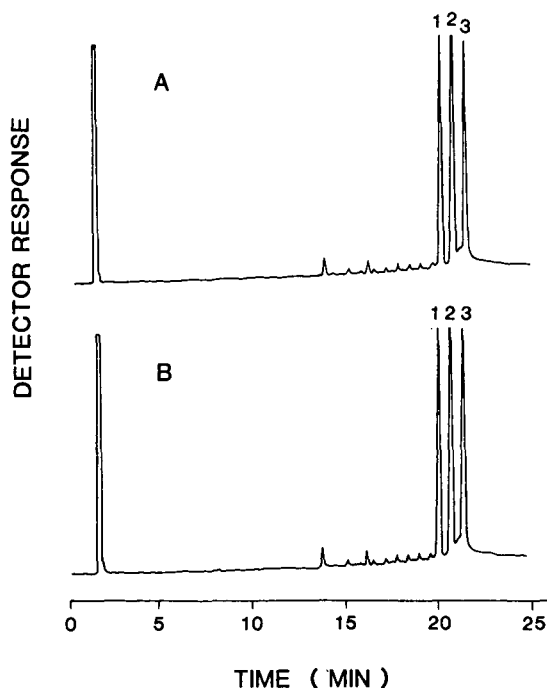
Fig. 3. Cold on-column injection capillary GC separation of a standard mixture of (1) D-517 (IS), (2) verapamil and (3) norverapamil using a FS SE-54 column. Conditions: column dimensions, 30 m × 0.32 mm I.D.; film thickness, 0.1 μm; temperature program, 90°C for 1 min, 90–280°C at 10°C/min; column flow 43 cm/s helium; detection, FID; FID temperature, 330°C. (A) Column with a deactivated (OV-1701-vinyl) 0.07 m × 0.52 mm I.D. FS pre-column, (B) column with a deactivated (OV-1701-vinyl) 3.00 m × 0.52 mm I.D. FS pre-column.
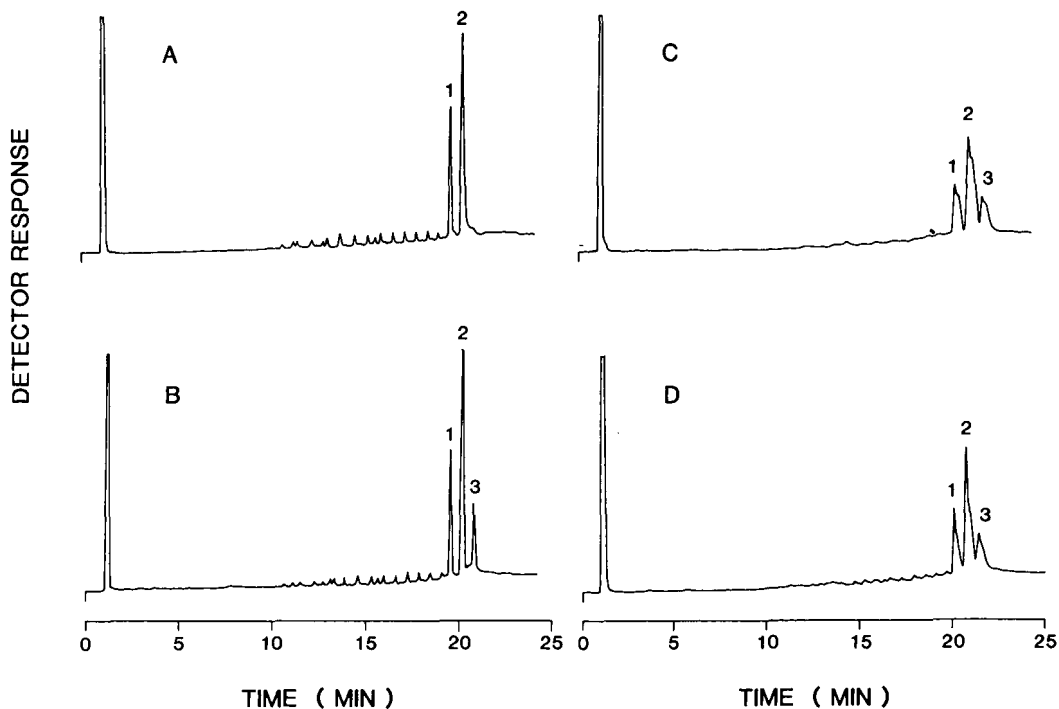
Fig. 4. Cold on-column injection capillary GC separations of a standard mixture of (1) D-517 (IS), (2) verapamil and (3) norverapamil using a 30 m × 0.32 mm I.D. FS SE-54 column with a 0.1 μm film thickness. Conditions: see Fig. 3. (A) Column with a 0.1 μm film thickness. Blank (undeactivated) 0.5 m × 0.52 mm I.D. FS pre-column, (B) column with a deactivated (OV-1701-vinyl) 0.5 m × 0.52 mm I.D. FS pre-column, (C) column with a 0.5 m × 0.52 mm I.D. FS pre-column which had a 0.33-μm film of SE-54 and (D) column with a 0.07 m × 0.52 mm I.D. FS pre-column which had a 0.33-μm film of SE-54.

SE-54 also results in peak splitting (Fig. 4D). The addition of TEA to the solvent (0.01%) did not affect the results.

One means of reducing the number of active sites in a column, or in this case a pre-column, is the repeated injection of large amounts of the species of interest. Separation of the standard mixture at μg/ml levels using a blank (undeactivated) pre-column produced the expected absorption of norverapamil (Fig. 5A). Injection of a concentrated solution of norverapamil (Fig. 5B) yielded a small, broad peak. Analysis of the standard mixture (Fig. 5C) showed that the activity of the pre-column was reduced as a peak for norverapamil was present although its height was less than expected. The second injection of the concentrated solution of norverapamil (Fig. 5D) yielded a much larger peak, but repeated injection of the standard mixture (Fig. 5E) showed little change. Injection of the μg/ml solution of norverapamil using a column with a 1-m deactivated (OV-1701-vinyl) pre-column (Fig. 5F) produced a large peak indicating that absorption of norverapamil even at the relatively high μg/ml levels was still occurring in the undeactivated pre-columns (Fig. 5B and D). The response (peak area) of verapamil in comparison to the IS (D-517) remained constant regardless of the pre-column used (Fig. 5).
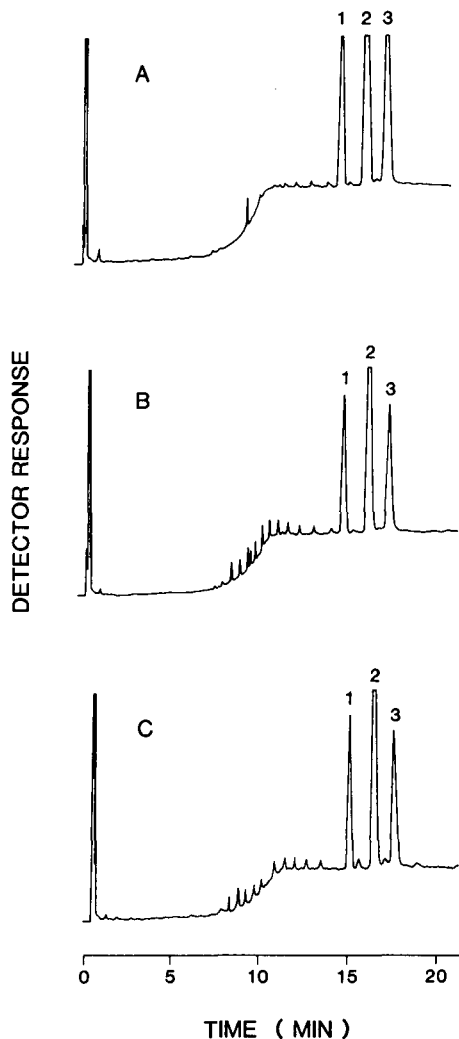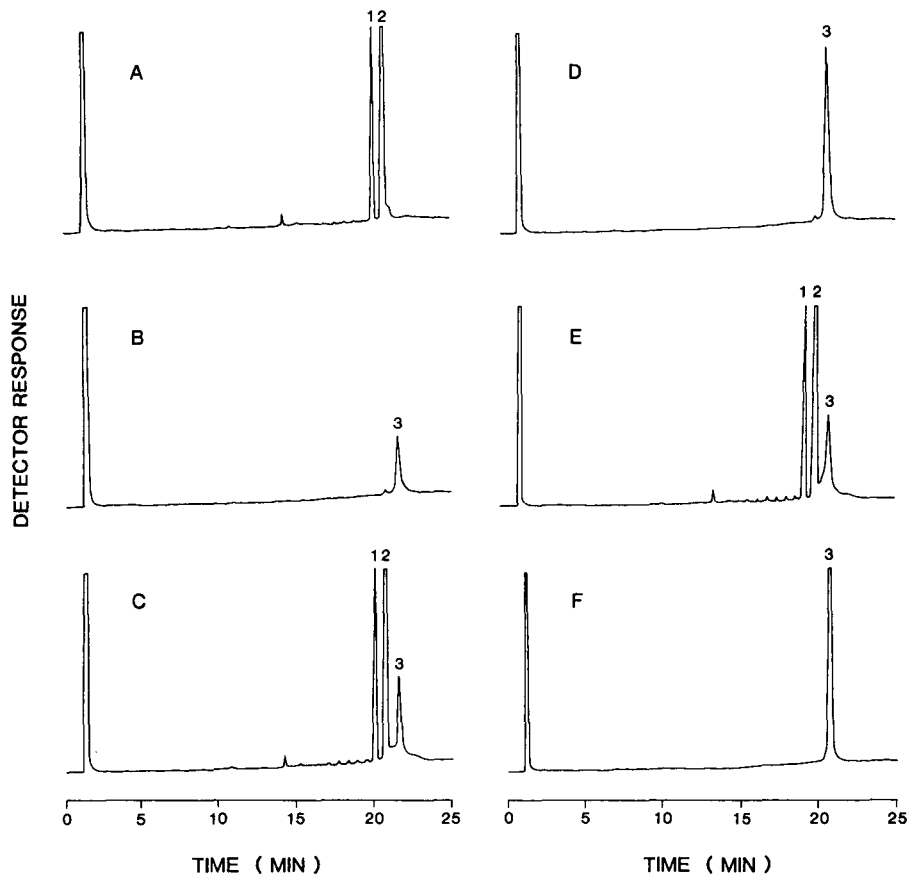
Fig. 5. Cold on-column injection capillary GC separations of (1) D-517 (IS), (2) verapamil and (3) norvera-
pamil using a FS SE-54 column. Conditions as in Fig. 3. (A) Analysis of all three components using a
column with a blank (undeactivated) 1 m × 0.52 mm I.D. FS pre-column, (B) analysis of a concentrated
sample of norverapamil again using the column and blank pre-column, (C) analysis of the three-compo-
nent mixture after injection of the concentrated norverapamil sample also using the column with blank
pre-column, (D) second separation of the concentrated norverapamil sample, (E) third analysis of the
three-component mixture and (F) separation of the concentrated verapamil sample using the column with
a deactivated (OV-1701-vinyl) 1 m × 0.52 mm I.D. FS pre-column.

    The effects of the deactivated (OV-1701-vinyl) pre-column and the press-fit
connector on the GC analysis at low levels (ng/ml)) were investigated using a wide-
bore, thick-film, FS capillary column with NPD (Fig. 6). First, our concentrated
mixture (µg/ml) was chromatographed using FID (Fig. 6A). Next, the pre-column
was removed and the ng/ml-level standard mixture was separated using the column
without a pre-column, using NPD (Fig. 6B). Finally, the deactivated pre-column was
re-connected and the sample (ng/ml) was chromatographed once again. Results were
the same with or without the pre-column (Fig. 6B and C) indicating that the deacti-
vated (OV-1701-vinyl) pre-column and the press-fit connector did not contribute to
peak absorption, tailing, or broadening, especially in the case of the more reactive
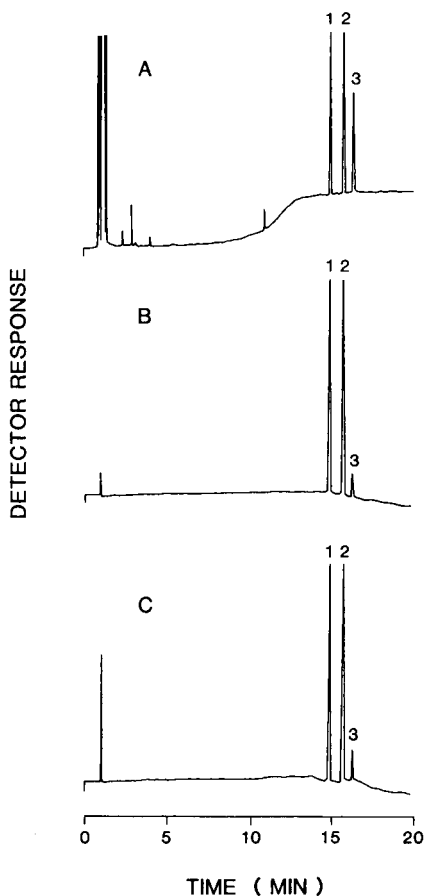
Fig. 6. Separation of (1) D-517 (IS), (2) verapamil and (3) norverapamil with a wide-bore, thick-film, FS DB-5 column at high (μg/ml) concentrations using FID and at low, therapeutic (ng/ml) levels using NPD. Conditions: column dimensions, 30 m × 0.52 mm I.D.; film thickness, 1.5 μm; column flow, 63 cm/s helium; temperature program, 90°C for 1 min, 90–310°C at 20°C/min; FID temperature, 330°C; NPD temperature 280°C. (A) Separation of concentrated (μg/ml) mixture using FID and a deactivated 0.75 m × 0.52 mm I.D. FS pre-column, (B) separation of the low-level (ng/ml) mixture using NPD and the column only (no pre-column) and (C) separation of the low-level (ng/ml) mixture using NPD and the column with a deactivated 0.75 m × 0.52 mm I.D. FS pre-column.

norverapamil. The response factors (K) for verapamil in relation to the IS (D-517) were constant even when those at high levels (μg/ml) (Fig. 6A) were compared to those obtained at low, therapeutic levels (ng/ml) (Fig. 6B and C) using two different detector systems (FID and NPD). However, the response factors (K) of norverapamil were 5 × less at ng/ml levels using NPD compared to those at μg/ml levels using FID. Some change in response was anticipated due to the difference in the detector systems, but the magnitude (5 ×) of that change was surprising. Although the peak shapes were unaffected (Fig. 6B and C), the huge unexplained difference in response could

result from absorption of the relatively reactive norverapamil at ng/ml levels even using a very-low-surface-activity, commercially produced column.

The repeated injection of large amounts of norverapamil to improve its response was studied at therapeutic levels (ng/ml) using a 30 m × 0.32 mm I.D. FS SE-54 column with a 0.25 μm film thickness and a 1-m deactivated pre-column (Fig. 7). Initial separation of the standard mixture (Fig. 7A) was almost identical to the results obtained after repeated injection of a concentrated solution of norverapamil (Fig. 7B).
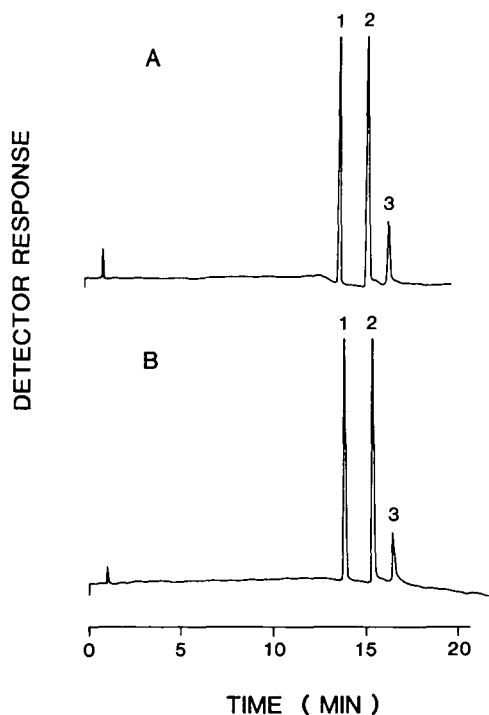
Fig. 7. Separation of (1) D-517 (IS), (2) verapamil and (3) norverapamil at therapeutic (ng/ml) levels using a FS SE-54 column. Conditions: column dimensions, 30 × 0.32 mm I.D.; film thickness, 0.25 μm; column flow, 45 cm/s helium; temperature program, 90°C for 1 min, 90–280°C at 20°C/min; detection, NPD; NPD temperature, 280°C; pre-column, 1 m × 0.52 mm I.D. deactivated (OV-1701-vinyl) FS. (A) Analysis of standard three-component mixture and (B) analysis of mixture after several injections of a concentrated sample of norverapamil.

The analysis of the three-component mixture at μg/ml and ng/ml levels using a 12 m × 0.2 mm I.D. FS methylsilicone (HP-1) capillary column with a 0.3-m deactivated pre-column is shown in Fig. 8. Peaks shapes are not as good at low levels (Fig. 8B and C), and the response of norverapamil decreases by over 50% after only 12 repeated analyses (Fig. 8C), while the response of verapamil remained constant.

Using a wide-bore FS SE-54 column, we again demonstrated that analysis of D-517 (IS), verapamil and the more reactive norverapamil at therapeutic (ng/ml) levels was unaffected by the attachment of a 1-m deactivated (OV-1701-vinyl) FS
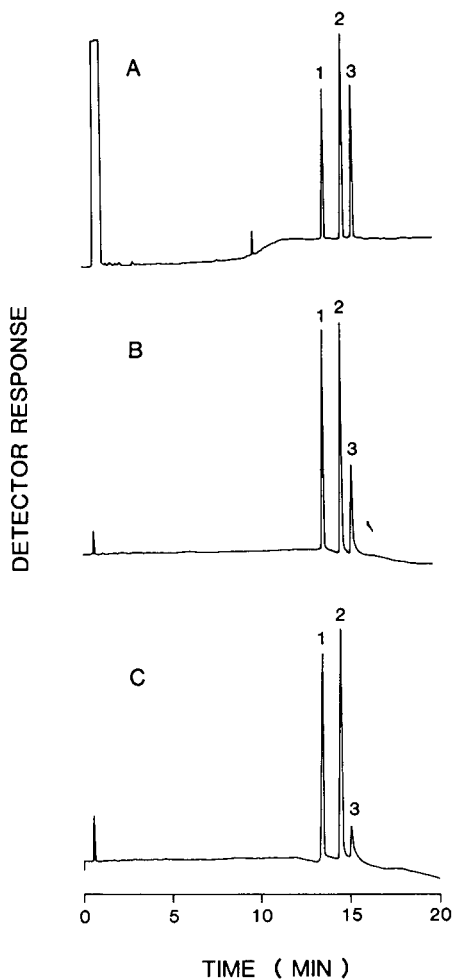
Fig. 8. Separation of (1) D-517 (IS), (2) verapamil and (3) norverapamil, using a narrow-bore, methyl silicone (HP-1) FS column with a 0.3 m × 0.52 mm I.D. deactivated (OV-1701-vinyl) FS pre-column, at high (µg/ml) levels using FID and at therapeutic (ng/ml) levels using NPD. Conditions: column dimensions, 12 m × 0.2 mm I.D.; film thickness, 0.33 µm; column flow, 30 cm/s helium; temperature program, 90°C for 1 min, 90–280°C at 20°C/min; FID temperature, 330°C; NPD temperature, 280°C. (A) Separation of concentrated (µg/ml) mixture using FID, (B) separation of the low-level (ng/ml) mixture using NPD and (C) separation of the low-level mixture after 12 repeated analyses.

pre-column using a press-fit connector (Fig. 9A and B). A blank undeactivated pre-column had little or no effect on D-517 and verapamil, but norverapamil was again completely absorbed (Fig. 9C). This was in sharp contrast to the appearance of the chromatogram showing the separation of a concentrated sample of norverapamil also using the blank undeactivated pre-column (Fig. 9D). The well-defined, symmetrical peak at higher ng/ml levels belies the complete absorption of norverapamil at therapeutic concentrations.
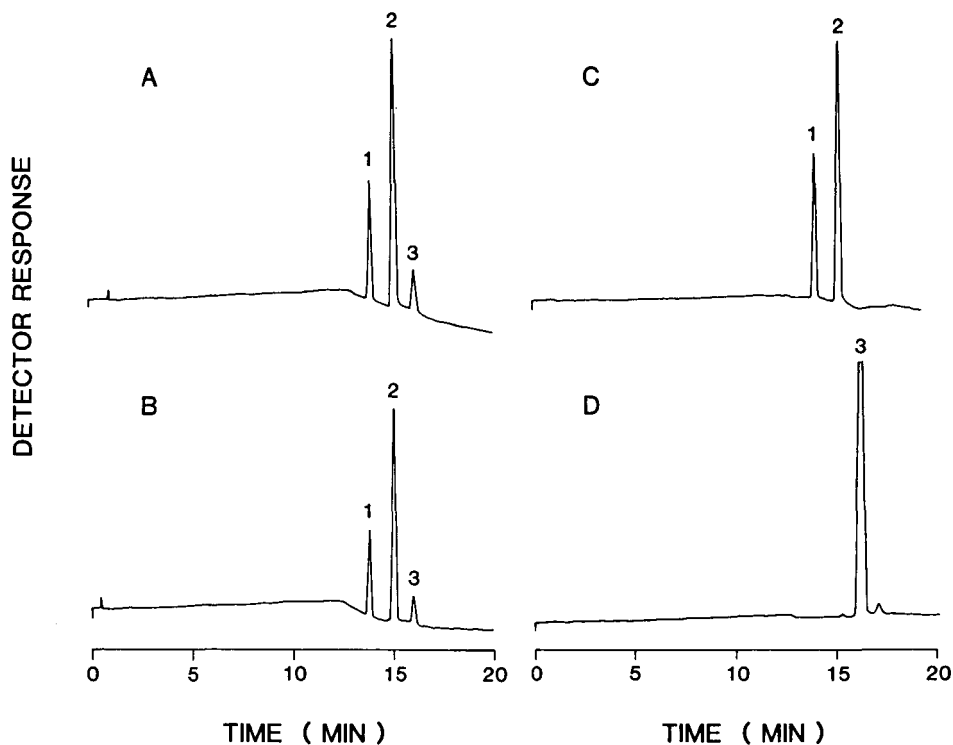
Fig. 9. Separation of (1) D-517 (IS), (2) verapamil and (3) norverapamil using a wide-bore FS SE-54 column. Conditions: column dimensions, 20 m × 0.52 mm I.D.; film thickness, 0.25 μm; column flow, 66 cm/s helium; temperature program, 90°C for 1 min, 90–280°C at 20°C/min; detection, NPD; NPD temperature, 280°C. (A) Column only, (B) column with a 1 m × 0.52 mm I.D. deactivated FS pre-column; (C) column with a 1 m × 0.52 mm I.D. blank pre-column and (D) a concentrated sample of norverapamil separated on the column with a blank pre-column.

CONCLUSIONS

The relatively new press-fit connectors are an excellent means of attaching pre-columns to coated capillary columns. They did not significantly increase the activity of our capillary columns even at ng/ml levels. Their insertion into columns had no detectable effects even on the analysis of the more reactive norverapamil. Deactivation with OV-1701-vinyl was an acceptable means of preparing FS tubing for pre-columns as their use had no effect upon the analysis of D-517, verapamil and norverapamil at therapeutic (ng/ml) concentrations. The addition of TEA to the samples or the repeated injection of large amounts of norverapamil were ineffective in the elimination of surface activity of a column and/or pre-column. The active metabolite norverapamil exhibited much higher reactivity toward active sites in chromatographic systems than verpamil, and detector response for norverapamil increased as the amount injected increased, while the response of verapamil remained constant. In addition, repeated analyses of norverapamil at ng/ml levels yielded a decrease in response over time using both commercially and laboratory-prepared columns with

and without deactivated pre-columns. Thus, conditions which are acceptable for the analysis of verapamil may be unacceptable for the determination of norverapamil. These data indicate that the reliable analysis of norverapamil by GC requires that it first be converted to a more stable derivative. However, the attachment of a deactivated pre-column had no effect on the analysis of verapamil or norverapamil.

REFERENCES

1 K. Grob and B. Schilling, *J. Chromatogr.*, 391 (1987) 3.
2 E. R. Rohwer, V. Pretorius and P. J. Apps, *J. High Resolut. Chromatogr. Chromatogr. Commun.*, 9 (1986) 295.
3 B. Schilling, K. Grob, P. Pickler, R. Dubs and B. Breckbuhler, *J. Chromatogr.*, 435 (1988) 204.
4 M. Eichelbaum, A. Somogyi, G. E. von Unruh and H. J. Dengler, *Eur. J. Clin. Pharmacol.*, 19 (1981) 13.
5 D. R. Abernathy, E. L. Todd and J. R. Mitchell, *Pharmacology*, 29 (1984) 264.
6 H. G. Hege, *Arzneim. Forsch./Drug Res.*, 29 (1979) 1681.
7 J. Vasiliades, K. Wilkerson, D. Ellul, M. Anticoli and A. P. Rocchini, *Clin. Chem.*, 28 (1982) 638.
8 D. J. Hoffman and J. Higgins, *J. Chromatogr.*, 374 (1986) 170.
9 K. Grob, *On-column Injection in Capillary Gas Chromatography*, Hüthig, New York, 1987.
10 R. F. Arrendale and R. M. Martin, *J. High Resolut. Chromatogr. Chromatogr. Commun.*, 11 (1988) 157.

Tracer pulse chromatographic method for the determination of nitrogen BET isotherms and surface areas

HENGCHANG SONG, JOSEPH R. STRUBINGER and JON F. PARCHER*

Department of Chemistry, University of Mississippi, University, MS 38677 (U.S.A.)

(Received March 28th, 1990)

ABSTRACT

A new method for the determination of surface areas and nitrogen isotherms at 77 K has been developed. The method utilizes mass spectrometric tracer pulse chromatography with $^{15}N_2$ as the isotopic probe. The technique was used to measure the BET surface area of silica, chemically bonded silica, graphitized carbon black, glass beads and diatomaceous earth chromatographic adsorbents. The results were compared with the surface areas measured by volumetric methods for 5-μm silica and 5-μm C_{18}-bonded silica. The agreement was within the experimental error of the two experimental techniques.

In addition, the total surface areas of three packed high-performance liquid chromatography columns were determined *in situ* without unpacking or disturbing the column in any way. It was shown that the measured total surface area agreed within 10% with the specific surface area times the packing weight for a column packed with 5-μm silica particles.

The method is fast, accurate and simple. The primary experimental data are retention times, rather than peak areas, and the method is applicable to any vapor or inert gas adsorbate. The major disadvantages are the requirements for a mass-selective detector and labeled isotopic solute probes.

INTRODUCTION

In 1958, Nelsen and Eggertsen [1] proposed a continuous-flow, thermal desorption chromatographic method for the determination of BET isotherms and surface areas from nitrogen adsorption at 77 K. This method was improved and developed to provide the basis for commercial instrumentation commonly used today. In addition to this thermal desorption method, at least three other chromatographic procedures have been used for the measurement of solid surface areas. Frontal, tracer pulse and elution chromatography have all been used to determine the adsorption isotherms of inert gases or other probe solutes on solid surfaces. The surface areas could be calculated from the isotherm by fitting the data to an adsorption model, such as that of Brunauer, Emmett and Teller [2].

Two other chromatographic techniques for the determination of surface areas are based on the "Point B" method [3] for the estimation of the monolayer capacity of an adsorbent. Kuge and Yoshikawa [4] developed an elution method for measuring the monolayer capacity of type II and IV adsorbents. The method is based on the formation of a shoulder or other anomaly in the shape of the elution peak when the sample size of the eluted probe solute is sufficient to cover the adsorbent surface with a monolayer of the solute. A second, rather unique type of single-point method was

developed by Serpinet [5]. In this method several columns with different liquid loadings were required, and the monolayer capacity was determined from the breakpoint in a plot of the retention volume of a probe solute versus the reciprocal of the liquid loading. The plots showed two linear regions corresponding to adsorption on the liquid-modified adsorbent and partition into the liquid coated on the adsorbent. The breakpoint in the plot indicated the transition from one mechanism to the other which presumably occurred at the point of complete surface coverage. This method has the advantage of being independent of any adsorption model; however, it also requires the preparation of multiple columns with a range of liquid loadings.

All of these chromatographic methods for the determination of isotherms and surface areas have been extensively reviewed in several monographs [6–8]. The commonly cited advantages of chromatographic methods compared to the classical gravimetric and volumetric methods are speed, simplicity and low maintenance requirements. The latter advantage arises because the methods do not require high vacuum, and commercial gas chromatography (GC) instrumentation is adequate for all of the chromatographic techniques.

More recently, mass spectrometric tracer pulse chromatography [9] has been used to determine the adsorption isotherms of organic vapors on chromatographic adsorbents [10,11]. The same technique has also been used to measure binary isotherms [12,13] to study the interactions between adsorbates in the condensed, two-dimensional adsorbed phase.

This technique, however, has not been used to study the adsorption of inert gases at low temperatures, although the method is theoretically applicable for such systems. The possible advantages of the tracer pulse procedures over the other chromatographic methods for BET surface area measurements would be that (i) the primary measured data are retention times rather than peak areas, (ii) the system remains isothermal rather than alternating between adsorption at 77 K and desorption at 300 K, (iii) the system is isocratic so there is no "sorption effect", (iv) only one packed column is required and (v) a full isotherm can be determined rather than a single point. The thermal desorption method of Nelsen and Eggertsen [1] is popular, but suffers from the need for frequent detector calibration and sample blanks required to correct for the flow-rate and baseline disturbances caused by the thermal excursions.

The primary objectives of the present work were to investigate the application of tracer pulse chromatography to the determination of nitrogen isotherms at 77 K and to determine the feasibility and accuracy of the method for the measurement of surface areas and pore-size distributions.

EXPERIMENTAL

Instrumentation
A schematic diagram of the instrument is shown in Fig. 1. The GC–mass spectrometric (MS) system was a Hewlett-Packard 5995, and the only major modification of the instrument was the incorporation of very precise flow regulators and pressure sensors. The flow controllers were Matheson Model 8202 regulators with Model 8102 flow sensors (0–50 ml STP[a]/min). The pressure transducers were Setra

_____
[a] STP = Standard temperature and pressure.
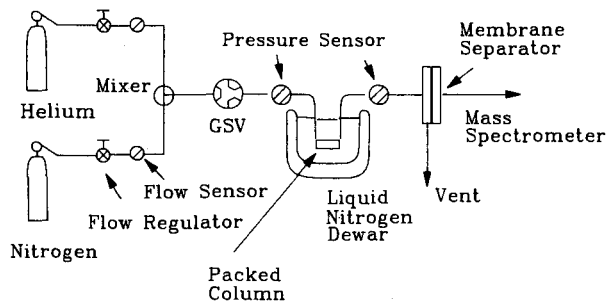
Fig. 1. Schematic diagram of the instrumentation. GSV = Gas-sampling valve.

Model 204 (0–100 p.s.i.g.). The flow regulators were controlled from a microcomputer via a digital-to-analog converter with an output of 0–5 V d.c. The pressure transducers were monitored through an analog-to-digital converter with an input range of 0–5 V d.c. Precise control of the mixed flow of gases was a critical factor in the precision of the apparatus. The probe solutes were injected with a pneumatically controlled gas-sampling valve which was actuated via the RS-232 port of the computer.

Columns

The columns were packed in metal tubing of various dimensions determined by the specific surface area of the adsorbents. The materials studied included silica, chemically bonded silica, graphitized carbon black, glass beads and diatomaceous earth adsorbents. A complete description of the chromatographic columns is given in Table I.

In addition, three packed HPLC columns were used for *in situ* determination of the total surface area of the stationary phase. The commercial columns were Models 2060250 (5-μm silica) and 2060210 (5-μm C_{18}-bonded silica) (SGE), 150 mm × 2 mm I.D. The weight of packing material in these columns was not determined, although the weights were probably in the range 0.4–0.6 g. A third column was packed in the laboratory with 0.205 g of C_{18}-bonded silica (SGE) in a stainless-steel tube 100 mm × 2 mm I.D.

TABLE I

DESCRIPTION OF CHROMATOGRAPHIC COLUMNS AND ADSORBENTS

Adsorbent material	Particle size (μm)	Column dimensions (mm)	Packing weight (mg)
Carbopack A	180–250	100 × 3	150.0
Carbopack B	180–250	60 × 3	44.1
Carbopack C	150–180	400 × 3	831.3
Silica	5	50 × 3	49.1
C_{18}-Bonded silica	5	50 × 3	75.4
Diol-bonded silica	5	50 × 3	40.3
Cyano-bonded silica	5	50 × 3	59.6
Glass beads	180–250	400 × 6.4	9320
Chromosorb P	180–250	300 × 3	304.2

All of the columns were conditioned prior to the isotherm measurements. The conditioning strategy varied with the type of adsorbent. In general, the procedure involved temperature programming from 30 to 100–150°C with the temperature maintained at the upper temperature until no effluent was monitored by the mass spectrometer. The use of MS in the scan mode to sense the type and quantity of outgassing effluent allowed the use of variable conditioning procedures for each type and batch of adsorbent.

Procedure

The flow-rates and mixing ratios of He and N_2 were set and allowed to stabilize for 5–10 min. A mixture of Ne, Ar and $^{15}N_2$ was injected via the gas-sampling valve at the same time the MS system was activated. The MS system was operated in a "selected ion monitor" mode to detect m/e values of 20, 30 and 40 and ignore the N_2 background at m/e 28. The nitrogen probe solute was 98.8% $^{15}N_2$ (MSD Isotopes, Montreal, Canada).

The use of labeled nitrogen introduces the possibility of an "isotope effect" on the retention of $^{15}N_2$ compared with $^{14}N_2$. In an attempt to determine the magnitude of this effect, a sample containing natural and labeled nitrogen along with neon was injected into a silica column at 77 K with pure helium as the carrier gas. The experiment showed that there was an isotope effect of about 1.05. That is, the ratio of the retention times of the unlabeled and labeled solute was approximately 1.05. This correction factor was used to adjust all of the reported data.

Calculations

The amount of nitrogen adsorbed, Γ_j (μmol/g), was calculated from the retention times of neon, t_0, and the isotopic nitrogen probe, $t_{R,i}$ (min), by the relation:

$$\Gamma_j = (t_{R,i} - t_0)\left(\frac{P_r F_c Y_j}{RT_r W_s}\right) \tag{1}$$

where F_c is the flow-rate, P_r and T_r are the pressure and temperature for which the flow regulators were calibrated, *i.e.*, ambient conditions, Y_j is the mole fraction of nitrogen in the carrier gas, W_s is the weight of the solid adsorbent in the column and R is the molar gas constant.

The surface areas of the adsorbents were determined from the calculated monolayer capacity, V_m, obtained from linear regression of the BET equation in the form:

$$\frac{P_j}{\Gamma_j(P_j^0 - P_j)} = \left(\frac{1}{CV_m}\right) + \frac{C-1}{CV_m}\left(\frac{P_j}{P_j^0}\right) \tag{2}$$

where P_j and P_j^0 are the pressure of nitrogen in the column and the vapor pressure of liquid nitrogen at the column temperature, and C is an empirical parameter which is related to the heat of adsorption and the shape of the isotherm in the region of monolayer formation.

RESULTS AND DISCUSSION

One of the major problems in the determination of adsorption isotherms by a chromatographic or any other method is the accurate determination of the void volume of the column or apparatus. This measurement is particularly critical with chromatographic methods for gas–solid adsorption at very low temperatures and/or high pressures. The commonly used probes, such as air or methane, were not useful because they were significantly adsorbed under the conditions used in this study. The "hypothetical perfect gas" perturbation method of Kobayashi and co-workers [14,15], which is commonly used for chromatographic isotherm measurements, was also inapplicable in the present study because of the significant retention of argon and the higher inert gases. However, it was found that, although the retention time of argon and the other inert gases varied with the amount of N_2 adsorbed, the retention time of neon was independent of surface coverage with nitrogen. This effect is shown in Fig. 2. The constant retention times of neon indicated that neon, like helium, was not adsorbed on the solid and could serve as an accurate probe for the determination of t_0.
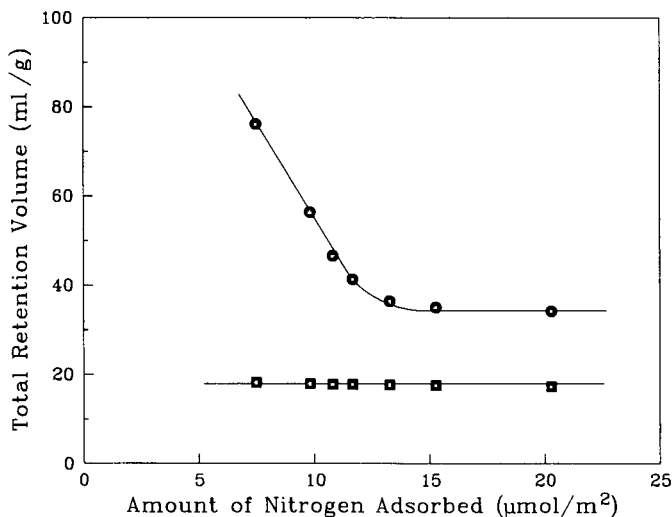
Fig. 2. Retention times of eluted samples of argon and neon with different amounts of nitrogen adsorbed on the surface of Carbopack C. ● = Argon; ◻ = neon.

Another potential problem in the proposed experiment is the possible adsorption of nitrogen on the walls of the column and connecting tubing. This effect would be particularly significant for low surface area adsorbents. To check the magnitude of this effect, the solutes were injected into an empty column at 77 K at several flow-rates. It was observed that the three solutes, Ne, Ar and $^{15}N_2$ all eluted concurrently. Thus the amount of nitrogen adsorbed in the instrumental apparatus was less than the lowest limit for the experimental measurement.

The tracer pulse experimental procedure was used to measure the isotherm of nitrogen on 5-μm silica gel at 77 K. The full isotherm was obtained by using three
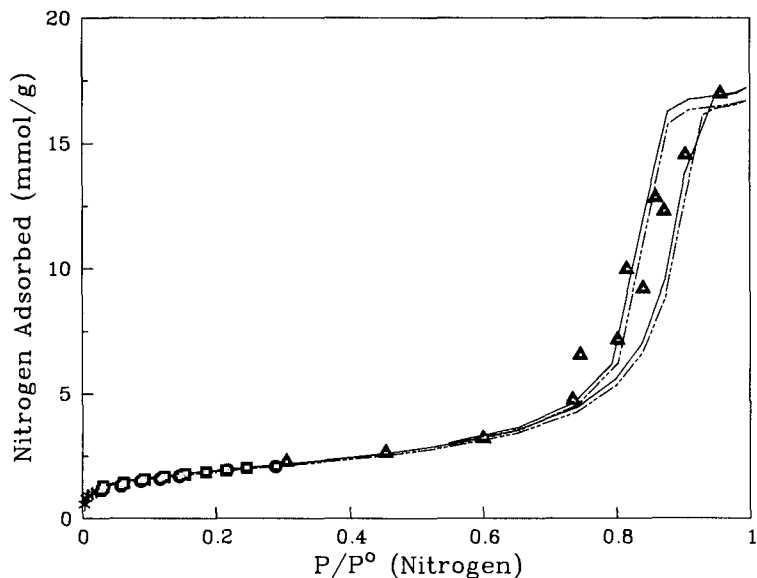
Fig. 3. Experimentally measured adsorption isotherms of nitrogen on 5-μm silica. $*$ = 2% N_2 in He; $\mathbf{O}$, $\square$ = 20% N_2 (duplicate experiments); $\blacktriangle$ = 100% N_2; $-\cdot-$ = volumetric data (duplicate experiments) [16].

different compositions of the He + N_2 carrier gases. Tanks with compositions of 2, 20 and 100% N_2 were used to cover the low, intermediate and high ranges of P/P^0 required for the full isotherm. Within each range, smaller incremental changes in composition were controlled by variation of the ratio of flows through the two flow controllers. The range required for the BET analysis, 0.05 $\leqslant P/P^0 \leqslant$ 0.35, could be studied with only a single tank containing 20% N_2. The measured isotherm is shown in Fig. 3. The lines in the figure show the duplicate isotherms measured by the classical, volumetric method [16]. The agreement with the volumetric data is excellent at relative pressures of less than 0.7. Above this pressure, the mesoporous-silica adsorbent shows a hysteresis loop which the chromatographic method could not follow accurately because of the significant pressure drop across the column. Fig. 4 shows the BET plot for the measured isotherm in the applicable range of P/P^0. In both cases, the agreement between the volumetric (static) and chromatographic data were within the experimental uncertainty of either method. The BET surface areas were determined for all of the absorbents listed in Table I. The results of this analysis are given in Table II.

One of the potential applications of this technique is the determination of the total surface areas of packed GC, high-performance liquid chromatography (HPLC) or supercritical fluid chromatography columns *in situ* without disturbing the column packing in any way. This application would be significant for high-efficiency columns packed with very small particles, *i.e.*, < 10 μm, because of the difficulty of packing and weighing these particles. The pressure drop across the columns was large due to the very small particle size. However, the viscosity of the helium and nitrogen mixtures was also diminished at 77 K, so a reasonable flow-rate could be obtained without an excessive pressure drop across the column. Typically with commercial packed (5-μm)
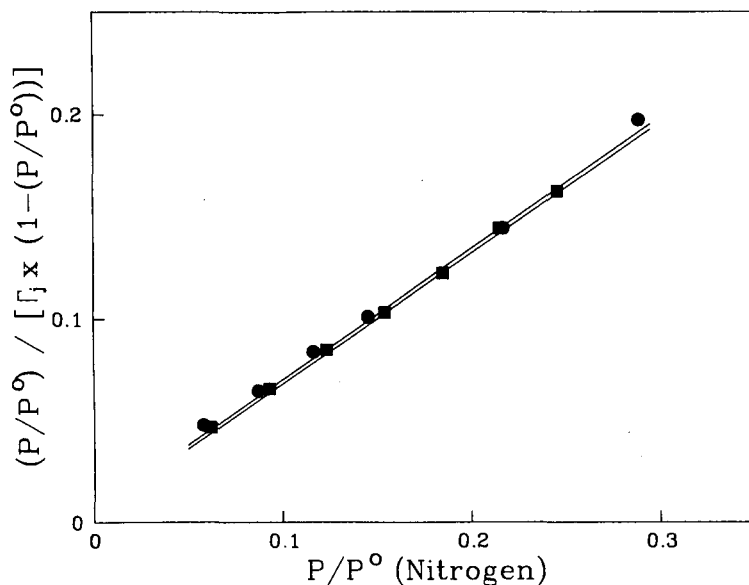
Fig. 4. BET plots for 5-μm silica. ●, ■ = this work (duplicate experiments); ——— = volumetric data [16].

columns a head pressure of 30 p.s.i. gave a flow-rate in the order of 10 ml/min at 77 K. The results for the total surface areas in the two commercial columns were 34 m^2 and 42 m^2 for the C_{18} and silica columns, respectively.

The surface area of the stationary phase in the laboratory-packed column was measured *in situ* at several flow-rates to determine the influence of the column pressure drop on the measured surface areas. The specific surface area was also measured for the packing material alone. The results of both experiments are given in Table III.

TABLE II

LINEAR REGRESSION DATA FOR VARIOUS CHROMATOGRAPHIC ADSORBENTS

Adsorbent	Linear regression results		Surface areas (m^2/g)	
	V_m (μmol/g)	C	This work	Volumetric
Carbopack A	124	280	12.0	15 [17]
Carbopack B	834	150	80.4	100 [17]
Carbopack C	94.8	341	9.1	9 [17]
Silica	1530	108	147.8	155.4 [16]
				150.9 [16]
C_{18}-Bonded silica	974	26	93.9	89.7 [16]
				97.6 [16]
Diol-bonded silica	2500	56	241.0	
Cyano-bonded silica	1158	40	111.6	
Glass beads	0.90	29	0.09	0.01–0.1
Chromosorb P	56.1	27	5.4	

TABLE III

COMPARISON OF SPECIFIC AND TOTAL SURFACE AREAS FOR A C_{18}-BONDED SILICA HPLC COLUMN

(Specific surface area) × (packing weight) = (93.9 m^2/g) (0.205 g) = 19.2 m^2

Carrier gas flow-rate (ml/min)	Inlet pressure (p.s.i.)	Compressibility correction factor, j	Measured total surface area (m^2)
3.5	20.6	0.81	22.4
5.5	24.0	0.74	22.6
10.5	30.3	0.62	21.2
20.4	40.3	0.49	20.6

The two measurements agreed within about 10%. However, there appears to be a slight, but systematic, dependence of the calculated isotherms and surface areas on the flow-rate and/or the pressure drop across the column. The *in situ* isotherm method for packed HPLC columns can only provide an average of the amount of nitrogen adsorbed because of the significant difference between the partial pressure of N_2, and consequently the amount of N_2 adsorbed, at the inlet and outlet of the column. These pressures may differ by a factor 2–3 (Table II). This effect would be most deleterious in the regions of the isotherm where $(\partial \Gamma / \partial P)$ is large, *i.e.*, at very low pressures. In the relative pressure range of 0.05–0.35, which is the range where eqn. 2 is valid, the effect of pressure drop is not as critical. The use of an average pressure, *e.g.*, P_{out}/j, produced linear BET plots and acceptable surface areas. Fig. 5 shows the BET data for the experiments described in Table III along with the results from the volumetric
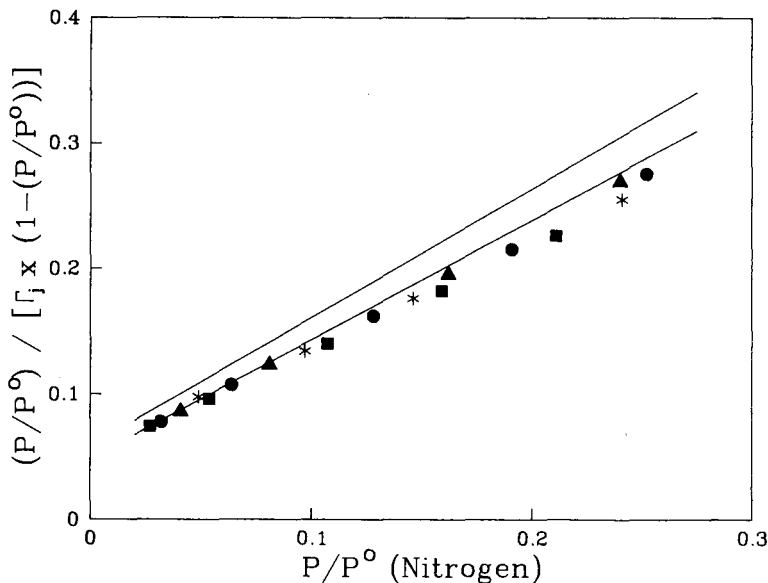
Fig. 5. BET plots for C_{18}-bonded silica. ✳, ●, ▲, ■ = this work (each different symbol in the figure corresponds to a row in Table II); — ·— = volumetric data [16].

measurements [16]. The variations caused by the significant pressure drop in the *in situ* experiments are less than the repeatability of the volumetric procedure.

The tracer pulse method for the determination of BET isotherms requires a mass-specific detector to measure the retention time of an isotopically labeled tracer of the adsorbable component of the gas. The requirements for the MS system are, however, minimal, and the simplest instruments, such as the mass-specific detector or ion trap detector are adequate for the isotherm measurements described above. The required isotopes can be expensive or difficult to prepare, although this is not the case for the $^{15}N_2$ probes used in this study. The method suffers from all of the disadvantages inherent in the BET model [3]; however, the experimental technique is not limited to N_2 as the adsorbate. Other solutes and perhaps other adsorption models could be used for t. e surface areas calculations.

The flow-through systems used for all chromatographic techniques have the advantage that equilibrium is established rapidly, but the disadvantage is that the inlet of the column must be at a higher pressure than the outlet. This means that the measured isotherm data are always some type of "average" although this effect does not appear to significantly influence the surface-area measurements as shown in Table III and Fig. 5. However, this effect can be minimized by the use of low flow-rates, short columns, or coarse particles.

One disadvantage of the tracer pulse method, as well as any other chromatographic method, is that it is inherently a "batch process". This disadvantage is partially off-set by the slightly reduced experiment time per sample. The primary experimental datum is the retention time of the $^{15}N_2$ probe. This retention time was typically in the range 2–20 min, and the equilibration time for a gas-phase composition change was 5–10 minutes. A complete BET plot requires at least 5 data points. The estimated time for a complete BET surface-area measurement by this technique would be 0.5–2 h. This time can be reduced by minimizing the retention time of the probe solute. Volumetric measurements require 10–20 h for a full (50 point) isotherm, or about 1–2 h for a 5-point surface-area measurement.

The method is easily automated with a computer-controlled GC–MS system and gas-sampling valve. The only actions required are periodic injections and adjustments of the flow-rates.

CONCLUSIONS

Mass spectrometric tracer pulse chromatography can be used to measure the adsorption isotherms of nitrogen on solid adsorbents. If the measurements are carried out at 77 K, the adsorption data in the range $0.05 \leqslant P/P^0 \leqslant 0.35$ can be fit to the BET model to determine the surface area of solid adsorbents. The method has been applied to a variety of different adsorbent types with surface areas from 0.09 to 240 m^2/g.

The method is comparable in accuracy and reproducibility with the static volumetric methods. Commercially available, simple GC–MS systems are adequate for the instrumentation, and the MS can serve to monitor the outgassing effluent to minimize the preparation time and to ensure that the outgassing process has been completed.

The method is fast, accurate, and simple. The major disadvantages are the need for a GC–MS system and isotopically labeled solutes. The method is not limited to

a particular adsorbate or temperature, and the adsorption isotherms of two or more adsorbates can be measured simultaneously.

The variation of the retention volume of one probe, such as argon, can also be determined as a function of the surface coverage by another adsorbate, such as nitrogen. This phenomenon is illustrated in Fig. 1. If this type of experiment can be used to determine the monolayer capacity of an adsorbent, it would lead to a surface area measurement technique that, like Serpinet's [5] method, would not require a theoretical model for interpretation of the data.

ACKNOWLEDGEMENTS

REFERENCES

1 F. M. Nelsen and F. T. Eggertsen, *Anal. Chem.*, 30 (1958) 1387.
2 S. Brunauer, P. H. Emmett and E. Teller, *J. Am. Chem. Soc.*, 60 (1938) 309.
3 S. J. Gregg and K. S. W. Sing, *Adsorption, Surface Area and Porosity*, Academic Press, New York, 1982, Ch. 2.
4 Y. Kuge and Y. Yoshikawa, *Bull. Chem. Soc. Jpn.*, 38 (1965) 948.
5 J. Serpinet, *J. Chromatogr.*, 119 (1976) 483.
6 A. V. Kiselev and Y. I. Yaskin, *Gas-Adsorption Chromatography*, Plenum, New York, 1969, Ch. IV.
7 J. R. Conder and C. L. Young, *Physicochemical Measurement by Gas Chromatography*, Wiley-Interscience, New York, 1979, Ch. 10.
8 R. J. Laub and R. L. Pecsok, *Physicochemical Applications of Gas Chromatography*, Wiley-Interscience, New York, 1978, Ch. 7.
9 J. F. Parcher and M. I. Selim, *Anal. Chem.*, 51 (1979) 2154.
10 P. J. Lin and J. F. Parcher, *J. Colloid Interface Sci.*, 91 (1983) 76.
11 K. J. Hyver and J. F. Parcher, *Anal. Chem.*, 56 (1984) 274.
12 J. F. Parcher and P. J. Lin, *Anal. Chem.*, 53 (1981) 1889.
13 J. F. Parcher and K. J. Hyver, *J. Chromatogr.*, 302 (1984) 195.
14 S. Masukawa and R. Kobayashi, *J. Gas Chromatogr.*, 6 (1968) 257.
15 Y. Hori and R. Kobayashi, *J. Chem. Phys.*, 54 (1971) 1226.
16 Micromeritics, Inc., Atlanta, GA, personal communication, 1989.
17 *Bulletin 738A*, Supelco, Inc., Bellefonte, PA, 1976.

Hydrogen bonding

XV. A new characterisation of the McReynolds 77-stationary phase set

MICHAEL H. ABRAHAM* and GARY S. WHITING

Department of Chemistry, University College London, 20 Gordon Street, London WC1H 0AJ (U.K.)

RUTH M. DOHERTY

Naval Surface Warfare Center, White Oak Laboratory, Silver Spring, MD 20910 (U.S.A.)

and

WENDEL J. SHUELY

U.S. Army Chemical Research, Development and Engineering Center, Aberdeen Proving Ground, MD 21010 (U.S.A.)

ABSTRACT

The following equation has been applied to all the phases in the McReynolds 77-stationary phase set.

$$\log V_G^0 = c + rR_2 + s\pi_2^* + a\alpha_2^H + b\beta_2^H + l \log L^{16}$$

In this equation, V_G^0 is the specific retention volume for a series of solutes on a given stationary phase, and the explanatory variables are R_2 a modified solute molar refraction, π_2^* the solute dipolarity, α_2^H the solute hydrogen-bond acidity, β_2^H the solute hydrogen-bond basicity, and $\log L^{16}$ where L^{16} is the solute Ostwald absorption coefficient on hexadecane at 25°C. The constants in the equation are obtained by multiple linear regression analysis, using about 150 data points in each regression, and values of r, s, a, b and l are regarded as characteristic constants of the phases that serve to classify the 77-phase set. It is shown that the classification of the phases into clusters is in accord with chemical principles, and is in excellent agreement with previous work using hierarchical clustering, minimum spanning tree techniques, and pattern cognition methods. The above equation allows the factors that lead to gas–liquid chromatographic separations to be identified, and provides quantitative information on the various solute–solvent interactions that give rise to these factors.

INTRODUCTION

The largest sets of gas chromatographic retention data are those of McReynolds, who determined retention volumes (V_G^0) and retention indices (I) of 376 solutes on 77 phases at two temperatures [1], and retention indices of 10 solutes on 226 phases at 120°C [2]. Numerous workers have classified both the 77-phase set and the 226-phase set by various methods. McReynolds himself [2] assigned a single polarity index to the 226 stationary phases, using the sum of the ΔI values for benzene, butanol,

2-pentanone, nitropropane and pyridine. Later workers refined this method [3] and also calculated a polarity index from the Gibbs energy of solvation of the methylene increment, $\Delta G_s^0(CH_2)$, on a given stationary phase [4]. Other workers assigned a number of characteristic parameters to phases. Thus Figgins *et al.* [5] derived ΔG_s^0 values for six functional groups on 75 of the 226-phase set, and Fellous *et al.* [6] assigned a polarity index (ρ^*) to the same six functional groups on 72 of the 226-phase set.

Various sophisticated methods have been used to classify the McReynolds phases into groups. They include nearest neighbour techniques [7], information theory [8], numerical taxonomy [8,9], principal components analysis [10], pattern cognition methods [11,12] and factor analysis [13]. All these methods reduce the 226-phase set or the 77-phase set to a smaller number of clusters each of which represents a collection of similar phases. This is a very useful and helpful outcome, but, in addition, several of these methods lead to the estimation of the number of factors that influence chromatographic retention data. Wold and Andersson [10] suggested three main factors, (1) polarity, (2) a factor difficult to identify and (3) a factor that was due to hydrogen-bonding of the phase with alcohols. Chastrette [13] showed that five factors accounted for 99% of the total variance: three factors were difficult to account for, and the other two were polarity and a factor connected to, but not identical with, hydrogen-bonding. A polarity factor was identified by McCloskey and Hawkes [14], who also suggested that a factor related to the ability of a phase to retain *cis*-hydrindane was important.

It seems, therefore, that although a single "polarity" parameter is still often used to characterise stationary phases [4,15], analytical methods suggest that a number of factors must be involved, perhaps three [10] to five [13], although identification of these factors with particular chemical interactions has not proved possible. Our analysis starts with a model for solvation of a solute, and then deduces from the model various possible interactions. Once these interactions are set out, the necessary parameters required to quantify these interactions have to be obtained (from data other than the chromatographic results to be analysed). These parameters then, in effect, take the place of the various factors identified by methods such as principal components analysis [10] or factor analysis [13].

On our model, the process of dissolution of a gaseous solute into a liquid stationary phase or solvent can conceptually be broken down into a number of stages, *viz.* (1) the creation of a cavity in the phase of suitable size, (2) reorganisation of solvent molecules round the cavity and (3) introduction of the solute into the cavity. The first stage involves the endoergic breaking of solvent–solvent bonds: the larger the solute, the more bonds are broken to create a cavity, and the more endoergic is the process. On this step alone, the larger the solute the less soluble it would be, and the smaller would be the retention volume (V_G^0) or the Ostwald solubility coefficient (L). The second stage is not very important in terms of Gibbs energy, although it probably is in terms of enthalpy and entropy. In the third stage, various solute–solvent interactions will be set up, all of which will be exoergic and will lead to increased solubility of the solute. Possible interactions include: (i) General dispersion interactions that will invariably be larger or more exoergic the larger is the solute. It is these interactions that account for the solubility of inert solutes such as the alkanes. And since such solutes are more soluble the larger they are, these dispersion interactions must be

strong enough to overcome the endoergic cavity effect. (ii) Dipolar interactions, including dipole–dipole or dipole–induced dipole effects. (iii) Hydrogen-bonding interactions between solute acid–solvent base and solute base–solvent acid. (iv) Possible specific interactions involving π- or n-electron pairs. In view of this complexity of solute–solvent systems, it is not surprising that only limited identification of the factors governing such systems has hitherto been made, but it is clearly of considerable importance if stationary phases could be characterised in terms of these fundamental interactions.

We have now developed solute parameters that, we believe, correspond to either simple fundamental properties, or to known combinations of properties [16–23]. These are as follows: R_2 a modified polarisability parameter that characterises the ability of a solute to interact via π- or n-electron pairs [16,17], δ_2 a polarisability correction term [18–20] taken as zero except for polyhalogenated aliphatics (0.5) or aromatics (1.0) and which is probably an approximation to R_2, π_2^* the solute dipolarity[a] [18–20], α_2^H the solute hydrogen-bond acidity [21], β_2^H the solute hydrogen-bond basicity [22] and log L^{16} where L^{16} is the solute Ostwald solubility coefficient on hexadecane at 25°C [23]. This latter parameter is a combination of a cavity term and a general dispersion interaction term [24]. Various multiple linear regression equations can then be constructed to account for solubility-related properties (SP) of a series of solutes in a given solvent or stationary phase, eqns. 1–3, where SP can be V_G^0, L (or K, the gas–liquid partition coefficient), but *cannot* be the retention index.

$$\log \text{SP} = c + rR_2 + s\pi_2^* + a\alpha_2^H + b\beta_2^H + l \log L^{16} \tag{1}$$

$$\log \text{SP} = c + d\delta_2 + s\pi_2^* + a\alpha_2^H + b\beta_2^H + l \log L^{16} \tag{2}$$

$$\log \text{SP} = c + rR_2 + q\mu_2^2 + a\alpha_2^H + b\beta_2^H + l \log L^{16} \tag{3}$$

In eqn. 3, μ_2 is the solute dipole moment. We have applied eqns. 1–3 to a number of sets of gas chromatographic retention data, and also to the solubility of gases and vapours in some common solvents, with considerable success [16,17,25]. Now since the parameters, or explanatory variables, in eqns. 1–3 represent solute properties, the various constants found by multiple linear regression analyses, will represent solvent or stationary phase properties. The most useful equation in this respect is eqn. 1 for which we have r the tendency of the phase to interact with π- and n-solute electron pairs, s the phase dipolarity, a the phase hydrogen-bond basicity (because basic phases will interact with acidic solutes), b the phase hydrogen-bond acidity, and l representing a combination of general dispersion interactions and cavity effects. These constants r, s, a, b and l (together with possibly q, another measure of phase dipolarity) thus serve to characterise the phase in terms of particular chemical interactions. That up to five constants are needed to characterise a given stationary phase reflects the complexity of solute–solvent interactions. The number of constants,

---

[a] We use this term in the Kamlet–Taft sense [18], namely the ability of a molecule to undergo molecular interactions of a dipole–dipole or a dipole–induced dipole nature. Thus dioxane and 1,4-dichlorobenzene are regarded as "dipolar", even though they have no permanent dipole moment.

however, is certainly in accord with principal components analysis [10] and factor analysis [13], which both show that several factors are required to account for retention data.

RESULTS

We now apply eqns. 1–3 to the data of McReynolds [1] on 367 solutes on 77 phases. Of the solutes studied, we have all the necessary parameters for about 160, and our analysis uses up to 157 solutes on the 77 phases at two temperatures[a]. As pointed out, above, retention indices are not suitable for use as SP values in eqns. 1–3, and all our analyses are in terms of the log V_G^0 values reported by McReynolds [1]. We first test, as a necessary preliminary, whether the solute parameters used as explanatory variables are, indeed, independent. In Table I are given the correlation constants, R, between the explanatory variables in eqn. 1. It can be seen that the intercorrelations are insignificant, with the possible exception of that between π_2^* and β_2^H for which $R = 0.474$ (and $R^2 = 0.225$ only). We also test eqns. 1–3 for two typical phases, ethyleneglycol adipate and dibutyltetrachlorophthalate; results are in Table II. Both the overall correlation coefficient and the standard deviation, S.D., are almost identical for eqn. 1 and eqn. 2. Since the molar refraction parameter R_2 can be identified with a specific type of solute–solvent interaction, whereas the empirical δ_2 parameter cannot, we shall list results in terms of the preferred eqn. 1 only. Although the correlations in terms of eqn. 3 are quite useful, they are in all cases not as good as eqn. 1, and so we shall not give all the details of eqn. 3, but list where necessary values of the q constant only.

TABLE I

CORRELATION COEFFICIENTS BETWEEN THE EXPLANATORY VARIABLES, FOR THE 155-SOLUTE DATA SET USED FOR FLEXOL

	R_2	π_2^*	α_2^H	β_2^H
π_2^*	0.295			
α_2^H	0.111	−0.210		
β_2^H	−0.243	0.474	0.247	
$\log L^{16}$	0.016	−0.171	−0.061	−0.169

The results of application of eqn. 1 to the entire set of stationary phases at 120°C are summarised in Table III, where also the q constant in eqn. 3 is given. For a few phases, data were available at 80 and 100°C only, and we have estimated the various constants at 120°C from values at the lower temperatures. For completeness, we applied the various equations to results at the other given temperatures used in the work of McReynolds [1], and details are shown in Table IV. Before attempting to

---

[a] McReynolds studied a large number of difunctional compounds for which we lack most of the required parameters in eqns. 1 and 2; these include many formals, acetals, dihydric alcohols, etc. Note that not all solutes were studied on all phases, so that the number of solutes used in our regressions varies from 130 to 157.

TABLE II

COMPARISON OF EQNS. 1–3 IN REGRESSIONS OF LOG V_G^0 AT 120°C

S.D. = Overall standard deviation; R = overall correlation coefficient; n = number of solutes.

Eqn.	c	r	d	s	q	a	l	S.D.	R	n
Ethyleneglycol adipate										
1	−0.900	0.357		1.425		1.720	0.443	0.093	0.9857	143
	0.038[a]	0.048		0.048		0.053	0.007			
2	−0.871		0.116	1.480		1.867	0.438	0.094	0.9849	143
	0.038		0.030	0.047		0.053	0.007			
3	−0.360	0.784			0.073	1.405	0.394	0.160	0.9476	143
	0.055	0.079			0.006	0.089	0.013			
Dibutyltetrachlorophthalate										
1	−0.615	0.249		0.692		0.600	0.600	0.048	0.9969	150
	0.019	0.025		0.025		0.028	0.004			
2	−0.615		0.112	0.752		0.687	0.599	0.050	0.9967	150
	0.020		0.016	0.025		0.029	0.004			
3	−0.410	0.547			0.038	0.420	0.586	0.070	0.9920	150
	0.024	0.039			0.003	0.040	0.006			

[a] These are the standard deviations in the constants.

classify the phases, we note that the correlation eqn. 1 yields results that are reasonably good for "all solute" correlations, and, as we shall see, these results are chemically sensible. Thus the s, a and b constants, when statistically significant, are always positive, because increase in solute–solvent interactions must lead to an increase in solubility of the gaseous solute, and hence to an increase in V_G^0. The r constant is nearly always positive, except in the case of fluorinated phases, e.g. Dow fluid 1265, where the polarisability is even less than in hydrocarbon systems. As mentioned in the introduction, the l constant reflects a combination of an endoergic cavity term and an exoergic solute–solvent general dispersion interaction term. The latter always dominates, giving rise to positive l constants.

The effect of temperature is very important with regard to characterisation of solubility-related phenomena, although it has generally been overlooked as regards characterisation of stationary phases. In general, the main characteristic constants s, a, b and l, all decrease, often quite markedly, with temperature. Now if the relevant solute–solvent interactions are not only exoergic but are exothermic as well, the Van 't Hoff equation requires that these interactions will decrease with increase in temperature, hence leading to a decrease in the numerical values of the characteristic constants. On thermodynamic grounds it thus follows that any correlation equation set up in terms of solute–solvent or solute–stationary phase interactions must incorporate this temperature dependence. Our eqn. 1 does so via the characteristic constants.

As a final check on our method of analysis, we can compare regression equations obtained from the set of solutes used by McReynolds [1] with those [16] from the quite different set of solutes used by Patte et al. [26] for Carbowax 1540, diethyleneglycolsuccinate, polyphenyl ether and Zonyl-E7. Details are in Table V, and show that there is very good agreement between the two sets of regressions using eqn. 1.

TABLE III

CLASSIFICATION OF PHASES AT 120 °C

S.D. and R are the overall deviation and correlation coefficient on application of eqn. 1 to log V_G^0. The number of data points is No. q = The coefficient of μ_2^2 in eqn. 3.

Group	Stationary phase	Characteristic constants in eqn. 1					S.D.	R	No	q
		c	r	s	a	l				
1	Squalane[a]	−0.33	0.12	0.02	0.00	0.619	0.026	0.9990		0.001
2	Apiezon M	−0.45	0.26	0.10	0.11	0.600	0.035	0.9982	147	0.006
	Apiezon N	−0.48	0.27	0.12	0.10	0.601	0.037	0.9978	149	0.008
	Apiezon J	−0.48	0.27	0.13	0.13	0.594	0.034	0.9984	148	0.010
	Apiezon L	−0.48	0.27	0.14	0.13	0.596	0.036	0.9982	149	0.006
3	Versilube P50	−0.37	0.03	0.25	0.17	0.538	0.036	0.9978	149	0.010
	SE-31	−0.36	0.03	0.24	0.17	0.520	0.039	0.9971	156	0.012
	SE-30	−0.32	0.03	0.27	0.29	0.523	0.040	0.9971	152	0.014
	SE-30 NPGA	−0.40	0.06	0.27	0.33	0.525	0.042	0.9969	152	0.016
	SE-52	−0.38	0.06	0.32	0.22	0.532	0.041	0.9971	155	0.018
4	Dioctylsebacate	−0.35	0.12	0.49	0.79	0.594	0.047	0.9967	153	0.029
	Di-2-ethylhexylsebacate	−0.36	0.13	0.51	0.83	0.591	0.045	0.9969	153	0.028
	Tripelargonate	−0.42	0.16	0.53	0.82	0.583	0.051	0.9964	151	0.032
	Isooctyldecyladipate	−0.37	0.13	0.55	0.81	0.586	0.048	0.9964	154	0.031
	Di-2-ethylhexyladipate	−0.36	0.13	0.55	0.87	0.590	0.047	0.9967	150	0.030
	Diisodecylphthalate	−0.52	0.13	0.65	0.73	0.589	0.055	0.9958	155	0.038
	Dioctylphthalate	−0.52	0.14	0.67	0.77	0.587	0.053	0.9960	153	0.039
5	Ucon LB-1715	−0.56	0.18	0.71	1.22	0.543	0.072	0.9923	153	0.038
	Flexol 8N8	−0.48	0.11	0.73	1.27	0.573	0.065	0.9932	155	0.043
	Pluronic L81	−0.49	0.20	0.77	1.29	0.537	0.075	0.9913	152	0.040
6	Polyphenyl ether, 5 rings	−0.70	0.21	0.88	0.54	0.564	0.064	0.9940	155	0.048
	Polyphenyl ether, 6 rings	−0.74	0.21	0.90	0.56	0.563	0.066	0.9935	155	0.048
7	Tricresylphosphate	−0.68	0.15	1.06	1.23	0.550	0.074	0.9930	154	0.057
	Sucrose acetate isobutanoate	−0.56	0.05	1.05	1.29	0.509	0.071	0.9928	157	0.056
8	Hallcomid M18	−0.35	0.11	0.60	1.55	0.592	0.062	0.9947	154	0.037
	Hallcomid M180L	−0.45	0.10	0.71	1.59	0.592	0.068	0.9930	153	0.040

9	Pluronic L42	−0.52	0.21	0.88	1.45	0.529	0.081	0.9898	154	0.045
	Pluronic L72	−0.54	0.17	0.89	1.41	0.531	0.077	0.9917	153	0.042
	Pluronic L61	−0.53	0.20	0.91	1.42	0.526	0.079	0.9905	151	0.044
	Pluronic L63	−0.54	0.24	0.92	1.46	0.519	0.080	0.9900	153	0.046
	Polytergent J300	−0.55	0.16	0.94	1.49	0.536	0.081	0.9901	154	0.052
	Pluronic P84	−0.57	0.20	0.94	1.44	0.516	0.079	0.9908	152	0.047
	Pluronic P85	−0.57	0.28	0.94	1.46	0.512	0.082	0.9902	153	0.052
	Pluronic L44	−0.56	0.26	0.96	1.52	0.515	0.084	0.9899	154	0.049
	Oronite NIW	−0.62	0.25	0.96	1.46	0.524	0.085	0.9898	155	0.053
	Ucon HB-2000	−0.60	0.28	0.97	1.48	0.514	0.081	0.9907	154	0.053
	Ethofat 60-25	−0.60	0.26	0.99	1.54	0.523	0.078	0.9916	154	0.052
	Pluronic P65	−0.60	0.28	1.01	1.50	0.513	0.086	0.9893	155	0.050
	Pluromic P46	−0.61	0.30	1.02	1.56	0.505	0.085	0.9893	154	0.052
	Tergitol NPX	−0.57	0.19	1.02	1.47	0.518	0.078	0.9917	154	0.058
10	Neopentylglycoladipate, term	−0.68	0.21	1.08	1.45	0.510	0.070	0.9929	152	0.057
	Ethyleneglycolsebacate	−0.78	0.27	1.10	1.44	0.518	0.078	0.9911	145	0.054
	Diethyleneglycolsebacate	−0.76	0.32	1.14	1.45	0.498	0.074	0.9910	141	0.052
	Neopentylglycoladipate	−0.67	0.24	1.14	1.47	0.491	0.073	0.9916	150	0.060
	Neopentylglycolsuccinate	−0.71	0.23	1.24	1.49	0.466	0.082	0.9884	153	0.065
11	Pluronic F88	−0.63	0.34	1.10	1.60	0.483	0.086	0.9887	153	0.058
	Pluronic F68	−0.66	0.35	1.13	1.61	0.485	0.087	0.9884	154	0.059
	Pluronic F77	−0.63	0.32	1.09	1.61	0.496	0.083	0.9897	151	0.051
	Igepal CO 880	−0.66	0.28	1.16	1.61	0.488	0.084	0.9885	152	0.059
	Triton X 305	−0.83	0.29	1.17	1.65	0.492	0.086	0.9894	154	0.059
12	Ethyleneglycoladipate	−0.90	0.36	1.43	1.72	0.443	0.093	0.9857	143	0.073
	Diethyleneglycoladipate	−0.91	0.40	1.46	1.73	0.438	0.089	0.9847	139	0.065
13	XF-1150	−0.69	0.06	1.44	1.38	0.417	0.084	0.9856	150	0.092
	Sucrose octaacetate	−0.73	0.12	1.48	1.59	0.426	0.090	0.9852	154	0.071
14	Carbowax 20M	−0.73	0.40	1.23	1.78	0.465	0.091	0.9880	153	0.059
	Carbowax 6000	−0.75	0.40	1.28	1.80	0.469	0.090	0.9878	150	0.059
	Carbowax 4000	−0.76	0.32	1.31	1.85	0.470	0.090	0.9867	149	0.059
	Carbowax 1540	−0.75	0.31	1.34	1.87	0.457	0.093	0.9866	151	0.069
	Carbowax 1000	−0.76	0.29	1.37	1.89	0.457	0.094	0.9867	152	0.071

TABLE III (continued)

Group	Stationary phase	Characteristic constants in eqn. 1					S.D.	R	No	q
		c	r	s	a	l				
15	Carbowax 600	-0.82	0.31	1.46	2.12	0.455	0.093	0.9847	149	0.073
	Carbowax 400	-0.77	0.28	1.50	2.18	0.440	0.090	0.9883	149	0.077
	Carbowax 300	-0.79	0.33	1.50	2.28	0.434	0.093	0.9877	149	0.074
	Quadrol	-0.77	0.07	1.47	2.38	0.471	0.103	0.9858	153	0.087
	Hyprose SP80	-0.87	0.11	1.53	2.40	0.414	0.103	0.9835	151	0.088
16	Triethyleneglycolsuccinate	-1.05	0.39	1.71	1.87	0.416	0.090	0.9858	145	0.078
	Diethyleneglycolsuccinate	-0.99	0.43	1.74	1.68	0.379	0.114	0.9755	145	0.073
	Dow Corning Fluid 550	-0.46	0.09	0.56	0.29	0.547	0.047	0.9963	152	0.032
	Casterwax	-0.45	0.10	0.63	1.09	0.562	0.060	0.9944	150	0.040
	Dibutyltetrachlorophthalate	-0.62	0.25	0.69	0.60	0.600	0.048	0.9969	150	0.038
	Citroflex A4[a]	-0.43	0.12	0.85	0.94	0.552	0.061	0.9951		0.046
	Bis(2-ethoxyethyl)phthalate	-0.64	0.13	1.23	1.25	0.529	0.074	0.9923	152	0.067
	Dow Corning Fluid FS 1265	-0.76	-0.25	1.29	0.29	0.451	0.083	0.9851	153	0.086
	Kroniflex THPP	-0.72	0.22	1.34	2.28	0.498	0.083	0.9913	152	0.071
	Zonyl E-7	-0.82	-0.28	1.63	0.69	0.449	0.071	0.9902	150	0.083

[a] Values extrapolated from 80 and 100 °C.

CHARACTERISATION OF PHASES

Details of the application of eqn. 1 to the 77 McReynolds phases are given in Tables III, IV, VI and VII. In Table III are results at a common temperature of 120°C, with values for squalane and Citroflex A4 extrapolated from those at 80 and 100°C. Table IV contains results at temperatures other than 120°C, usually at 100 or at 140/160°C, so that all of McReynolds data sets have been analysed. We do not list the chemical formulation of the 77 phases, even though some of them are rather obscure, because Fellous et al. [6] have detailed the 77 stationary phases already. It should be noted that many of these phases contain a non-ionic surfactant (2%, w/w), and hence our obtained constants, Table III, refer to the phases as specifically formulated by McReynolds [1]. Although many of the McReynolds phases are no longer in current use, we list results for all the phases in order to show the utility of our method and in order to compare our classification with previous characterisation [12] of the total 77-phase set.

Furthermore, no corrections were made by McReynolds for effects such as interfacial adsorption, and his results for solutes such as alkanes in the more polar phases may be subject to additional error. We have no way of correcting the raw data of McReynolds, and rather than exclude particular subsets of compounds on some arbitrary basis, we have chosen to use all the available results. This may well account for part of the large standard deviations observed for regressions with phases such as diglycerol and sorbitol, and suggests also that the obtained constants for these phases should be viewed with some caution.

In principle, a given stationary phase at a given temperature is characterised by the six constants in eqn. 1. However, the constant c, although important as regards the absolute values of $\log V_G^0$, is not a very useful characteristic constant, whilst the constant r plays only a minor role, at least for the present data set. We are thus left with the four constants s, a, b and l. But we can effect further simplification by noting that only three out of the 77 phases give rise to statistically significant b constants, and hence show hydrogen-bond acidity. These are docosanol, diglycerol and sorbitol with b values of 0.34, 0.52 and 0.34 respectively at 120°C (see Table VI). A number of the other phases might be expected to show hydrogen-bond acidity, but the analysis given in Table VIII reveals that the $b\beta_2^H$ term is not significant. We can therefore regard docosanol, diglycerol and sorbitol as singular phases, and analyse the remaining 74 phases with the omission of the $b\beta_2^H$ term altogether (see Tables III and IV). For these 74 phases, the three major characteristic constants are thus s, a and l only.

We begin the analysis of the 74 phases in Table III by noting that there is some connection between s, a and l. In general, basic phases will also be dipolar, so that a and s will tend to run together. Furthermore, solvent–solvent interactions will be greater in dipolar, basic phases, thus giving rise to a larger endoergic cavity term, leading to a smaller value of the l constant. Since a and s are likely to be related, we can first group the 74 phases through a plot of a against s, shown in Fig. 1. Quite clearly, there are several groups or clusters of phases with about the same a and s values, and we have drawn up Table III to show the 16 clusters indicated in Fig. 1. Of course, there is an arbitrary element in the choice of clusters. Thus groups 9 and 11 might be subsumed into a common group, or group 4 might be divided into two groups, but this is a feature of any method that reduces the 77 phases down to a

TABLE IV

REGRESSIONS AT VARIOUS TEMPERATURES

Stationary phase	c	r	s	a	l	S.D.	R	No	Temperature (°C)
Squalane	−0.21	0.11	0.08	—	0.735	0.043	0.9970	133	80
	−0.27	0.12	0.05	—	0.674	0.034	0.9983	147	100
Apiezon M	−0.57	0.28	0.13	0.06	0.504	0.044	0.9971	153	160
Apiezon N	−0.62	0.28	0.15	0.09	0.504	0.045	0.9969	153	160
Apiezon J	−0.62	0.28	0.17	0.11	0.501	0.038	0.9977	150	160
Apiezon L	−0.57	0.29	0.10	0.05	0.502	0.037	0.9975	151	160
Versilube F50	−0.48	0.08	0.22	0.09	0.444	0.037	0.9972	152	160
SE-31	−0.48	0.05	0.22	0.14	0.430	0.038	0.9968	157	160
SE-30	−0.45	0.06	0.23	0.18	0.441	0.036	0.9968	154	160
SE-30 NPGA	−0.50	0.05	0.30	0.28	0.486	0.039	0.9970	139	140
SE-52	−0.51	0.07	0.29	0.17	0.442	0.040	0.9966	157	160
Dioctylsebacate	−0.31	0.13	0.55	0.94	0.646	0.049	0.9969	154	100
Di-2-ethylhexylsebacate	−0.31	0.13	0.55	0.95	0.646	0.050	0.9969	154	100
Tripelargonate	−0.53	0.15	0.49	0.65	0.486	0.051	0.9957	154	160
Isooctyldecyladipate	−0.33	0.11	0.60	0.96	0.645	0.054	0.9964	155	100
Di-2-ethylhexyladipate	−0.31	0.11	0.61	1.04	0.644	0.052	0.9966	152	100
Diisodecylphthalate	−0.55	0.14	0.59	0.62	0.537	0.050	0.9964	156	140
Dioctylphthalate	−0.55	0.15	0.61	0.64	0.532	0.052	0.9960	155	140
Ucon LB-1715	−0.69	0.20	0.61	0.88	0.459	0.061	0.9924	152	160
Flexol 8N8	−0.54	0.07	0.69	1.09	0.524	0.057	0.9953	157	140
Pluronic L81	−0.44	0.18	0.84	1.56	0.589	0.081	0.9910	151	100
Polyphenyl ether, 5 rings	−0.86	0.23	0.82	0.44	0.482	0.060	0.9936	156	160
Polyphenyl ether, 6 rings	−0.87	0.24	0.82	0.46	0.478	0.063	0.9929	156	160
Tricresylphosphate	−0.62	0.15	1.14	1.44	0.600	0.078	0.9920	142	100
Sucrose acetate isobutanoate	−0.65	0.06	0.86	0.99	0.429	0.060	0.9925	155	160
Hallcomid M18	−0.31	0.11	0.65	1.89	0.649	0.066	0.9943	141	100
Hallcomid M180L	−0.38	0.10	0.74	1.90	0.646	0.069	0.9934	141	100

Pluronic L42	−0.59	0.20	0.82	1.26	0.486	0.074	0.9902	155	140
Pluronic L72	−0.61	0.23	0.81	1.23	0.489	0.072	0.9917	155	140
Pluronic L61	−0.50	0.21	1.02	1.67	0.581	0.088	0.9890	141	100
Pluronic L63	−0.47	0.17	1.01	1.71	0.571	0.083	0.9890	140	100
Polytergent J300	−0.49	0.15	1.01	1.76	0.584	0.089	0.9901	155	100
Pluronic P84	−0.52	0.25	1.00	1.70	0.564	0.090	0.9893	153	100
Pluronic P85	−0.52	0.27	1.03	1.71	0.562	0.091	0.9892	154	100
Pluronic L44	−0.62	0.25	0.89	1.31	0.473	0.078	0.9899	155	140
Oronite NIW	−0.81	0.20	0.90	1.12	0.458	0.071	0.9906	154	160
Ucon HB-2000	−0.52	0.29	1.03	1.67	0.560	0.094	0.9884	153	100
Ethofat 60-25	−0.57	0.19	1.08	1.78	0.575	0.086	0.9909	151	100
Pluronic P65	−0.50	0.27	1.05	1.76	0.560	0.090	0.9881	143	100
Pluronic P46	−0.46	0.30	0.94	1.38	0.466	0.079	0.9893	156	140
Tergitol NPX	−0.66	0.24	0.86	1.13	0.437	0.066	0.9916	152	160
Neopentylglycoladipate, term	−0.76	0.16	1.03	1.31	0.475	0.065	0.9928	140	140
Ethyleneglycolsebacate	−0.81	0.22	1.02	1.32	0.478	0.067	0.9930	132	140
Diethyleneglycolsebacate	−0.83	0.27	1.06	1.34	0.460	0.073	0.9909	136	140
Neopentylglycoladipate	−0.67	0.18	1.02	1.32	0.444	0.064	0.9926	140	140
Neopentylglycolsuccinate	−0.72	0.16	1.15	1.39	0.418	0.070	0.9905	139	140
Pluronic F88	−0.58	0.28	1.21	1.83	0.531	0.095	0.9878	153	100
Pluronic F68	−0.60	0.29	1.24	1.81	0.530	0.098	0.9878	156	100
Pluronic F77	−0.57	0.32	1.19	1.87	0.547	0.094	0.9871	141	100
Igepal CO 880	−0.66	0.27	1.28	1.88	0.540	0.096	0.9890	152	100
Triton X 305	−0.86	0.31	0.94	1.26	0.407	0.072	0.9890	152	160
Ethyleneglycoladipate	−0.97	0.24	1.37	1.68	0.412	0.083	0.9868	129	140
Diethyleneglycoladipate	−0.92	0.30	1.34	1.61	0.399	0.079	0.9865	130	140
XF-1150	−0.82	0.06	1.30	1.12	0.344	0.076	0.9843	152	160
Sucrose octaacetate	−0.84	0.12	1.29	1.30	0.362	0.076	0.9852	154	160
Carbowax 20M	−0.82	0.37	1.07	1.36	0.392	0.076	0.9879	151	160
Carbowax 6000	−0.79	0.40	1.15	1.56	0.431	0.083	0.9877	152	140
Carbowax 4000	−0.81	0.37	1.18	1.64	0.431	0.080	0.9889	150	140
Carbowax 1540	−0.71	0.38	1.42	2.17	0.499	0.100	0.9874	150	100
Carbowax 1000	−0.73	0.30	1.49	2.24	0.500	0.100	0.9875	149	100

TABLE IV *(continued)*

Stationary phase	c	r	s	a	l	S.D.	R	No	Temperature (°C)
Carbowax 600	−0.78	0.29	1.61	2.39	0.496	0.104	0.9866	148	100
Carbowax 400	−0.73	0.28	1.60	2.44	0.481	0.104	0.9867	150	100
Carbowax 300	−0.76	0.26	1.64	2.56	0.476	0.106	0.9866	149	100
Quadrol	−0.72	0.12	1.50	2.76	0.521	0.106	0.9879	152	100
Hyprose SP80	−0.84	0.09	1.61	2.77	0.461	0.110	0.9848	150	100
Triethyleneglycolsuccinate	−1.06	0.33	1.57	1.67	0.381	0.086	0.9840	133	140
Diethyleneglycolsuccinate	−1.07	0.35	1.60	1.77	0.342	0.099	0.9746	133	140
Dow Corning Fluid 550	−0.56	0.11	0.47	0.20	0.456	0.041	0.9967	154	160
Casterwax	−0.56	0.13	0.60	0.93	0.519	0.053	0.9953	152	140
Dibutyltetrachlorophthalate	−0.57	0.24	0.75	0.68	0.658	0.057	0.9956	142	100
Citroflex A4	−0.29	−0.06	1.05	1.47	0.658	0.072	0.9923	136	80
	−0.36	0.04	0.94	1.19	0.602	0.066	0.9938	150	100
Bis(2-ethoxyethyl)phthalate	−0.58	0.18	1.29	1.46	0.575	0.085	0.9899	143	100
Dow Corning Fluid FS 1265	−0.86	−0.21	1.13	0.27	0.367	0.071	0.9853	155	160
Kroniflex THFP	−0.79	0.23	1.25	2.02	0.461	0.082	0.9901	153	140
Zonyl E-7	−0.78	−0.29	1.78	0.78	0.494	0.077	0.9905	138	100

TABLE V

CHARACTERISATION OF PHASES USING EQN. 1 WITH McREYNOLD'S AND LAFFORT'S DATA AT 120 °C

M = McReynold's set, this work; L = Laffort's set, ref. 16.

Stationary phase	Set	r	s	a	l
Carbowax 1540	M	0.31	1.34	1.87	0.457
	L	0.26	1.37	2.11	0.442
Diethyleneglycolsuccinate	M	0.43	1.74	1.68	0.379
	L	0.35	1.70	1.92	0.396
Polyphenyl ether, 6 rings	M	0.21	0.90	0.56	0.563
	L	0.19	0.98	0.59	0.552
Zonyl E-7	M	−0.28	1.63	0.69	0.449
	L	−0.38	1.61	0.70	0.442

TABLE VI

STATIONARY PHASES WITH SIGNIFICANT HYDROGEN-BOND ACIDITY

Stationary phase	c	r	s	a	b	l	S.D.	R	No	Temperature (°C)
Docosanol[a]	−0.41	0.13	0.29	0.75	0.34	0.603	−	−	−	120
	−0.37	0.15	0.30	1.13	0.39	0.657	0.061	0.9951	148	100
	−0.33	0.16	0.31	1.56	0.45	0.717	0.077	0.9925	134	80
Diglycerol	−1.26	0.55	1.63	2.77	0.52	0.225	0.148	0.9589	146	120
Sorbitol	−1.72	0.35	0.81	1.77	0.34	0.360	0.161	0.9217	130	120

[a] Extrapolated from results at 80 and 100 °C.

TABLE VII

TEST FOR STATIONARY PHASE HYDROGEN-BOND ACIDITY

Stationary phase	c	r	s	a	b	l	S.D.	R
Castorwax	−0.47	0.13	0.59	1.06	0.08	0.563	0.059	0.9945
	−0.45	0.10	0.63	1.09	−	0.562	0.060	0.9944
Flexol 8N8	−0.49	0.12	0.71	1.25	0.03	0.573	0.065	0.9932
	−0.48	0.11	0.73	1.27	−	0.573	0.065	0.9932
Hyprose SP80	−0.86	0.09	1.56	2.42	0.05	0.414	0.103	0.9835
	−0.87	0.11	1.53	2.40	−	0.414	0.103	0.9835
Quadrol	−0.77	0.08	1.45	2.37	0.03	0.472	0.103	0.9858
	−0.77	0.07	1.47	2.38	−	0.471	0.103	0.9858

TABLE VIII

EFFECT OF CHAIN LENGTH ON THE CHARACTERISTIC CONSTANTS FOR SOME STA-
TIONARY PHASE ESTERS

Stationary phase	r	s	a	l
Dioctylsebacate	0.12	0.49	0.79	0.594
Ethyleneglycolsebacate	0.27	1.10	1.44	0.518
Diethyleneglycolsebacate	0.32	1.14	1.45	0.498
Isooctyldecyladipate	0.13	0.55	0.81	0.586
Ethyleneglycoladipate	0.36	1.43	1.72	0.443
Diethyleneglycoladipate	0.40	1.46	1.73	0.438
Diethyleneglycolsebacate	0.32	1.14	1.45	0.498
Diethyleneglycoladipate	0.40	1.46	1.73	0.438
Diethyleneglycolsuccinate	0.43	1.74	1.68	0.379

relatively small number of clusters. We can then examine the 16 groups to see if any futher subdivision is necessary on the basis of the r and l constants. However, within each group, the r and l constants do not vary overmuch. Only in the case of group 7 and group 16 is there a clear subdivision into high and low values of l, although groups 10 and 15 do contain a rather wide spread of l values.

We can conclude that an analysis in terms of s and a (and also b for phases that are hydrogen-bond acids) enables us to group the 74 McReynolds phases into a number of clusters of similar phases, leaving some 11 stationary phases (8 in Table III plus the three acidic phases) as singular phases that cannot be substituted by any other of the 77-phase set. Our grouping is based entirely on chemical principles, and it
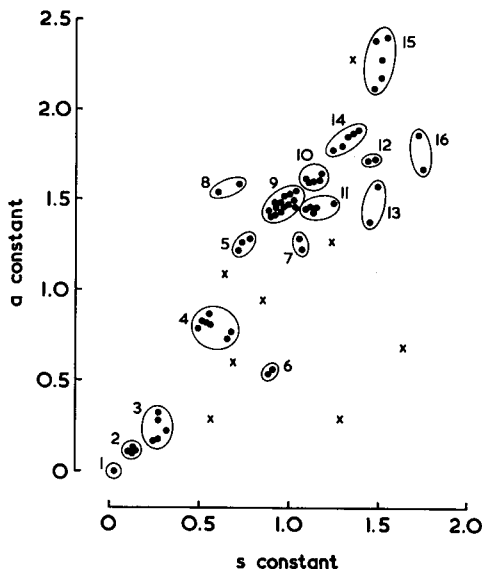
Fig. 1. Classification of stationary phases according to the a constant and the s constant in eqn. 1. ● = Groups as shown in Table III; × = singular phases.

is very instructive to compare results with other work carried out on more mathematical lines.

Huber and Reich [12] have analysed the 77-phase set, using both hierarchical clustering and the minimum spanning tree method. Their results, especially by the latter technique, are almost identical to those we have obtained. Differences, such as there are, are trivial. For example Huber and Reich [12] class Castorwax and our groups 5 and 8 together, but reference to Table III and Fig. 1 shows that this is quite reasonable on our analysis as well. Wold [11] used a pattern cognition method to group the 226-phase set into clusters. Where there are common phases between the 226- and the 77-phase sets, there is again excellent agreement between our result and those of Wold [11]. As pointed out by Wold, the nearest neighbour technique used by Leary et al. [7] leads to a rather peculiar set of clusters. However, the numerical taxonomy method of Massart et al. [9] applied to the 226-phase set leads to groups not too dissimilar to those in Table III, although there are some outstanding exceptions. Thus Massart et al. [9] class didecylphthalate and Flexol 8N8 in the same group, whereas we find the latter to be considerably more basic (a = 1.27 as against a = 0.73 for diisodecylphthalate). Our method of clustering, therefore, is in excellent agreement with results of Huber and Reich [12] and of Wold [11], but not so much with results of Leary et al. [7] or of Massart et al. [9].

A general survey of our classification, Table III, shows that it is completely consistent with the chemical formulation of the phases. Thus group 1 contains the saturated hydrocarbon squalane, and would include other hydrocarbons such as hexadecane (by definition), octacosane, $C_{87}H_{176}$ etc. The apiezons in group 2 are slightly dipolar and basic due to the presence of some aromatic groups, whilst the silicones in group 3 are rather more dipolar and basic through the silicon–oxygen bond. Thus the hydrogen-bond basicity of $(CH_3)_3SiOSi(CH_3)_3$ as a solute, β_2^H = 0.16, can be compared to values of β_2^H for di-tert.-butylether of 0.38, and values of around 0.45 for straight-chain aliphatic ethers [22]. All the simple esters of carboxylic acids cluster in group 4, the two amides appear in group 8, and so forth. The Carbowaxes fall into an exact sequence from Carbowax 20M to Carbowax 300, with values of s and a monotonically increasing along the series, where the cut-off point between groups 14 and 15 is clearly arbitrary. The sebacates (C_{10}), adipates (C_6) and succinates (C_4) are worthy of attention (see Table VIII). The sebacates are always less dipolar and less basic than the adipates or succinates, and the simple dialkylesters are always less dipolar and less basic than the corresponding ethyleneglycol or diethyleneglycol ester.

The constant r does not vary widely over the particular set of 77 phases, but, significantly, the r constant is negative in the case of the only fluorinated stationary phases in the set, viz. Dow Corning Fluid FS 1265 and Zonyl E-7. The ability of these phases to interact with solute π- and n-electron pairs is even less than that of a simple alkane.

Finally, we consider the characteristic constant l, a resultant of an endoergic solvent cavity term tending to decrease the value of l and an exoergic general dispersion interaction term tending to increase the value of l. We have previously shown [16] that the methylene increment for solvation of a homologous series[a] of gaseous

---

[a] That is a series in which CH_2 groups are successively inserted at the same part of the molecule.

TABLE IX

VALUES OF ΔLOG V_G^0 FOR 1-ALKANOLS ON SOME STATIONARY PHASES

R and No = Correlation coefficients and number of points in plots of log V_G^0 against carbon number of the 1-alkanols.

Stationary phase	Temperature (°C)	l	Δlog V_G^0	R	No
Squalane	80	0.735	0.398	0.9991	5
Squalane	100	0.674	0.358	0.9988	7
Squalane[a]	120	0.619	0.322	--	--
Apiezon N	120	0.601	0.314	0.9993	7
SE-30	120	0.523	0.280	0.9996	7
Carbowax 400	120	0.440	0.235	0.9998	7
Diethyleneglycolsuccinate	120	0.379	0.198	0.9989	7
Diglycerol	120	0.225	0.110	0.9987	7

[a] Extrapolated values.

solutes in a given solvent, $\Delta G_s^0(CH_2)$, depends on a combination of a solvent cavity term and a general dispersion interaction term. Now $\Delta G_s^0(CH_2)$ is related to Δlog V_G^0, since $\Delta G_s^0(CH_2) = -2.303RT \, \Delta$log V_G^0, where Δlog V_G^0, is the average increase in log V_G^0, along an homologous series. It therefore follows that the constant l must also be related to the important term Δlog V_G^0, or $\Delta G_s^0(CH_2)$.

In Table IX are given values of Δlog V_G^0, for the homologous series of 1-alkanols in a few representative stationary phases covering the range of l constants we have encountered. A plot of Δlog V_G^0, against the l constant (Fig. 2) yields an excellent straight line passing through the origin, since Δlog V_G^0 must approach zero as l approaches zero. We can thus show from experiment, as well as theory, that the l constant in eqn. 1 is a measure of the ability of a stationary phase to separate mem-
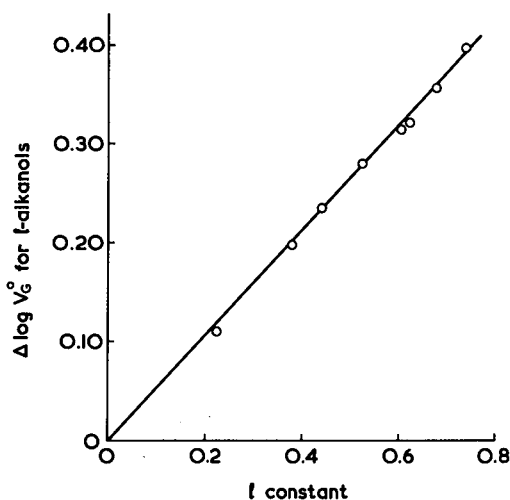
Fig. 2. Plot of Δlog V_G^0 against the l constant.

TABLE X

CHARACTERISTIC CONSTANTS FOR OTHER PHASES AT 120°C

Phase	r	s	a	l
N-methylpyrrolidinone [17]	–	1.42	2.70	0.472
N-Formylmorpholine [17]	–	1.52	2.24	0.442
Tricyanoethoxypropane [16]	0.23	2.12	1.94	0.379

bers of an homologous series. The l constant is entirely equivalent to $\Delta G_s^0(CH_2)$, so that eqn. 1 actually incorporates this latter parameter.

We have not considered eqns. 2 and 3 other than to compare them with eqn. 1 in Table II. Eqn. 2 offers no advantage over eqn. 1 and suffers from the disadvantage of containing the empirical parameter δ_2. Eqn. 3, although giving rise to significantly worse fits than eqn. 1 has the advantage that the q constant, especially, can be related to a theoretical model of solute dipole–solvent interactions via the Kirkwood equation [27]. However, in practice the correlation constant between q and s is so high, 0.970 for the 77 stationary phases at 120°C, that no extra information is contained in q. At present, therefore, eqn. 3 is not necessary for the characterisation of stationary phases. However, the dipole moment term is theoretically very useful, and it might be possible to incorporate other solute parameters, and to obtain an improved version of eqn. 3 that retains the dipole moment as a dipolarity parameter.

In Table X we list a few phases that we have previously [16,17] characterised through eqn. 1. The two amides are highly basic, whilst tricyanoethoxypropane is the most dipolar phase we have examined to data. Finally, we give in Table XI a selection of phases to show how the characteristic constants s, a, b and l relate to the chemical

TABLE XI

CHEMICAL CHARACTERISTICS OF SOME PHASES

Phase	Polarity	Basicity	Acidity	Separation of homologues
Hexadecane } Squalane }	Zero	Zero	Zero	High
Apiezon	Low	Low	Zero	High
Polyphenylether	Medium	Low	Zero	High
Hallcomid } Kroniflex THFP }	Medium	High	Zero	Medium
Carbowax 300 } Quadrol } Hyprose SP80 }	High	High	Zero	Medium
Zonyl E-7	High	Low	Zero	Medium
N-Methylpyrrolidinone	High	Very high	Zero	Medium
Tricyanoethoxypropane	Very high	High	Zero	Low
Docosanol	Low	Medium	Low	High
Diglycerol	High	Very high	Medium	Very low

nature of the stationary phase. From such a list, it is easy to select a phase that will effect separations mainly through dipole–dipole interactions (*e.g.* Zonyl E-7), or a phase that will effect separations mainly through interactions of the type solute hydrogen-bond acid–solvent hydrogen-bond base (e.g. Hallcomid M18 or M180L). We have not been able to list any phase that leads mainly to interactions of the type solute hydrogen-bond base–solvent hydrogen-bond acid. The most acidic phase we have encountered is diglycerol with $b = 0.52$ at 120°C, but this phase is actually the strongest hydrogen-bond base of all the phases listed. In any case, diglycerol is unsuitable as a general stationary phase because of the very low l constant. We hope to report in the near future on our attempts to synthesise phases that are strong hydrogen-bond acids but weak hydrogen-bond bases.

In conclusion, we have been able to set up a new classification of stationary phases, based on fundamental chemical interactions. The characteristic constants r, s, a, b and l provide information on the propensity of a given phase to undergo specific interactions with solutes, and hence lead to criteria for the choice of a phase to effect particular separations. The method does not have the disadvantages of the McReynolds–Rohrschneider procedures, and although retention data on not less than about 25 solutes are required, it is necessary only to determine relative retention times. Another advantage of the present method is that eqn. 1 can be applied to equilibria involving any condensed phase, for example the solubility of gaseous solutes in simple organic solvents [17], or even the adsorption of gases on solids. We hope to report on these processes in the near future.

SOLUTE–SOLVENT INTERACTIONS

Our main aim in this paper has been to characterise the set of 77 McReynolds phases in terms of eqn. 1, where SP = V_G^0. However, we can now use the results given in Tables III–VI to analyse the factors that influence solute retention on stationary phases. We give in Table XII a breakdown of eqn. 1, term-by-term for two typical solutes, butanone and 1-butanol, in a variety of stationary phases. In the less polar

TABLE XII

ANALYSIS OF THE FACTORS THAT INFLUENCE LOG V_G^0, USING EQN. 1 AT 120°C

Solute	Phase	Term					Dispersion[a]	Cavity[a]
		rR_2	$s\pi_2^*$	$a\alpha_2^H$	$b\beta_2^H$	$l \log L^{16}$		
Butanone	Apiezon M	0.04	0.07	0	0	1.37	3.36	−1.93
	Hallcomid M18	0.02	0.40	0	0	1.35	3.26	−1.88
	Zonyl E-7	−0.05	1.09	0	0	1.03	1.90	−1.09
	Diglycerol	0.09	1.09	0	0.25	0.52	(0.48)	(−0.28)
1-Butanol	Apiezon M	0.06	0.40	0.04	0	1.56	4.10	−2.25
	Hallcomid M18	0.03	0.24	0.52	0	1.54	4.00	−2.20
	Zonyl E-7	−0.06	0.65	0.23	0	1.17	2.31	−1.27
	Diglycerol	0.12	0.65	0.91	0.23	0.59	(0.59)	(−0.32)

[a] See text. These do not add up to the $l \log L^{16}$ term because of a constant term and a small dipole–induced dipole term that have not been included.

phases, where the s constant is quite small, by far the main term is $l \log L^{16}$. The term $a\alpha_2^H$ can be substantial for the combination of a hydrogen-bond acidic solute and a hydrogen-bond basic phase, but for the present set of solutes and phases the $b\beta_2^H$ term is never substantial. Of course, for more acidic phases than diglycerol, the $b\beta_2^H$ term could be much more significant.

In eqn. 1, the $l \log L^{16}$ term covers both general dispersion interactions that lead to positive values of $\log V_G^0$, and the endoergic solvent–solvent cavity term that leads to negative values of $\log V_G^0$. These two effects are very difficult to unravel quantitatively, hence we have had to use a combined term in eqn. 1. Abraham and Fuchs [24], however, managed to dissect the $\log L^{16}$ values themselves into mainly a cavity term and a general dispersion interaction term. If we assume, as before [25], that the ratio of these two terms remains the same, then we can roughly separate the total $l \log L^{16}$ term shown in Table XII into cavity and general dispersion effects. Given that these are only approximations, expecially in the case of diglycerol, we can still see that the largest interaction term corresponds to general solute–solvent dispersion effects. It is these that control the separation of members of an homologous series. Eqn. 1 incorporates such an effect in the $l \log L^{16}$ term. Although dipolar and acid–base interactions tend to be smaller than the general dispersion interactions, they control separations of dissimilar solutes. Eqn. 1 incorporates these effects in the first four terms.

Thus our preferred eqn. 1 not only forms the basis of a classification of stationary phases, but also leads to a rationale for the separation of solutes, based on a number of possible solute–solvent interactions.

ACKNOWLEDGEMENTS

REFERENCES

1 W. O. McReynolds, *Gas Chromatographic Retention Data,* Preston Technical Abstracts, Evanston, IL, 1966.
2 W. O. McReynolds, *J. Chromatogr. Sci.,* 8 (1970) 685.
3 G. Tarján, A. Kiss, G. Kocsis, S. Mészáros and J. M. Takács, *J. Chromatogr.,* 119 (1976) 327; and references cited therein.
4 S. K. Poole, B. R. Kersten and C. F. Poole, *J. Chromatogr.,* 471 (1989) 91.
5 C. E. Figgins, T. H. Risby and P. C. Jurs, *J. Chromatogr. Sci.,* 14 (1976) 453.
6 R. Fellous, L. Luft and J.-P. Rabine, *J. Chromatogr.,* 160 (1978) 117; 166 (1978) 383.
7 J. J. Leary, J. B. Justice, S. Tsuge, S. R. Lowry and T. L. Isenhour, *J. Chromatogr. Sci.,* 11 (1973) 201.
8 A. Eskes, F. Dupuis, A. Dijkstra, H. De Clercq and D. L. Massart, *Anal. Chem.,* 47 (1973) 2168.
9 D. L. Massart, P. Lenders and M. Lauwereys, *J. Chromatogr. Sci.,* 12 (1974) 617.
10 S. Wold and K. Andersson, *J. Chromatogr.,* 80 (1973) 43.
11 S. Wold, *J. Chromatogr. Sci.,* 13 (1975) 525.
12 J. F. K. Huber and G. Reich, *J. Chromatogr.,* 294 (1984) 15.
13 M. Chastrette, *J. Chromatogr. Sci.,* 14 (1976) 357.
14 D. H. McCloskey and S. J. Hawkes, *J. Chromatogr. Sci.,* 13 (1975) 1.
15 J. A. Garcia-Dominguez, J. Garcia-Munoz, V. Menendez, M. J. Molera and J. M. Santiuste, *J. Chromatogr.,* 393 (1987) 209.
16 M. H. Abraham, G. S. Whiting, R. M. Doherty and W. J. Shuely, *J. Chem. Soc., Perkin Trans. 2,* in press.

17 M. H. Abraham, G. S. Whiting, R. M. Doherty and W. J. Shuely, *J. Chem. Soc., Perkin Trans. 2*, in press.
18 M. J. Kamlet, R. M. Doherty, J.-L. M. Abboud, M. H. Abraham and R. W. Taft, *Chemtech*, 16 (1986) 566.
19 M. H. Abraham, R. M. Doherty, M. J. Kamlet and R. W. Taft, *Chem. Britain*, 22 (1986) 551.
20 M. J. Kamlet, R. M. Doherty, M. H. Abraham and R. W. Taft, *Quant. Struct.–Act. Relat.*, 7 (1988) 71.
21 M. H. Abraham, P. L. Grellier, D. V. Prior, P. P. Duce, J. J. Morris and P. J. Taylor, *J. Chem. Soc., Perkin Trans. 2*, (1989) 699.
22 M. H. Abraham, P. L. Grellier, D. V. Prior, J. J. Morris and P. J. Taylor, *J. Chem. Soc., Perkin Trans. 2*, (1990) 521.
23 M. H. Abraham, P. L. Grellier and R. A. McGill, *J. Chem. Soc., Perkin Trans. 2*, (1987) 797.
24 M. H. Abraham and R. Fuchs, *J. Chem. Soc., Perkin Trans. 2*, (1988) 523.
25 M. H. Abraham, P. L. Grellier, I. Hamerton, R. A. McGill, D. V. Prior and G. S. Whiting, *Faraday Disc. Chem. Soc.*, 85 (1988) 107.
26 F. Patte, M. Etcheto and P. Laffort, *Anal. Chem.*, 54 (1982) 2239.
27 J. G. Kirkwood, *J. Chem. Phys.*, 2 (1934) 351.

High-performance size-exclusion chromatography of porcine colonic mucins

Comparison of Bio-Gel® TSK 40XL and Sepharose® 4B columns

ANDREW S. FESTE*, DOMINIQUE TURCK and CARLOS H. LIFSCHITZ

USDA/ARS Children's Nutrition Research Center, Baylor College of Medicine, 1100 Bates, Houston, TX 77030 (U.S.A.)

(First received February 27th, 1990; revised manuscript received July 4th, 1990)

ABSTRACT

A high-performance size-exclusion chromatography (HPSEC) method was developed for the separation of porcine colonic mucins using a Bio-Gel® TSK 40XL HPSEC column (300 mm × 75 mm). In addition, porcine gastric and bovine submaxillary mucin preparations were used to describe more fully the separation characteristics of the HPSEC column. For comparison, the same preparations were also separated using a Sepharose® 4B column (100 cm × 2.6 cm). The colonic and gastric mucins eluted in the void volume (V_0) of both columns. Bovine submaxillary mucin was in the elution volume (V_e) of both columns. Analytical HPSEC of fractions (V_0 and V_e) of the various preparations obtained by Sepharose 4B chromatography exhibited retention times identical to those for fractions obtained by HPSEC. After separation by both methods, purified mucins were obtained by $CsCl_2$ density gradient ultracentrifugation; analytical HPSEC profiles, protein contents, and monosaccharide compositions of both gastric and colonic mucins from either column were similar. The HPSEC method, however, is ideally suited to separate microgram to milligram quantities of colonic mucin preparations quickly: 2 to 4 h, compared with 24 to 30 h for the Sepharose 4B method.

INTRODUCTION

The mucus of the gastrointestinal tract is a complex mixture of glycoproteins, water, electrolytes, lipids, and proteins of serous or cellular origin. The visco-elastic character and lubricating nature of mucosal surfaces result mainly from the presence of high molecular weight, polydisperse glycoproteins, namely mucins, which are synthesized and secreted all along the gastrointestinal tract by goblet cells [1].

Gastrointestinal mucins generally have molecular weights greater than $2 \cdot 10^6$ dalton and carbohydrate compositions between 60% and 80%. Mucins also contain various amounts of sulfate and have various ratios of constituent monosaccharides (sialic acid, N-acetylglucosamine, N-acetylgalactosamine, galactose and fucose). The oligosaccharide moieties are generally linked to serine and threonine residues of the protein component through acetal bonds (O-glycosidic) [2,3].

To study the developmental pattern of colonic mucins, we used miniature pigs as model organisms, because intestinal development and function in pigs resemble those in the human infant. Infant miniature pigs, however, can provide only limited amounts of tissue; therefore, a suitable micropreparative method was required. Porcine colonic mucins have a molecular weight of approximately $15 \cdot 10^6$ dalton and have been separated by Sepharose® 4B gel filtration [4]. The objective of this investigation was to determine whether high-performance size exclusion chromatography (HPSEC) could be used in lieu of gel filtration to separate colonic mucins. To describe the separation characteristics of the HPSEC column more completely and to compare its capabilities with those of the Sepharose 4B column, porcine gastric mucins ($2 \cdot 10^6$ dalton) and bovine submaxillary mucins (375 000 dalton) were also studied.

EXPERIMENTAL

Materials

Concentrated hydrochloric acid was purchased from Fisher (Pittsburgh, PA, U.S.A.). Durapore® hydrophilic filters (0.22 μm, 48 mm) were purchased from Waters (Milford, MA, U.S.A.). Molecular weight markers (MW-GF-1000 dit), enzyme inhibitors, deoxyribonuclease I (Type IV), ribonuclease (Type III-A), porcine gastric mucin Type II, bovine submaxillary mucin Type I, Trizma®, sodium azide, cesium chloride, Sepharose 4B, carbohydrate standards and all analytical procedure chemicals, with the exception of the BCA protein reagent (Pierce, Rockford, IL, U.S.A.) were purchased from Sigma (St. Louis, MO, U.S.A.). The Bio-Gel® TSK 40XL analytical column and guard columns were purchased from Bio-Rad (Richmond, CA, U.S.A).

Methods

Colonic specimen. A 6-month-old pig was killed by electrocution; the colon was rapidly removed and washed extensively with phosphate-buffered saline (PBS) that contained the following additives: sodium azide, 0.02%; phenylmethanesulfonyl fluoride (PMSF) (dissolved in 2.5% ethanol), 2 mM; N-ethylmaleimide, 10 mM; and sodium EDTA, 10 mM. The colon was opened along its longitudinal axis and the mucosa was scraped with a glass slide. The scrapings were suspended in 25 ml of 0.01 M Tris–HCl (pH 8.0, 0.02% sodium azide), homogenized for 30 s with a Tekmar Tissumizer Mark II (Cincinnati, OH, U.S.A.), then centrifuged at 34 000 rpm (105 000 g) for 1.0 h at 4°C. The supernatant was dialyzed against Milli-Q (Millipore, Houston, TX, U.S.A.) water for 2 days at 4°C and then lyophilized.

RNase and DNase digestion. Colonic, gastric, and submaxillary mucin preparations were dissolved in 20 to 40 ml of PBS, pH 7.0, that contained 0.02% sodium azide, 10 mM magnesium sulfate, 50 g/ml DNase, and 50 μg/ml RNase [5]. The mixtures were incubated at ambient temperature for 16.0 h. After incubation, each mixture was centrifuged for 30 min at 6000 g and 4°C. Each supernatant was then dialyzed extensively against Milli-Q water. The dialysates were frozen in liquid nitrogen and subsequently lyophilized.

Lipid extraction. Delipidation of the colonic mucin preparation was carried out by extraction with chloroform–methanol; two extractions were performed, first at 2:1, then 1:2 [6].

Sepharose 4B chromatography. Lyophilized colonic, gastric, and submaxillary mucin preparations (90 to 103 mg) were dissolved in 1.0 to 2.5 ml of 0.01 M Tris–HCl, pH 8.0, then loaded onto a 100 cm × 2.6 cm column containing Sepharose 4B that was previously equilibrated in 0.01 M Tris–HCl, pH 8.0, containing 0.02% sodium azide [7]. After elution at 18.0 ml/hour with equilibration buffer, 4.5-ml fractions were collected and peaks were located by determining the absorption of each fraction at 230 nm and 280 nm. Fractions that contained carbohydrates were detected at 492 nm using the phenol–sulfuric acid reaction [8].

High-performance size-exclusion chromatography. Size-exclusion chromatography was performed on a Waters 840 liquid chromatography system. A DEC 380 Professional computer (Digital Equipment Co., Maynard, MA, U.S.A.) was used for data acquisition and system control. Communication between the DEC 380 and the liquid chromatography components was established via a system interface module. A Model 510 pump was used for flow-rate control. Sample injections (10 to 150 μl) were performed by a Model 712 WISP auto-injector. Protein peaks were detected at 230 and 280 nm by using a Waters Model 490 Multiwavelength Detector.

A Bio-Gel TSK 40XL (7.5 mm × 300 mm, 10 μm) column was used to separate each mucin preparation. The column was equilibrated with 0.05 m Tris–HCl buffer (pH 8.0), and the proteins were eluted with the same buffer at a flow-rate of 1.0 ml/min. Before chromatography, the eluent was filtered through a Durapore hydrophilic filter (0.22 μm).

When the column was used preparatively, 4 to 12 mg of lyophilized material was dissolved in 100 to 150 μl of starting buffer and injected into the high-performance liquid chromatograph; 6 min after injection, 250-μl fractions were collected every 0.25 min. After separation of the sample, 20-μl aliquot was removed from each fraction and analyzed by HPSEC; the fractions that contained the void volume peak were pooled.

Molecular weight calibration. The HPSEC column was calibrated by injecting 20 μl of 1.0 mg/ml (in 0.05 M Tris–HCl, pH 8.0 buffer) solutions of carbonic anhydrase, bovine serum albumin, yeast alcohol dehydrogenase, sweet potato β-amylase, horse spleen apoferritin and bovine thyroglobulin. The peaks were detected by their absorbance at 230 nm.

To calibrate the Sepharose 4B column, the proteins were divided into two groups that were chromatographed separately. Carbonic anhydrase (3.0 mg), alcohol dehydrogenase (5.0 mg) and horse spleen apoferritin (10.0 mg) comprised the first group; the proteins were dissolved in 3.0 ml of Tris–HCl, pH 8.0, then loaded onto the column. The second group of proteins consisted of bovine serum albumin (10.0 mg), β-amylase (3.0 mg) and thyroglobulin (10.0 mg). After measuring the absorbance of each fraction at 230 nm, the elution volume of each peak was determined by measuring each fraction with a graduated cylinder.

Density gradient ultracentrifugation. Lyophilized material was dissolved in 15 ml of a 68% (68 g CsCl$_2$/100 ml PBS) solution; the final density of CsCl$_2$ was 1.42 g/ml. Density gradient ultracentrifugation was performed in a Beckman (Palo Alto, CA, U.S.A.) Model L2-70M ultracentrifuge using a vertical rotor VTi 50. The sample was spun at 36 000 g for 48 h at 4°C. After the run was completed, ten sequential 1.5-ml fractions were collected in a Beckman fraction recovery system. The density of each fraction was determined by weighing a 100-μl aliquot. Each fraction was exten-

sively dialyzed against Milli-Q water at 4°C. After dialysis to remove cesium chloride, the absorption of each fraction was measured at 230, 280 and 492 nm. In addition, 50-μl aliquots of each fraction were analyzed by HPSEC.

Protein assay. Protein concentrations were measured using the bicinchoninic acid (BCA) method [9].

Hydrolysis [10]. A 10-μg amount of separate mucin fractions (in 10 to 80 μl water) were placed into Waters Pico Tag® reaction vials; the vials were then placed into a hydrolysis chamber and dried under vacuum. For neutral monosaccharide determination, 200 μl of 2.0 M HCl were placed into the bottom of the hydrolysis chamber. The chamber was attached to a Waters Pico Tag hydrolysis station, and the interior of the chamber was evacuated, then flushed three times with nitrogen. The sealed chamber was placed into an oven and hydrolyzed for 4.0 h at 100°C. After gas-phase hydrolysis, the chamber was opened to release HCl. The residual HCl was removed under vacuum. The procedure was identical for the hydrolysis of amino sugars, except that 4.0 M HCl was used for a period of 6.0 h.

Neutral and amino sugar analysis [10].
After hydrolysis, 100 μl of Milli-Q water was added to each vial, and a 50-μl sample was analyzed by chromatography on a Dionex (Sunnyvale, CA, U.S.A.) CarboPak® anion-exchange column. An isocratic gradient using 16 mM NaOH at 1.0 ml/min was used to elute the monosaccharides. The monosaccharides were detected by a Dionex pulsed amperometric detector employing a gold electrode.

Sialic acid analysis. Sialic acid was determined by the method of Warren [11] after hydrolysis with 0.1 H_2SO_4 for 1 h at 80°C.

RNA, DNA and glucuronic acid determinations. RNA content was assessed by measuring the absorbance at 260 and 232 nm [12]. The DNA content was determined by using a fluorimetric method [13]. The glucuronic acid content was measured using the method of Bitter and Muir [14].

RESULTS AND DISCUSSION

As shown in Fig. 1, on both the Bio-Gel TSK 40XL and Sepharose columns, proteins with molecular weights between 150 000 and 669 000 dalton demonstrated a linear relationship between V_e/V_0 and the log of the molecular weight (where V_0 = void volume and V_e = elution volume). Neither carbonic anhydrase (29 000 dalton) nor bovine serum albumin (66 000 dalton) showed a linear relationship on either column. The deviation, however, was less for the HPSEC column than for the Sepharose 4B column. This result was expected because the approximate molecular weight fractionation range for globular proteins is 60 000 to 20 · 10^6 dalton [15] on the Sepharose 4B column and 10 000 to 4 · 10^6 dalton [16] on the Bio-Gel TSK 40XL (HPSEC) column.

The analytical profile (Fig. 2a) confirmed the presence of a high-molecular-weight component in the V_0 (6.74 min) of the HPSEC column after separation of the colonic mucin preparation. Non-mucin components that had a lower molecular weight eluted in a single peak at 10.0 min. The HPSEC micropreparative profile shown in Fig. 2b demonstrates column overloading (10.5 mg in 150 μl). Even so, Fig. 2d–f demonstrates the separation of the mucin fraction (V_0, 6.30 min) from the lower molecular weight components. The V_0 fraction (mucin) was obtained by pooling the
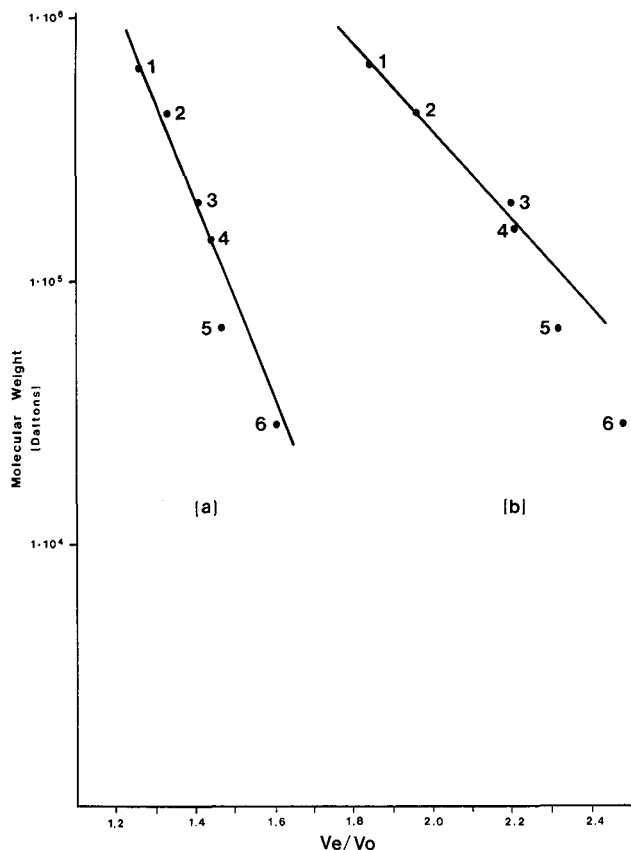
Fig. 1. Molecular weight calibration of the HPSEC (a) and Sepharose 4B (b) columns. The proteins were separated and the elution volumes were determined as described in the *Methods* section. Proteins: 1 = thyroglobulin (669 000); 2 = apoferritin (443 000); 3 = β-amylase (200 000); 4 = alcohol dehydrogenase (150 000); 5 = bovine serum albumin (66 000); 6 = carbonic anhydrase (29 000).

tubes collected from 6.00 to 7.50 min. Tubes collected from 7.75 to 12.0 min (Fig. 2e and f) demonstrated the presence of lower-molecular-weight components. The results obtained by Sepharose 4B chromatography (Fig. 2c) reflected those obtained by analytical HPSEC; the V_0 was easily separated from the lower-molecular-weight components. Both the analytical HPSEC and the Sepharose 4B chromatograms reflected, on the basis of absorbance at 230 and 280 nm respectively, the low amounts of V_0 material present in the colonic mucin preparation. After pooling, dialysis, lyophilization and weighing of the V_0 material, 2.7 and 4.7% (w/w) of the material applied to the HPSEC and Sepharose 4B columns, respectively, were recovered.

The results obtained in the separation of the gastric mucin preparation (Fig. 3a–f) were similar to those observed with colonic mucin. Although the molecular weight of porcine gastric mucin has been reported to be approximately $2 \cdot 10^6$ dalton [17], the mucin fraction eluted in the V_0 of both the HPSEC and Sepharose 4B columns. On the basis of the absorbance at 230 nm, analytical HPSEC reflected a
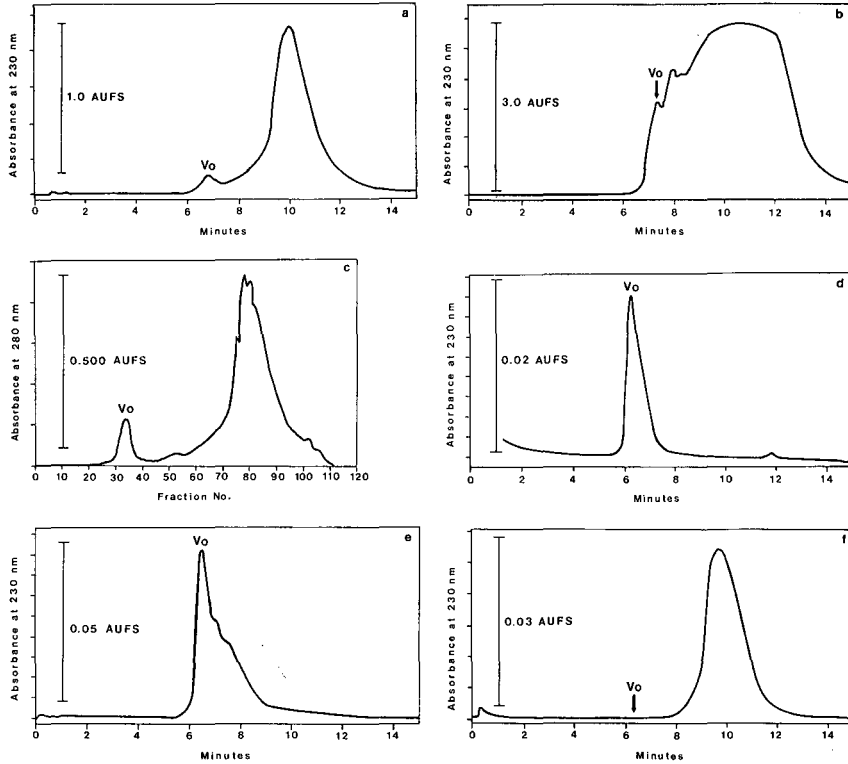
Fig. 2. Representation of the HPSEC and Sepharose 4B separations of adult porcine colonic mucin preparation after DNase and RNase treatment. (a) An analytical HPSEC injection (700 μg, 10 μl) was separated as described in the *Methods* section. The retention time of the mucin-containing fraction (V_0) was 6.74 min. (b) HPSEC micropreparative separation of 10.5 mg (150 μl). (c) Sepharose 4B separation of 101 mg (1.95 ml). Tubes 30–40 (V_0, fraction A), 48–54 (fraction B), and 70–95 (fraction C) were pooled. (d–f) 50-μl injections of HPSEC fractions collected between 6.75 and 7.0 min, 7.75 and 8.0 min, and 9.5 and 12.0 min, respectively. Tubes collected from 6.50 to 7.75 min (V_0, fraction A) and 9.75 to 12.0 min (fraction B) were pooled.

much larger V_0 population (relative to the included peak) than was present in the colonic preparation. After pooling, dialysis, lyophilization, and weighing, 16.8 and 19.4 (w/w) of the material applied to HPSEC and Sepharose 4B columns, respectively, was recovered in the V_0 fractions.

The molecular weight of bovine submaxillary mucins is approximately 375 000 dalton [18]; they would therefore be included in the elution volume of both columns. The analytical HPSEC profile (Fig. 4a) demonstrated the presence of one broad peak which eluted at 8.96 min. In contrast, the Sepharose 4B profile (280 nm monitoring) revealed a V_0 peak as well as an included peak. The Sepharose 4B V_0 fraction was collected, dialyzed, and lyophilized. The phenol sulfuric acid determination demonstrated the absence of carbohydrate, and because the material did not absorb at 230 nm (Fig. 4a), it was concluded that the V_0 fraction did not contain mucins. No further determinations were therefore made on the material.
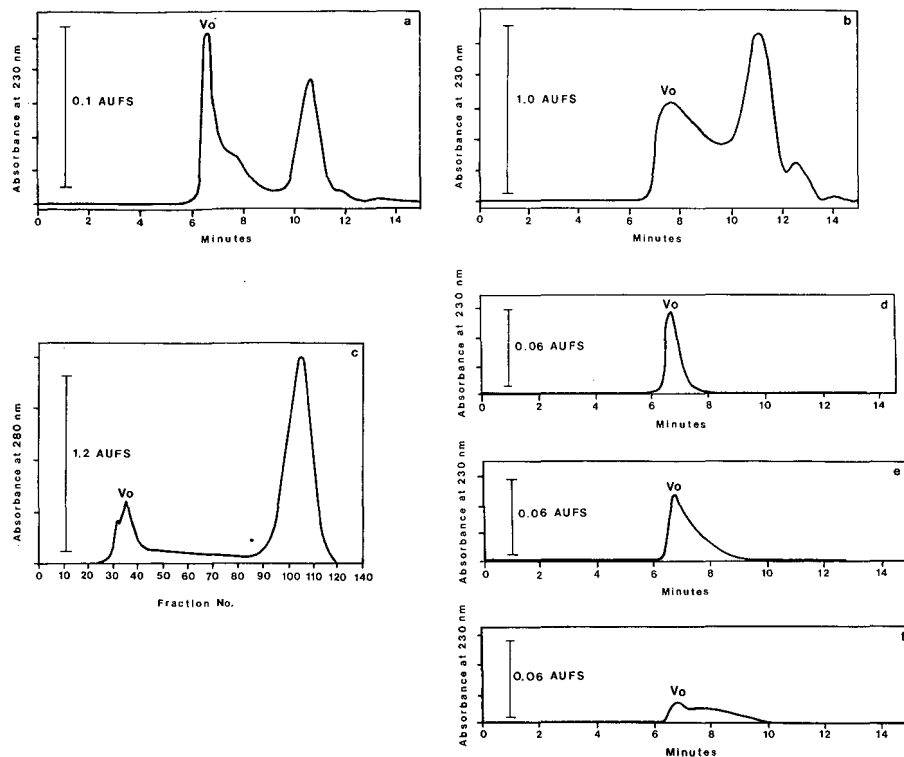
Fig. 3. Representation of the HPSEC and Sepharose 4B separations of porcine gastric mucin preparation after DNase and RNase treatment. (a) An analytical HPSEC injection (1.0 mg, 25 μl) was separated as described in the *Methods* section. The retention time of the mucin-containing fraction (V_0) was 6.61 min. (b) HPSEC micropreparative separation of 6.0 mg (150 μl). (c) Sepharose 4B separation of 209 mg (4.9 ml). Tubes 32–42 (fraction A) and 90–120 (fraction B) were pooled. (d–f) 50-μl injections of HPSEC fractions collected between 7.25 and 7.50 min, 8.00 and 8.25 min, and 9.25 and 9.50 min, respectively. Tubes collected from 6.75 to 7.75 min (V_0, fraction A) and 9.75 to 12.0 min (fraction B) were pooled.

The fractions obtained by HPSEC and Sepharose 4B separation were identical in retention times (Table I). Once the preparations were separated by HPSEC and Sepharose 4B chromatography, the pooled mucin-containing fractions were purified by $CsCl_2$ density gradient ultracentrifugation. After separation with either gel filtration or HPSEC followed by ultracentrifugation, the purified mucins were shown to be free of DNA, RNA and glucuronic acid. The monosaccharide and protein compositions of the HPSEC- and Sepharose 4B-separated colonic and gastric mucins (after ultracentrifugation) were similar to one another. The literature value for galactose in procine colonic mucin was 7% higher than the value we obtained, and the N-acetylglucosamine content was approximately 7% lower than either the HPSEC- or Sepharose 4B-separated mucins [4]. The composition of the HPSEC- and Sepharose 4B-separated porcine gastric mucins also agreed well with each other. However, the literature values were approximately 5% lower for N-acetylgalactosamine and 6% lower for sialic acid [17]. In contrast, the protein content reported in the literature was
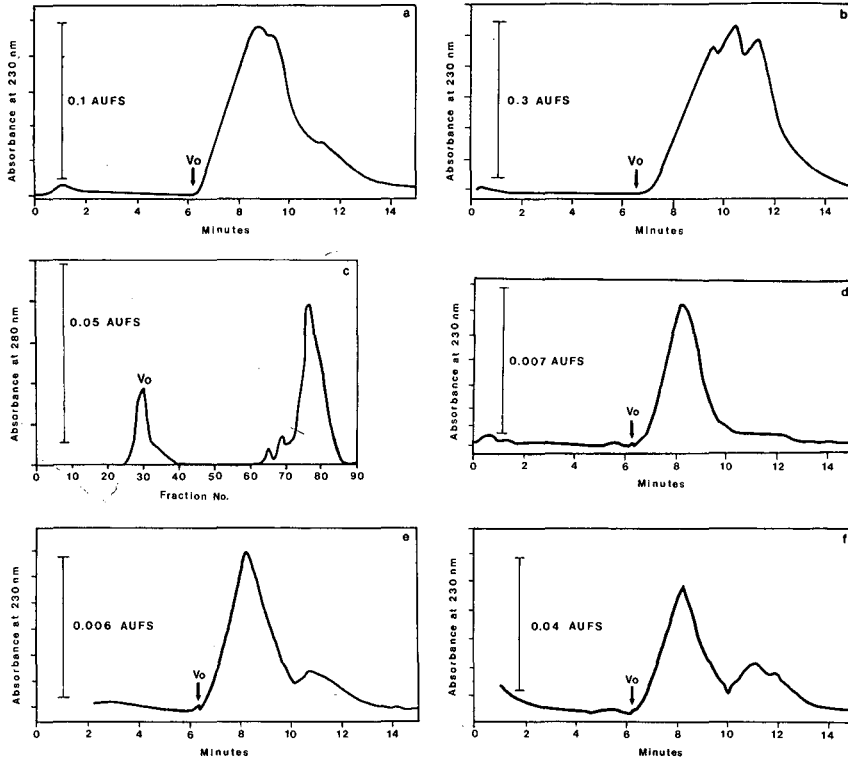
Fig. 4. Representation of the HPSEC and Sepharose 4B separations of bovine submaxillary preparation after DNase and RNase treatment. (a) An analytical HPSEC injection (2.12 mg, 20 μl) was separated as described in the *Methods* section. The single broad peak had a retention time of 8.96 min. (b) HPSEC micropreparative separation of 15.9 mg (150 μl). (c) Sepharose 4B separation of 103 mg (0.98 ml). Tubes 27–36 (V_0, fraction A) and 70–82 (fraction B) were pooled. (d-f) 50–μl injections of HPSEC fractions collected between 9.50 and 9.75 min, 10.75 and 11.0 min, and 11.75 and 12.0 min, respectively. Tubes collected from 9.0 to 10.75 min (fraction A) and 10.75 to 15.0 min (fraction B) were pooled.

TABLE I

RETENTION TIMES (t_R) OF POOLED FRACTIONATED MUCINS SEPARATED ON HPSEC AND SEPHAROSE 4B COLUMNS AND ANALYZED ON AN HPSEC COLUMN

Mucin	HPSEC		Sepharose 4B	
	Fraction	t_R (min)	Fraction	t_R (min)
Colonic	A (V_0)	6.43	A(V_0)	6.43
Gastric	A (V_0)	6.51	A (V_0)	6.49
Colonic	B	9.56	B	9.67
Gastric	B	10.6	B	10.6
Submaxillary	B	8.33	B	8.32

approximately 10% higher than the value we found. The starting material for this study was a commercial preparation, and the method by which the preparation was obtained was not available. Consequently, the differences between the values determined in this study and those in the literature may be result of different methods for isolation of the mucin fraction before chromatography and ultracentrifugation.

The compositions of the HPSEC- and Sepharose-separated submaxillary mucins were in fair agreement with each other. The relatively poorer agreement between the values of the two methods probably resulted from the inclusion of the mucins by both columns, and from the fact that the separations were not equivalent. The separation of submaxillary mucins was included in this investigation only for the purpose of comparing the HPSEC and Sepharose 4B methods; the values for submaxillary mucins reported in the literature (Table II) were obtained by using non-chromatographic methods of separation [18].

TABLE II

PROTEIN AND MONOSACCHARIDE COMPOSITION OF PURIFIED PORCINE COLONIC (PC), PORCINE GASTRIC (PG) AND BOVINE SUBMAXILLARY (BS) MUCINS (%, w/w)

Literature values are given without the sulfate content.

	Composition (%, w/w)								
	PC			PG			BS		
	HPSEC	Sepharose	Lit. [12]	HPSEC	Sepharose	Lit. [17]	HPSEC	Sepharose	Lit. [18]
Fucose	14.6	12.0	12.0	12.3	12.3	14.3	1.88	2.35	0.91
Galactose	17.3	17.4	24.0	29.0	30.6	32.9	6.51	5.31	5.15
N-Acetyl galactosamine	10.9	11.8	9.58	12.9	13.0	10.5	15.6	11.3	—
N-Acetyl glucosamine	32.4	34.8	27.6	32.6	29.2	24.7	—	—	18.8[a]
Sialic acid	13.0	11.4	11.4	6.51	8.72	0.25	25.5	28.1	21.2
Protein	11.8	12.8	15.3	6.74	7.10	17.2	50.6	52.8	53.9

[a] Total hexosamine content.

The objective of this study was to determine whether the HPSEC method could replace Sepharose 4B in the purification of colonic mucins. Preliminary experiments (data not shown) showed that very small amounts of mucins were present in colonic mucosal scrapings of infant miniature pigs. To harvest more mucins, we decided to see whether we could collect more of the lower molecular weight fractions and remove the contaminant components with the density gradient ultracentrifugation step; separation would be contingent on the lower-molecular-weight protein/glycoprotein having a lower density. Secondly, the density gradient ultracentrifugation step was originally implemented to separate a low-density, high-molecular-weight, non-mucin glycoprotein (present in the HPSEC or Sepharose 4B V_0 fractions) from the high-density, high-molecular-weight mucins [19]. To date, only high-molecular-weight, high-density colonic mucins have been described [11]. In Fig. 5a, one can observe the
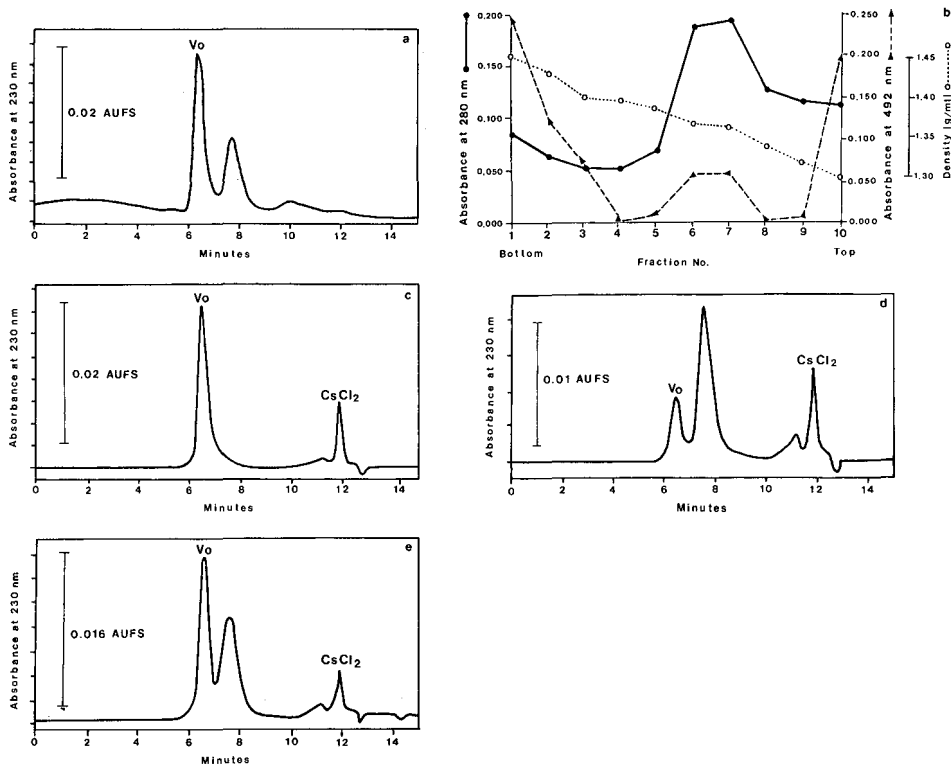
Fig. 5. HPSEC demonstration of the removal of two non-mucin components by density gradient ultracentrifugation. (a) Depiction of an HPSEC analytical profile of an HPSEC-purified preparation obtained by pooling fractions from 6.50 min to 8.35 min (instead of 6.5 min to 7.75 min). The V_0 peak eluted at 6.42 min and the second peak eluted at 7.77 min. (b) Density gradient ultracentrifugation separation of the sample depicted in (a). (c–e) Representation of HPSEC analytical profiles of ultracentrifuge fractions: density = 1.452 (highest density), 1.338 and 1.323 g/ml (lowest density), respectively. The retention time of the V_0 peak found in the density = 1.452 g/ml fraction was 6.49 min while the retention times of the two peaks found in the density = 1.338 g/ml and density = 1.32 g/ml fractions were 6.48, 7.62 min, and 6.58, 7.62 min, respectively.

lower-molecular-weight peak at 7.77 min that was purposely included into the pooled mucin fraction. Fig. 5b represents the density gradient separation of the mixture depicted in Fig. 5a. The high-density fraction (Fig. 5c) contained only the V_0 (mucin) peak. The middle density fractions (data not shown) contained trace amounts of V_0 material. The two low-density fractions (Fig. 5e and f) contained the high-molecular-weight V_0, non-mucin, glycoprotein and the lower-molecular-weight contaminant which eluted at 7.77 min.

Our results indicate that the HPSEC method is ideally suited for the separation of colonic mucins, and although the composition determined for gastric mucins differed from literature values, the monosaccharide and protein compositions of the HPSEC and Sepharose 4B mucins were similar. In contrast to the Sepharose 4B separation, which requires larger samples and longer elution times (24 to 30 h), the

HPSEC method can separate microgram to milligram quantities in 15.0 min. Even if 5 to 10 preparative injections must be made for the same sample, total separation time will require only 2 to 3 h. In addition, the HPSEC method can be used analytically to locate mucins in various chromatographic or ultracentrifugation fractions, which enable conservation of small quantities of mucins.

ACKNOWLEDGEMENTS

REFERENCES

1 M. R. Neutra and J. F. Forstner, in L. R. Johnson (Editor), *Physiology of the Gastrointestinal Tract*, Raven Press, New York, 1987, pp. 975–1009.
2 P. Roussel, G. Lamblin, M. Lhermitte, N. Houdret, J. J. Lafitte, J. M. Perini, A. Klein and A. Scharfman, *Biochimie*, 70 (1988) 1471–1482.
3 C. L. Laboisse, *Biochimie*, 68 (1986) 611–617.
4 T. Marshall and A. Allen, *Biochem. J.*, 173 (1978) 569–578.
5 A. E. Haviland, M. J. Borowitz, M. S. Lan, B. Kaufman, A. Khorrami, P. C. Phelps and R. S. Metzgar, *Gastroenterology*, 95 (1988) 1302–1311.
6 W. J. Esselman, R. A. Laine and C. C. Sweeley, *Methods Enzymol.*, 28 (1972) 140–156.
7 D. K. Podolsky and K. J. Isselbacher, *J. Clin. Invest.*, 72 (1983) 142–153.
8 M. Dubois, K. A. Gilles, J. K. Hamilton, P. A. Rebers and F. Smits, *Anal. Chem.*, 28 (1956) 350–356.
9 P. K. Smith, R. I. Krohn, G. T. Hermanson, A. K. Mallia, F. K. Gartner, M. D. Provenzano, E. K. Fujimoto, N. M. Goeke, B. J. Olson and D. C. Klenk, *Anal. Biochem.*, 150 (1985) 76–85.
10 M. R. Hardy, R. R. Townsend and Y. C. Lee, *Anal. Biochem.*, 170 (1988) 54–62.
11 L. Warren, *J. Biol. Chem.*, 234 (1959) 1971–1977.
12 A. Fleck and H. N. Munro, *Biochim. Biophys. Acta*, 55 (1962) 571–583.
13 C. F. Cesarone, C. Bolognesi and I. Santi, *Anal. Biochem.*, 100 (1979) 188–197.
14 T. Bitter and H. M. Muir, *Anal. Biochem.*, 4 (1962) 330–334.
15 *Products Catalog*, Pharmacia LKB Biotechnology, Piscataway, NJ 1989, p. 162.
16 *Product Catalog*, Bio-Rad, Richmond, CA, 1990, p. 88.
17 B. J. Starkey, D. Snary and A. Allen, *Biochem. J.*, 141 (1974) 633–639.
18 A. Gottschalk, A. S. Bhargava and V. L. N. Murty, in A. Gottschalk (Editor), *Glycoproteins, Their Composition, Structure and Function*, Elsevier, Amsterdam, New York, 1966, pp. 810–829.
19 J. M. Creeth and M. A. Denborough, *Biochem. J.*, 117 (1970) 879–891.

Analysis of 2,4,6-trinitrotoluene and its transformation products in soils and plant tissues by high-performance liquid chromatography

SCOTT D. HARVEY*, ROBERT J. FELLOWS, DOMINIC A. CATALDO and ROGER M. BEAN

Pacific Northwest Laboratory, Battelle Boulevard, P.O. Box 999, Richland, WA 99352 (U.S.A.)

(Received May 9th, 1990)

ABSTRACT

Previous studies have failed to provide an acceptable mass balance for 2,4,6-trinitrotoluene (TNT) in soils and plants due to deficiencies in analytical methodology. A high-performance liquid chromatographic (HPLC) method for soil analysis is reported which allowed for a mass balance in excess of 88% during a 2-month study. A method for plant analysis was developed which involved fractionation of organic extracts on Florisil adsorbent, to remove interfering pigments, followed by HPLC analysis of TNT and the primary metabolites, 2-amino-4,6-dinitrotoluene and 4-amino-2,6-dinitrotoluene. Chromatographic recovery of TNT from spiked tissues was 85 ± 6%. The methodology was utilized to investigate TNT uptake and metabolism in plants grown in TNT hydroponic solutions.

INTRODUCTION

Wastewaters contaminated with 2,4,6-trinitrotoluene (TNT) are produced by munitions manufacturing and packaging facilities, which use water to rinse TNT residues from equipment, rejected shells, and the interior surfaces of the facilities. The waste effluents contain up to 100 mg/l TNT [1,2]. The fact that approximately $2 \cdot 10^6$ liters of such wastewater are produced daily from a single facility emphasizes the magnitude of the potential pollution problem [3]. In the past, wastewater has been directed to lagoons for settling of solid material prior to release to rivers and streams [4,5]. Over time, explosive residues and their transformation products have accumulated in large areas of soil formerly occupied by the settling lagoons. Concerns about the environmental fate of these residues are now intensified because recent revegetation of these contaminated plots allows for the possible introduction of TNT, TNT transformation products, and plant-produced TNT metabolites into the food chain.

There is a basis for concern about the toxicity of TNT. Cases of liver damage and anemia among chronically exposed munition workers are well documented [6–8]. Exposure to TNT has been shown to be toxic to a large variety of biota including green algae, oyster larvae [9], fungi, Gram-positive bacteria [5], fish [10,11], rats and mice [12] as well as plants [1]. In addition, TNT has been found to be mutagenic in the Ames bacterial assay [13].

A number of investigations have examined the metabolism of TNT in bacterial, animal, and plant systems. In a study conducted by McCormick *et al.* [6], bacteria

were shown to reduce TNT to 2-amino-4,6-dinitrotoluene (2-AMDNT) and 4-amino-2,6-dinitrotoluene (4-AMDNT) through the successive formation of nitroso and hydroxylamino intermediates. Interestingly, reduction was found to occur most extensively in the para position [6]. Several studies examining the uptake and metabolism of TNT by plants have identified the AMDNT isomers as TNT metabolites [1,14,15]. The metabolic pathway in plants also favors the formation of 4-AMDNT over reduction to 2-AMDNT. Metabolic studies involving animals have identified 4-AMDNT, 2,4-diamino-6-nitrotoluene, 2,2',6,6'-tetranitro-4,4'-azoxytoluene, or the corresponding gulcuronide conjugates in urine of experimental animals that had been fed TNT [6]. There has been no evidence for the biological cleavage of the aromatic ring of TNT [6]. This universal metabolism of TNT by bacteria, animals, and plants to the AMDNT isomers is significant, as both the toxicity and mutagenicity of the AMDNT isomers have been demonstrated [13].

In order to assess the impact of TNT on food-chain transfer, the transformations of TNT in soils, as well as the uptake and metabolism of parent compound and associated transformation products by plants, need to be delineated. Although a variety of analytical methods have been described for recovery and analysis of TNT and tranformation products in soils, demonstration of an acceptable mass balance has not been realized. Analysis for TNT, TNT transformation products, and TNT-related metabolic products in plant tissues presents a new dimension in difficulty due to the highly complex nature of biological matrices. It is not surprising that previous attempts to delineate these complex phenomena have been plagued by analytical interferences, poor reproducibility, and low material balance [1,14,15]. The analytical approach to these problems mandate the use of both high-resolution analytical techniques and radiolabeled analyte. For instance, a study by Palazzo and Leggett [1] utilized tissue from plants grown in hydroponic solutions containing cold TNT. The plant tissues were subjected to acid hydrolysis, benzene extraction, and analysis by gas chromatography (GC) with electron-capture detection. These authors were able to identify and quantitate both the AMDNT isomers and TNT; however, since radiolabeled TNT was not used, it was impossible to determine what percentage of plant-sequestered TNT was ultimately present in these three chemical forms. Radiolabeled studies have the additional advantage of allowing for unambiguous identification of metabolic transformation products.

Accurate assessment of environmental and health risks demand analytical methods that provide for an acceptable mass balance. The primary goal of the study was therefore to develop an analytical methodology for the examination of TNT and TNT transformation and/or metabolic products in soils and plant tissues that would satisfy the mass balance criterion. Due to the limited thermal stability of explosives residues, a method utilizing high-performance liquid chromatography (HPLC) was developed.

MATERIALS AND METHODS

Uniformly ring-labeled [^{14}C]TNT (specific activity of 5.3 mCi/mmol) was obtained from E.I. du Pont de Nemours (Boston, MA, U.S.A.). Radiopurity, based on HPLC radiochromatography, was 99.86%. 2-Amino-4,6-dinitrotoluene was a Standard Analytical Reference Material (SARM) obtained from the U.S. Army Toxic and Hazardous Materials Agency (Aberdeen Proving Ground, MD, U.S.A.).

Soil characterization and sampling

Palouse soil, representing a typical Washington State agricultural soil, was used for all studies. Palouse is a silt-loam, mixed mesic Pachic Ultic Haploxeroll. The sample was collected at Pullman, WA, U.S.A., and consisted of the Ap horizon [23]. This soil is 77% silt, and 21% clay, contains 2% organic matter, and has a cation-exchange capacity of 23.8 mequiv./100 g and a pH of 5.6. For soil experiments, a solution containing appropriate proportions of labeled and vacuum-desiccated unlabeled TNT (Chem Service, West Chester, PA, U.S.A.) was prepared in 2.0 ml of methanol and amended with 400 g of air-dried soil to give a final concentration of 60 ppm TNT containing 10 μCi of labeled TNT. Amended soils were immediately brought to and maintained at 0.66 of field capacity with water. After initial sampling, which occurred no later than 2 h after amendment, the soils were maintained in a growth chamber environment that simulated the luminous intensity and spectral dispersion of sunlight during the 16-h daily light cycle. Sampling occurred at 0, 10, and 60 days and consisted of placing approximately 10 g of soil into a pre-weighed Soxhlet extraction thimble.

Plant cultivation and sampling

The chemical fate of TNT in plants was evaluated using bush beans (*Phaseolus vulgaris*, tendergreen) grown from seed. Plants were grown for 21 to 26 days on hydroponic nutrient solutions as described previously [16], at which time solutions were amended with a total of 10 ppm TNT, containing 5 μCi of radiolabel per 500 ml. These solutions were filter sterilized and placed in autoclaved 500-ml beakers to minimize bacterial contamination, which could promote transformation of TNT. Bush bean plants were placed in these solutions and maintained in a growth chamber until harvested at 1 and 7 days. The beakers were jacketed in an opaque sheath to protect the roots from light, as well as to minimize the photolysis of TNT. Solutions were analyzed by HPLC and liquid scintillation spectrometry at 0, 1 and 7 days. At harvest, plants were removed from the hydroponic solutions and the roots rinsed with 0.10 M calcium chloride followed by a rinse in methanol–water (80:20). Plants were then separated into roots, stems, and leaves; the tissues were minced, thoroughly mixed, and stored at $-80°$C until analysis.

Soil extraction

Soils were subjected to exhaustive Soxhlet extraction with 200 ml of methanol (J. T. Baker HPLC Grade) for 48 h. The soil extracts were filtered through a 0.22-μm nylon 66 filter (Alltech, Deerfield, IL, U.S.A.) before reducing the volume to approximately 20 ml by rotary evaporation. The concentrated extract was again filtered through a 0.22-μm filter, and the final volume was adjusted to a total of 25.0 ml. Extracted soils were dried at 105°C overnight, cooled in a desiccator, and weighed to obtain an accurate oven-dry weight. Portions of the extracted soils were further analyzed by total combustion in a Packard Model 306 oxidizer (Packard, Downers Grove, IL, U.S.A.) to determine the amount of irreversibly bound TNT residues that were not removed by Soxhlet extraction. The extraction efficiency of the procedure was obtained by comparing the amount of radiolabel contained in the final methanol extract to the amount of label originally added to the soil (both values were determined by liquid scintillation spectrometry). The methanol extract was subsequently analyzed for TNT and transformation products by HPLC as described below.

Tissue extraction and fractionation

 The extraction and fractionation scheme for plant tissues is outlined in Fig. 1. A 1.0-g sample of fresh weight tissue was homogenized for 2.5 min in a Sorvall Omni-Mixer (Newtown, CT, U.S.A.) with 10.0 ml of 1 M hydrochloric acid and approximately 0.5 g of dry ice. After transfer to a 25-ml Corex centrifuge tube, the tissue was subjected to acid hydrolysis by immersing the tube into a boiling water bath for 1 h. After cooling to room temperature, the hydrolyzed material was extracted with 10.0 ml of diethyl ether. The phases were separated by centrifugation for 10 min at 3000 g. The volume of each layer was recorded and 100-μl aliquots were removed for liquid scintillation spectrometry. The radioactivity remaining in the pellet was determined by oxidation followed by liquid scintillation spectrometry. To
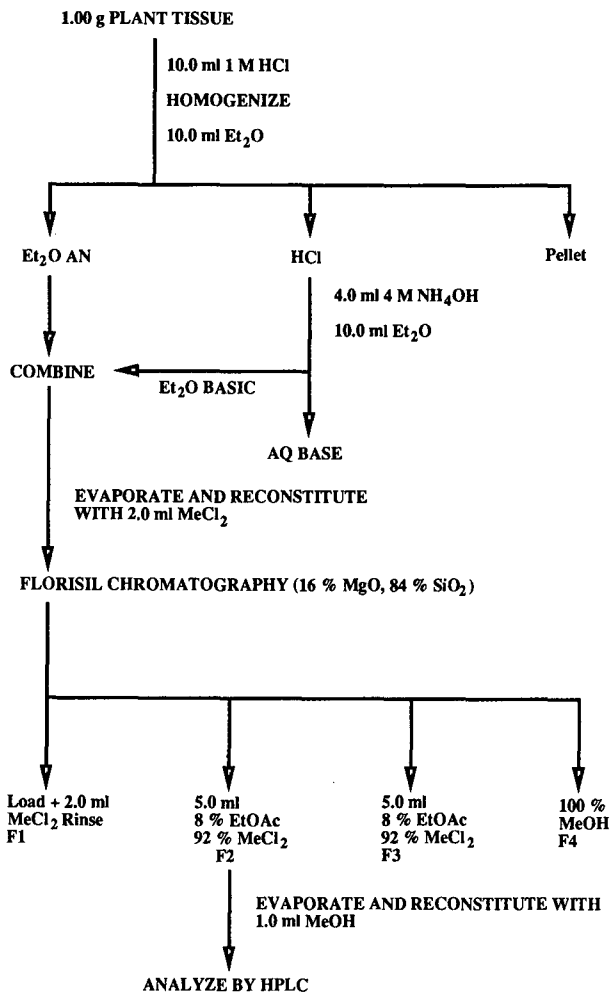
Fig. 1. Flow chart outlining the extraction and fractionation of plant tissues. AN = Acid–neutral; Et$_2$O = diethyl ether; MeCl$_2$ = methylene chloride; EtOAc = ethyl acetate; MeOH = methanol; AQ = aqueous.

obtain an extract of the basic organics, the hydrochloric acid layer was made basic by the addition of 4.0 ml of 4 M NH$_4$OH and extracted with a second 10.0-ml portion of diethyl ether. The layers were separated by centrifugation, the volumes recorded, and subsamples taken for liquid scintillation spectrometry. The two ether extracts were combined, evaporated to dryness with a stream of dry nitrogen, and reconstituted with 2.0 ml of methylene chloride.

The methylene chloride sample was applied to a Sep-Pak Florisil column (Waters, Milford, MA, U.S.A.) which had previously been equilibrated with methylene chloride. An additional 2.0 ml of methylene chloride was used to rinse the remaining residue from the sample vial to the Florisil column. The column eluate collected during the application of the sample comprised fraction 1. Fractions 2 and 3 were eluted from the column with successive 5.0-ml portions of methylene chloride–ethyl acetate (92:8). The final fraction (fraction 4) was eluted from the Florisil column by 5.0 ml of methanol. This strong solvent was chosen to strip the column of the maximal amount of adsorbed material. Volumes of the Florisil fractions were recorded and 100-μl aliquots were taken for liquid scintillation spectrometry. Prior to HPLC analysis, fraction 2 was evaporated to dryness and the residue was dissolved in 1.0 ml of methanol.

Residue analysis

The HPLC system consisted of a Waters Model 600E pump and system controller. The methanol extract (20 μl) of soil or plant tissue extracts was injected by a Waters WISP 710 automatic injector onto a Beckman Ultrasphere 5-μm octadecyl silica column and the components separated by a linear solvent program at a flow-rate of 1.0 ml/min. The solvent system was water–acetonitrile, with a 20-min gradient from 40% to 100% acetonitrile. Components were detected by UV absorption at 254 nm (Waters Model 490E detector), with a detector sensitivity of 0.008 a.u.f.s. Peak areas obtained from a Hewlett-Packard 3390 integrator were used for quantitative measurements.

Radiochromatographic detection was extensively used for unambiguous identification of transformation products arising from TNT. During selected chromatographic runs, the column eluate was collected in 0.5-ml increments for a total of 30 min. Each fraction was assayed for radioactivity by liquid scintillation spectrometry. Radiochromatograms were generated by plotting the disintegrations per min (dpm) in each successive aliquot as a function of retention time. Transformation products and/or metabolites identified in this manner were collected by repetitive HPLC runs to accumulate enough material for sebsequent mass-spectral studies.

GC–mass spectrometry (MS) studies utilized a Hewlett-Packard 5970 mass-selective detector interfaced to a Hewlett-Packard 5990A gas chromatograph. Transformation products were purified by HPLC as described above, evaporated to dryness with dry nitrogen, and dissolved in a small aliquot of hexane. Analysis consisted of a 1-μl splitless injection onto a 30 m × 250 μm I.D. DB-5 column containing a 1.0-μm film of stationary phase (J & W Scientific, Folsom, CA, U.S.A.). The separation was accomplished with helium carrier gas and a temperature program from 40 to 280°C at 6°C/min. Nominal resolution mass spectra were obtained by scanning the quadrupole mass spectrometer from 40 to 600 a.m.u. at a rate of 200 a.m.u./s.

Determination of $^{14}CO_2$ and volatile products

Evolution of volatile organics and $^{14}CO_2$ from plants and soils were examined by a previously described technique [17]. Soils were placed in a sealed canister and plants in a specially designed chamber that isolated the aerial portions from the roots. Air was drawn by vacuum sequentially through the chamber, two XAD columns (to trap volatile organics), and four bubbler traps (to trap $^{14}CO_2$) at a rate of 500 ml/min. Each bubbler initially contained 10.0 ml of 3 M sodium hydroxide. After each 24-h collection period, volumes remaining in the sodium hydroxide traps were recorded and material adsorbed on the XAD columns (100 $\times$ 5.0 cm) eluted with methanol. Radioactivity contained in methanol and sodium hydroxide samples were determined by liquid scintillation spectrometry.

Palouse soil, amended with 10-ppm TNT containing 20 μCi ^{14}C/400 g, was allowed 21 days to equilibrate prior to examining the evolution of volatiles and $^{14}CO_2$. The soil experiment was conducted for 6 consecutive days. Volatiles emanating from a mature hydroponically-grown bush bean plant were collected for three consecutive days. The plant was maintained on a 10-ppm TNT nutrient solution containing 5 μCi/500 ml during this experiment.

RESULTS

Purity of the radiolabeled TNT was determined to be 99.86% by radiochromatography. This purity was judged to be sufficient for subsequent metabolic studies and was used without further purification.

Soil fate of TNT

Chromatograms of methanol extracts from Palouse soil, a soil containing an intermediate organic content, produced blanks which were devoid of any interfering peaks. Chromatographic profiles of Palouse soil containing 60 ppm TNT are shown in Fig. 2. The top chromatogram is from an extraction initiated immediately after amendment of the soil with TNT. The retention time of TNT under the chromatographic conditions utilized in this study was 13.46 min. The chromatogram shown in the bottom of Fig. 2 is from a methanol extract of soil aged for 10 days with TNT. This chromatogram shows the presence of TNT as well as a peak that elutes immediately prior to TNT. The presence of radioactivity was verified in the first eluting peak, indicating that TNT had been transformed in the soil during the 10-day period. Co-injection experiments showed that 2-amino-4,6-dinitrotoluene and the unknown peak co-eluted. Further evidence for the identity of the unknown peak was provided by GC–MS studies. GC–MS analysis of this HPLC peak gave a chromatogram containing two peaks having identical mass spectra. One peak (retention time 29.24 min) was identified as 2-amino-4,6-dinitrotoluene as evidenced by a match of retention time and mass spectra with the SARM authentic standard. The mass spectrum of the second GC–MS peak (retention time of 28.41 min) indicated a structural isomer of 2-amino-4,6-dinitrotoluene, most likely the 4-amino-2,6-dinitrotoluene isomer. The 4-amino-2,6-dinitrotoluene isomer was found to be present at nearly twice (1.8 times) the abundance of the 2-amino-4,6-dinitrotoluene isomer.

The mass balance for TNT aged in Palouse soil for a 3-month period is presented in Table I. Average values from the triplicate analyses and the associated standard
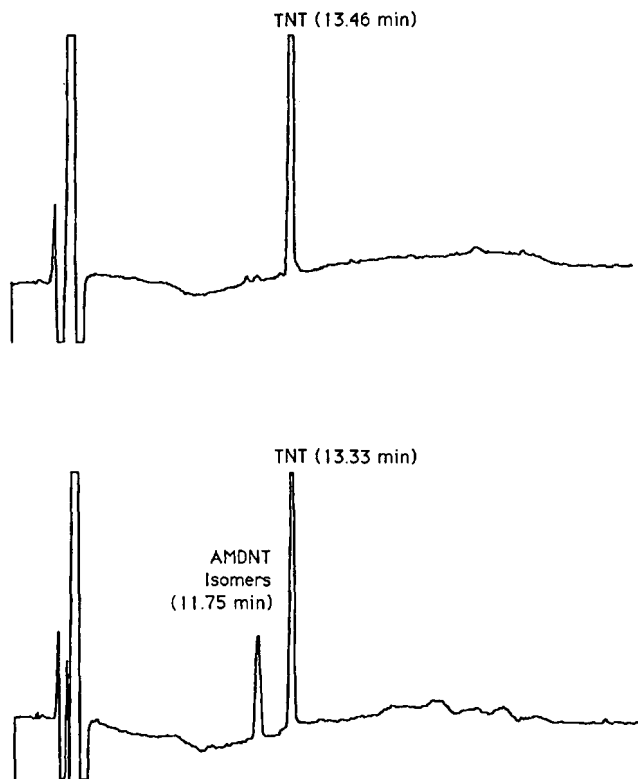
Fig. 2. Chromatographic profiles of methanol extracts of TNT in Palouse soil. The upper chromatogram is from an extract performed immediately after amendment; the bottom chromatogram is from an extract of soil aged with TNT for 10 days.

deviations are shown in Table I. The first column lists the percentage of total radio-activity added to the soil that was extracted by methanol during the Soxhlet extraction procedure. The second column presents the percentage of TNT that was recoverable in an unaltered form as determined by HPLC studies. The third column is the percentage of total TNT that was left in the soil after Soxhlet extraction as determined by oxidation of the extracted soil and quantitation of the resulting $^{14}CO_2$ by

TABLE I

MASS BALANCE OF PALOUSE SOIL CONTAINING TNT

Time (days)	Radiolabel in methanol extract (%)	Unaltered TNT (%)	Radiolabel in soil after extraction (%)	Mass balance deficit
0	94 ± 1	88 ± 1	0.7 ± 0.1	5%
10	71 ± 2	57 ± 4	17 ± 3	12%
61	60 ± 2	36 ± 3	30 ± 1	10%

liquid scintillation spectrometry. The last column shows the percentage of TNT that could not be accounted for in either the methanol extract or the extracted soil [100 − (column 1 + column 3)].

A small amount of $^{14}CO_2$ was observed to be evolved from Palouse soil during the 6-day collection of volatiles. Assuming a constant CO_2 generation rate during the 2-month study, a quantity equal to 4% of the TNT was oxidized to CO_2. Emission of volatile organics from Palouse soil was not observed.

Analysis of hydroponic solutions

Aerated control solutions of TNT that were shielded from the growth chamber lights showed only minimal losses of TNT during the 7-day study. Control solutions that were exposed to the growth chamber lights (both non-aerated and aerated) displayed a stab.° amount of radiolabel (average of 4.7 μCi, n = 6); however, the concentration of TNT was found to decline to an average of 3.0 ppm (n = 5) after 7 days. The disparity between radiolabel and TNT concentration was coincident with the appearance of a pink photodecomposition product. The pink product was not analyzed but was believed to be the same photodecomposition product observed and characterized by Spanggord et al. [18]. The aminodinitrotoluene isomers were not observed in control solutions even after 7 days.

Analysis of solutions used to support bush beans showed both plant uptake and root catalytic transformations. Radiolabel decreased from the initial 5.0 μCi/beaker to 3.5 and 0.6 μCi/beaker at 1 and 7 days, respectively. The amount of TNT as determined by HPLC decreased from 10 to 2 ppm within 24 h and was below the detection limit of 0.1 ppm by 7 days. Transformation products observed in the chromatographic profiles included the aminodinitrotoluene isomers and a smaller amount of an unknown compound eluting with a retention time of 17.38 min. Incorporation of radiolabel in this unknown compound was verified by radiochromatography.

Fate of TNT in plant tissue

Initial plant studies examined the extent of conjugation of the TNT-derived radiolabel present in plant tissues. Leaf tissue from a bush bean grown in hydroponic culture for 7 days was homogenized with water and subsequently extracted with diethyl ether. Only 4% of the total label was found to partition into the diethyl ether layer, while 57% of the label remained in the water layer. This indicated that the TNT was metabolized to very polar and perhaps conjugated forms. In an attempt to free possible conjugates, an acid hydrolysis was implemented immediately after homogenization. A subsample of the above leaf tissue was hydrolyzed with 1 M hydrochloric acid for 1 h prior to extraction with diethyl ether. It was found that 23% of the radiolabel was now ether extractable; 41% remained in the hydrochloric acid layer. By either extraction with acid hydrolysis or water extraction, slightly over 60% of the total radiolabel was found to be solubilized in the aqueous or ether layers. In all subsequent experiments the plant tissue was homogenized, hydrolyzed with acid, and then extracted with diethyl ether. The fractions resulting from the partitioning between the 1 M hydrochloric acid and the diethyl ether layers are referred to as the hydrochloric acid and the diethyl ether acid–neutral fractions, respectively.

Initial methanol and chloroform–methanol extraction of plant tissue indicated the need for further fractionation before HPLC analysis due to the the co-extraction

of interfering pigments. Radiolabeled TNT was spiked (2.93 ppm fresh weight) onto bush bean leaves, the tissue homogenized, and the mixture extracted with methylene chloride. The organic layer was then subjected to fractionation on Florisil adsorbent with the collection of four fractions (F1–F4). Radiolabeled TNT eluted in fraction F2; the plant pigments were found to elute in fractions F3 and F4. In order to demonstrate the recovery and reproducibility of this separation, triplicate samples were fractionated and fraction F2 was further examined by HPLC and liquid scintillation spectrometry. The recovery of TNT in fraction F2 as based on chromatographic peak areas was 85 ± 6%, whereas the recovery of radiolabel was 83 ± 4%. It was subsequently found that the aminodinitrotoluene isomers co-elute from the Florisil column in fraction F2 along with the TNT.

Bush bean tissue samples were acid hydrolyzed, extracted into diethyl ether, and subjected to Florisil fractionation as described above. The amount of radiolabel contained in the tissues and the percentage of total radiolabel in each chemical fraction for bush bean leaves, stems, and roots are shown in Table II. Interestingly, it was found that the aminodinitrotoluene isomers were extracted from 1 M hydrochloric acid into diethyl ether. The combined electron-withdrawing property of the nitro substituents is responsible for the neutral behavior of these compounds. This property permitted the co-extraction and quantitation of the aminodinitrotoluene isomers along with TNT. Representative HPLC chromatograms of the F2 fractions from bush bean leaf, stem, and root tissues are shown in Figure 3; Table III gives the concentrations based on the tissue fresh weight for TNT and the aminodinitrotoluene isomers.

TABLE II

TOTAL RADIOACTIVITY (AS BASED ON OXIDATION), PERCENTAGES OF TOTAL RADIO-
ACTIVITY IN CHEMICAL FRACTIONS AND MATERIAL BALANCE FOR THE ANALYSIS OF
BUSH BEAN TISSUES

Values are the averages from analysis of 3 plants, with the exception of stem values, which are based on 1 plant.

	Day 1			Day 7		
	Leaves	Stem	Roots	Leaves	Stem	Roots
Activity (dpm/g)	$(5 \pm 2) \cdot 10^4$	$6 \cdot 10^4$	$(4 \pm 1) \cdot 10^5$	$(6 \pm 2) \cdot 10^4$	$4 \cdot 10^4$	$(6 \pm 3) \cdot 10^5$
Fraction (% total activity)						
Hydrochloric acid	38 ± 6	23	23 ± 1	41 ± 1	31	17 ± 2
Aqueous base	25 ± 1	18	17 ± 0	27 ± 3	22	11 ± 1
Diethyl ether acid–neutral	28 ± 3	32	69 ± 8	19 ± 4	32	38 ± 6
Diethyl ether base	7 ± 4	6	3 ± 1	6 ± 3	8	4 ± 1
F1	0	0	0	0	0	0
F2	6 ± 1	11	23 ± 4	5 ± 1	10	14 ± 2
F3	3 ± 2	2	6 ± 2	1 ± 1	3	3 ± 1
F4	12 ± 5	12	26 ± 3	6 ± 5	13	14 ± 3
Pellet	18 ± 2	37	26 ± 2	24 ± 5	45	40 ± 5
Material balance						
(Hydrochloric acid + diethyl ether acid– neutral + pellet)	84	92	118	84	108	95

TABLE III

CONCENTRATIONS OF TNT AND THE AMDNT ISOMERS IN BUSH BEAN TISSUE AFTER 1 AND 7 DAYS OF GROWTH IN HYDROPONIC CULTURE

	Concentrations (ppm fresh weight)	
	TNT	AMDNT isomers
Day 1		
Leaves	0.32 ± 0.11	0.23 ± 0.07
Stem	0.63	0.35
Root	6.07 ± 2.19	4.06 ± 1.13
Day 7		
Leaves	0.18 ± 0.16	0.15 ± 0.08
Stem	0.88	0.12
Root	7.44 ± 3.14	1.49 ± 0.62

Results obtained during the oxidative metabolism study indicated that bush bean plants did not transpire volatile organics containing TNT-derived radiolabel or $^{14}CO_2$.

DISCUSSION

Soil fate of TNT

The results presented in Table I reveal that the extraction efficiencies for soils were quite high at time 0, and nearly all the radiolabel was recovered as TNT. As TNT aged in soil, the amount of extractable radiolabel decreased with an increase in the amount of non-extractable radiolabel that was irreversibly bound to the soil. It is unclear whether sorption of TNT and/or its transformation products are responsible for the decreased extractability of radiolabel over the 60-day period. The decrease in extractable radiolabel as a function of time in soil may result from sorption of organic residues to soil minerals and/or soil organic matter. This phenomenon has been described for chemically related compounds by several authors [19–21]. Discrepancies between the percent of extractable radiolabel and the amount of unaltered TNT represent the extent of transformation of parent TNT to the aminodinitrotoluene isomers. Transformation to these isomers continued throughout the 2-month study period. Radiochromatographic studies did not detect the presence of other extractable transformation products in this soil.

Previous studies have failed to provide a reasonable mass balance for TNT and TNT transformation products in soils. For example, Pennington [15] was able to account for only 50% of the added TNT radiolabel after TNT had aged in soils for 65 days. This low mass balance was attributed to the formation of volatile transformation products. In support of this view, our data show a trend for an increasing mass balance deficit with time (Table I). This may represent the formation of volatile transformation products and/or mineralization of the TNT in the soil to CO_2. Small amounts of CO_2 were evolved from TNT-amended Palouse soil which accounted for approximately 4% of the radiolabel during the 2-month study period. The methodology presented in this study provides for an acceptable mass balance over the study

period (Table I). An additional important feature of the present methodology is the high degree of reproducibility, as indicated by the small standard deviations of the triplicate analyses (Table I).

Fate of TNT in plant tissues

Initial plant studies examining the effects of acid hydrolysis on the amount of ether-extractable TNT metabolites clearly indicated that 19% of the TNT metabolites in leaf tissue were present as hydrochloric acid hydrolyzable conjugates. Interestingly, acid hydrolysis did not increase the amount of radiolabel that was solubilized. In both the acid hydrolysis and water experimental conditions, approximately 60% of the radiolabel was solubilized, while about 40% remained in the pellet. It can only be assumed that the fraction of radiolabel remaining in the pellet following extraction was tightly bound, and probably conjugated.

The total activity per gram of fresh weight tissue is summarized in Table II. It is clear from the data that the majority of radiolabel was localized in the root tissue. Roots from both the 1- and 7-day bush bean plants contained approximately ten times the amount of radiolabel as an equal weight of the leaf tissue. Stem tissue contained an amount of radiolabel per gram of tissue similar to that of the leaf tissue. Localization of radiolabel primarily in the root tissue, with minimal translocation to the shoot, has been noted in studies of dinitroaniline herbicides [22]. The chemical similarity of the aminodinitrotoluene isomers, which were observed in hydroponic solutions containing bush beans, and the dinitroaniline herbicides may account for the similarity in radiolabel distribution.

Since the aminodinitrotoluene isomers were observed in all plant-containing hydroponic solutions and were absent from control solutions, it can be concluded that the presence of the root prompted formation of these compounds. It is not clear whether this transformation was due to metabolism of TNT by the root or to microorganisms associated with the root. Additionally, it is not clear whether plant uptake involves both TNT and the aminodinitrotoluene isomers or uptake of TNT followed by metabolic alteration to the aminodinitrotoluene isomers. These issues are difficult to experimentally address since, short of utilizing aseptic plants, root sterilization would damage the tissue resulting in impaired plant uptake. However, deconvolution of the above processes may not be imperative. If root microflora are responsible for transformation of TNT in hydroponic solutions, microorganisms normally associated with the rhizosphere would be expected to promote similar transformations in the environment.

The material balance summarized in Table II compares the percentage of total activity that can be accounted for in the hydrochloric acid, diethyl ether and pellet fractions. The average of these values is 97%, which indicates that practically all of the radiolabel can be accounted for at this stage of the fractionation. It should be noted that the sum of the diethyl ether acid–neutral and diethyl ether base fractions should equal the sum of the Florisil fractions. The actual material recovered in the Florisil fractions only accounts for an average of 65% of the material applied to the columns. This discrepancy is due either to radiolabel that was not solubilized when the ether-extractable residue was taken up in methylene chloride (before Florisil chromatography), adsorptive losses on the Florisil adsorbent, or to mechanical losses.

Fractionation on Florisil adsorbent prior to HPLC analysis of fraction F2

produced blanks with very little interference from indigenous plant components. Advantages of Florisil fractionation prior to HPLC analysis include prolonged analytical column life and the ability to determine TNT and the aminodinitrotoluene isomers without analytical interferences. The method was shown, by analysis of TNT-spiked leaf tissue, to give both high recoveries (84%) and good reproducibility.

The distribution of radiolabel among the chemical fractions (Table II) emphasizes the previously unknown polar nature of TNT plant metabolites. After acid hydrolysis, an average of 12% of the radiolabel over all analyses was found in fraction F2. Large quantities of more polar metabolites, found primarily in fraction F4 (average of 15% of the radiolabel) and the non-ether-extractable aqueous base (average of 29% of the radiolabel) fraction, accounted for an average of 44% of the radiolabel. The amount of radiolabel sequestered in non-extractable forms in the pellets averaged 29%. There is a clear indication from the data that the percentage of radiolabel found in fraction F2 was higher in the root tissue than in the leaves. The leaf tissue contained higher proportions of water-soluble metabolites present in the aqueous base fraction. These data suggest that TNT and its primary metabolites (the aminodinitrotoluene isomers) were transported from the roots to the aerial portions of the plant, where they underwent further modification to more polar metabolites. It should be emphasized that once plant uptake occurs, radiolabel remains within the plant tissues. Studies specifically designed to examine the release of $^{14}CO_2$ and ^{14}C-containing volatile organics failed to detect emission of such compounds by bean plants grown in ^{14}C-TNT containing solutions.

Comparisons between 1 and 7 day plants (Table II) show a trend consistent with metabolic immobilization of radiolabel in both leaf and root tissues. Leaf and root tissues from 1-day plants contained a higher percentage of radiolabel in the diethyl ether acid–neutral fraction than plants exposed for 7 days. After fractionation of the 1-day plant extracts on Florisil, the larger percentage of extractable radiolabel was reflected in fraction F4. Conversely, plants exposed for 7 days showed a higher percentage of immobilized radiolabel in the leaf and root pellets. These results suggest that a fundamental process associated with TNT metabolism in plants is the detoxification of TNT metabolic products by sequestration in non-extractable forms.

The chromatograms of the F2 fraction of bush bean leaf tissue exposed hydroponically in TNT solutions for 7 days show both TNT and the aminodinitrotoluene isomers at concentrations slightly above the detection limit of the analytical scheme (Fig. 3 top). The chromatogram in the bottom of Fig. 3 is from similarly exposed bush bean root tissue. Large quantities of these compounds are evident. Bush bean stem tissue contains concentrations of TNT and the aminodinitrotoluene isomers that are intermediate to those found in the leaves and roots (Fig. 3 center and Table III). The concentrations of TNT and the aminodinitrotoluene isomers given in Table III are consistent with the distribution of radiolabel as summarized in Table II. Note that only 5–6% of the radiolabel contained in leaves was speciated as TNT or the aminodinitrotoluene isomers.

Radiochromatograms of the F2 fraction from bush bean root tissue indicated the presence of an unknown TNT metabolite eluting with a retention time of 21.95 min. The peak corresponding to this metabolite is marked with an asterisk in Fig. 3. Incorporation of radiolabel into discrete metabolites, such as the unknown component identified above and the aminodinitrotoluene isomers, argues towards a defined
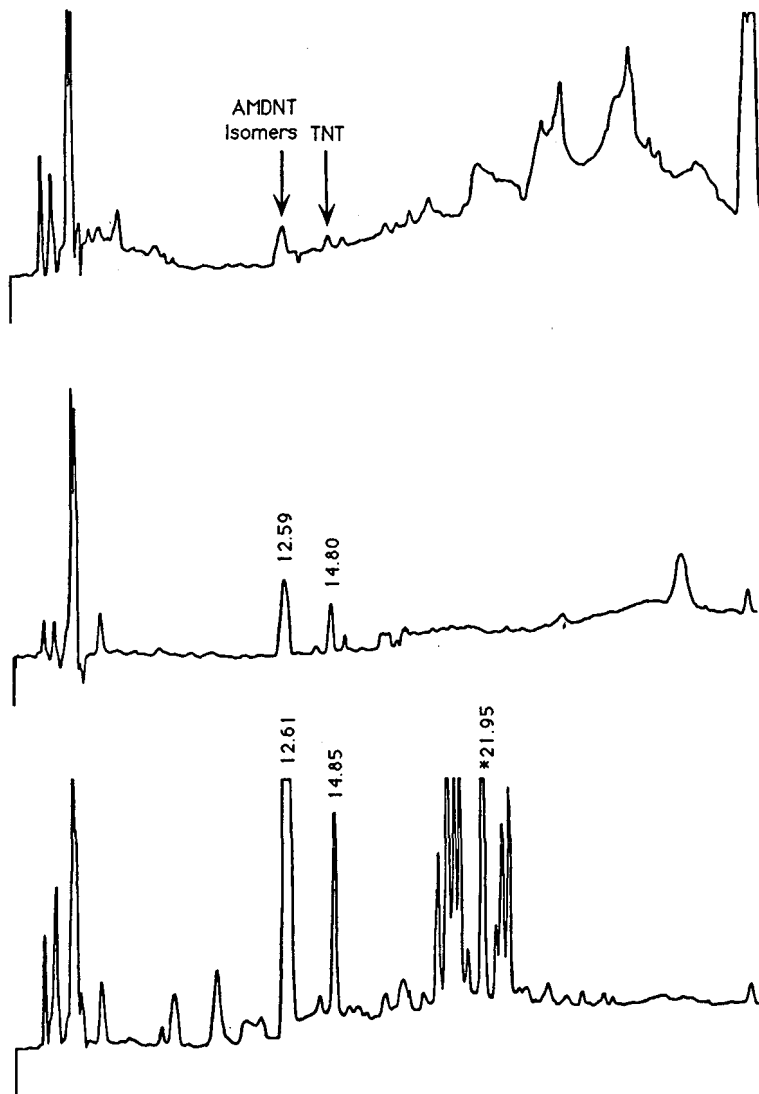
Fig. 3. Chromatograms of the F2 fraction of bush bean plants grown in hydroponic solutions containing 10 ppm TNT. The top chromatogram is from leaves, the center from stem, and the bottom from root tissue. The peak marked with an asterisk contains radiolabel and represents an unknown TNT metabolite. Numbers at peaks indicate retention times in min.

metabolism of TNT rather than nondescript incorporation of the radiolabel into a variety of metabolic paths. Structural elucidation of this metabolite, as well as the polar metabolites contained in the F4 and aqueous base fractions, should be the focus of future investigations.

ACKNOWLEDGEMENTS

REFERENCES

1 A. J. Palazzo and D. C. Leggett, *J. Environ. Qual.*, 15 (1986) 49.
2 D. L. Kaplan and A. M. Kaplan, *Environ. Sci. Technol.*, 16 (1982) 566.
3 J. T. Walsh, R. C. Chalk, and C. M. Merritt, *Anal. Chem.*, 45 (1973) 1215.
4 R. W. Traxler, *Biodegradation of Alpha TNT and Its Production Isomers, Technical Rep. 75-133-FSL*, U.S. Army Natick Development Center, Natick, MA, 1974.
5 R. E. Klausmeier, J. L. Osmon and D. R. Wells, *Dev. Ind. Microbiol.*, 15 (1973) 309.
6 N. G. McCormick, F. E. Feeherry and H. S. Levenson, *Appl. Environ. Microbiol.*, 31 (1976) 949.
7 A. Hamilton, *J. Ind. Hyg.*, 3 (1921) 102.
8 N. I. Sax, *Dangerous Properties of Industrial Materials*, Reinhold, New York, 2nd ed., 1963.
9 W. D. Won, L. H. DiSalvo and J. Ng, *J. Appl. Environ. Microbiol.*, 31 (1976) 576.
10 J. L. Osmon and R. E. Klausmeier, *Dev. Ind. Microbiol.*, 14 (1972) 247.
11 M. W. Nay, C. W. Randall and P. H. King, *J. Water Pollut. Control Fed.*, 46 (1974) 485.
12 C. C. Lee, J. V. Dilley, J. R. Hodgson, D. O. Helton, W. J. Wiegand, D. N. Roberts, B. S. Anderson, L. M. Halfpap and L. D. Kurtz, *Mammalian Toxicity of Munition Compounds, Phase 1, Acute Oral Toxicity Primary Skin and Eye Irritation, Dermal Sensitization, and Disposition and Metabolism, No. 3900-B*, Contract No. DAMD17-74-C-4073, Midwest Research Institute, Kansas City, MO, 1975.
13 J. V. Dilley, C. A. Tyson and G. W. Newell, *Mammalian Toxicology Evaluation of TNT Wastewaters*, Contract No. DAMD 17-76-C-6050, Vol. III, Stanford Research Institute, Menlo Park, CA, 1978.
14 B. L. Folsom, Jr., C. L. Teeter, M. R. Barton, J. A. Bright, *Plant Uptake of 2,4,6-Trinitrotoluene (TNT), Miscellaneous Paper EL-086*, U.S. Army Engineer Waterways Experiment Station, Vicksberg, MS, 1986.
15 J. C. Pennington, *Plant Uptake of 2,4,6-Trinitrotoluene, 4-Amino-2,6-Dinitrotoluene, and 2-Amino-4,6-Dinitrotoluene Using ^{14}C-Labeled and Unlabeled Compounds, Technical Report EL-88*, U.S. Army Engineer Waterways Experiment Station, Vicksberg, MS, 1987.
16 D. A. Cataldo, T. R. Garland and R. E. Wildung, *Plant Physiol.*, 62 (1978) 563.
17 R. J. Fellows, R. M. Bean and D. A. Cataldo, *J. Agric. Food Chem.*, 37 (1989) 1444.
18 R. J. Spanggord, T. Mill, T.-W. Chou, W. R. Maybe, J. H. Smith and S. Lee, *Environmental Fate Studies on Certain Munition Wastewater Constituents, Final Report, Phase II, Laboratory Studies, Contract No. DAMD17-78-C-8081*, SRI International, Menlo Park, CA, 1980.
19 J. M. Bollag, P. Blattmann and T. Laanio, *J. Agric. Food Chem.*, 26 (1978) 1302.
20 T. S. Hsu and R. Bartha, *Soil Science*, 116 (1974) 444.
21 R. Bartha and D. Pramer, *Science (Washington, D.C.)*, 156 (1967) 1617.
22 S. J. Parka and O. F. Soper, *Weed Science*, 25 (1977) 79.
23 R. L. Guthrie and J. E. Whitty, *Soil Sci. Soc. Am. J.*, 46 (1982) 443.

Analyse par chromatographie liquide du diamino-2,3 phénazine et de l'hydroxy-2 amino-3 phénazine dans les carbendazimes techniques et formulés

J.-C. VAN DAMME*, B. DE RYCKEL et M. GALOUX

Station de Phytopharmacie de l'État, 11 Rue du Bordia, B-5800 Gembloux (Belgique)
(Reçu le 30 mars 1990; manuscrit modifié reçu le 22 juin 1990)

ABSTRACT

Determination by liquid chromatography of 2,3-diaminophenazine and 2-hydroxy-3-aminophenazine in technical and formulated carbendazims

2,3-Diaminophenazine (DAP) and 2-hydroxy-3-aminophenazine (HAP) are highly mutagenic compounds that can be formed during the synthesis of carbendazim. A method has been developed to determine the DAP and HAP contents of technical and formulated carbendazims. The method is simple, rapid (20 min) and minimizes the degradation of phenazines in solution. All of the analyzed technical products (14) contained DAP, but only three wettable powders, among the twelve formulations analyzed, gave a result above the detection limit. HAP could be detected in none of the samples.

INTRODUCTION

La génotoxicité de certains fongicides de la famille des benzimidazoles, et notamment celle du carbendazime, est discutée depuis de nombreuses années [1–3]; certaines études ont attribué un pouvoir mutagène élevé au carbendazime tandis que d'autres ne faisaient état d'aucune activité mutagène. Après une revue systématique des publications sur le sujet, Oesch [4] a conclu que ni le carbedazime ni ses précurseurs biologiques (bénomyl et thiophanate) n'ont de propriétés mutagènes et a émis l'hypothèse que l'activité mutagène mise en évidence par le test de Ames, est à mettre à l'actif d'impuretés contenues dans les carbendazimes techniques utilisés lors de ces essais [5–6]. Des études ultérieures ont montré que des molécules du type phénazine ont une activité mutagène, notamment le diamino-2,3 phénazine (DAP) et l'hydroxy-2 amino-3 phénazine (HAP) (Fig. 1). Le DAP est formé à partir de deux molécules d'orthophénylènediamine (OPD), produit utilisé pour synthétiser le carbendazime (Fig. 2), et le HAP est obtenu par oxydation du DAP [7–10].

Pour déterminer les teneurs en DAP et HAP des produits techniques et formulés et vérifier une limite maximale éventuelle, il est nécessaire de disposer d'une méthode d'analyse relativement simple et rapide. Les méthodes d'analyse proposées par des fabricants de benzimidazoles (BASF et Dupont de Nemours) font appel à la détection par fluorescence pour obtenir une sensibilité suffisante. Dans la méthode BASF,
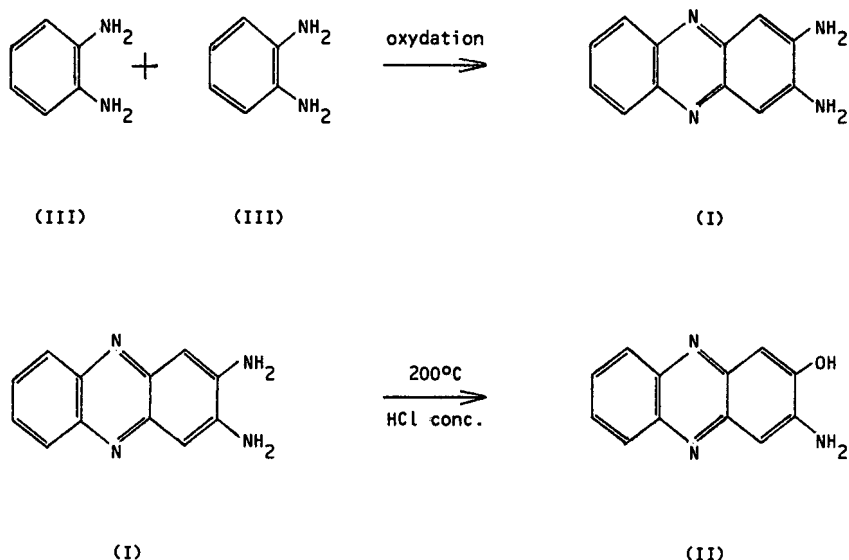
Fig. 1. Structure et formation des impuretés recherchées. I = DAP; II = HAP; III = OPD.
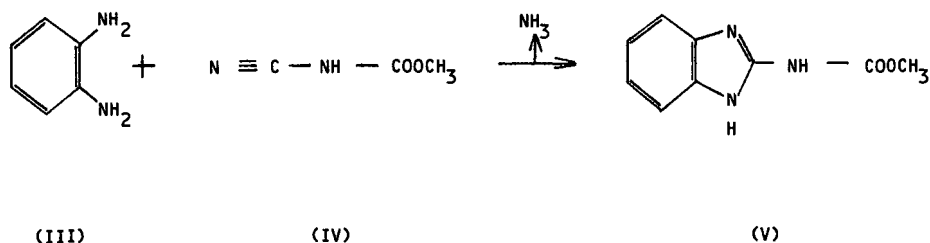
Fig. 2. Synthèse du carbendazime. III = OPD; IV = cyanocarbamate de méthyle; V = carbendazime.

l'étape d'extraction des phénazines, dans le cas des poudres mouillables, est assez longue et le taux de récupération est de 53%.

La méthode décrite a été mise au point pour permettre l'analyse de ces impuretés par chromatographie liquide avec un détecteur UV-visible. L'extraction est effectuée par une simple mise en solution et les taux de récupération dans les produits techniques et les formulations sont compris entre 95 et 100%.

MATERIEL ET MÉTHODE

Réactifs

Nous avons utilisé les réactifs suivants: méthanol pour chromatographie liquide (Alltech, 166170); acétonitrile pour chromatographie liquide (Alltech, 165690); acide sulfurique conc. min. 95%, pour analyse (Merck, 714); NaCl pour analyse (Merck, 6404); phase mobile: acétonitrile–méthanol à 0.1% H_2SO_4 (85:15 v/v); diamino-2,3

phénazine et hydroxy-2 amino-3 phénazine de pureté supérieure à 99% synthétisés par le Dr. Türk (BASF, Ludwigshafen, R.F.A.).

Appareillage et conditions chromatographiques

L'appareillage et les conditions chromatographiques étaient: bain à ultrasons Bransonic 521; tubes à centrifuger de 100 ml, fonds plats et bouchons à visser Pirex No. 22; centrifugeuse (2000 g) Beckman J-6B; chromatographe liquide comprenant une pompe isocratique Tracor 990, une vanne d'injection Rhéodyne 7125 munie d'une boucle de 20 μl, un détecteur spectrophotométrique UV-visible Perkin-Elmer LC-95, un enregistreur Linear Modèle 255 et un intégrateur Infotronics CRS 304, ou chromatographe liquide Hewlett-Packard HP 1090 comprenant une pompe iso-cratique, un système d'injection automatique, un détecteur UV-visible à barette de diodes, un enregistreur et un intégrateur; colonne HS-3 Silica (Perkin-Elmer, 0258-0167) 83 × 4,6 mm, diamètre des particules 3 μm; débit 1,25 ml min^{-1}; longueurs d'onde 453 nm pour le détecteur à longueur d'onde variable, 453 nm et 270 nm pour le détecteur à barette de diodes; température ambiante.

Mode opératoire

Préparation des solutions étalons. Opérer à l'abri de la lumière. Peser, à 0,01 mg près, environ 10 mg de DAP ou de HAP dans un ballon jaugé de 100 ml. Dissoudre et porter au volume avec du méthanol. Prélever immédiatement des aliquotes de 2 ml de cette solution dans des flacons de 50 ml avec bouchons à visser. Évaporer rapidement à sec sous courant d'azote et conserver au réfrigérateur à 4°C.

Le résidu sec (environ 0,2 mg de phénazine) est remis en solution avec un volume déterminé de méthanol à 0,02% H$_2$SO$_4$ concentré, et dilué pour obtenir la ou les concentration(s) désirée(s).

Extraction de l'échantillon. Opérer à l'abri de la lumière. Peser, à 0,01 g près, environ 1 g d'échantillon dans un tube à centrifuger. Ajouter 50 ml de méthanol et extraire pendant 5 min dans un bain à ultrasons. Dans le cas des suspensions concentrées, ajouter 1 g de NaCl pour obtenir un surnageant limpide. Centrifuger à 2000 g pendant 10 min. Prélever immédiatement 20 ml de surnageant dans un erlenmeyer de 25 ml et acidifier au moyen de 0,4 ml de méthanol à 1% H$_2$SO$_4$ concentré.

Dosage. Vérifier la linéarité et la stabilité de la réponse chromatographique en injectant 20 μl des solutions étalons dans les conditions décrites ci-dessus. La surface des pics de deux injections successives ne doit pas différer de plus de 2%. Injecter ensuite deux fois la solution échantillon, suivie d'une injection d'une solution étalon de concentration voisine.

La quantité de phénazine (DAP ou HAP) est calculée par la formule suivante:

$$\text{teneur en DAP (ou HAP)} = \frac{hcP}{Hp} \cdot 0,51 \text{ mg kg}^{-1}$$

dans laquelle h = hauteur du pic de la solution échantillon (moyenne de 2 injections); H = hauteur du pic de la solution étalon (moyenne de 2 injections); p = prise d'essai (en g) de l'échantillon; c = concentration en DAP (ou HAP) dans la solution de référence (en μg ml^{-1}); P = pureté du DAP (ou HAP) de référence (en %).

RÉSULTATS ET DISCUSSION

Stabilité et extraction des phénazines

Le DAP et le HAP se présentent sous forme de poudres cristallines de couleur jaune pour le DAP et brun-rouge pour le HAP. Ils sont solubles dans le benzène et le dichlorométhane et très solubles dans l'eau et les alcools. Les solutions aqueuses et méthanoliques de couleur jaune prennent rapidement une coloration brunâtre. Cette décoloration montre que ces molécules sont instables et leur stabilité dépend de la lumière et du pH.

La décomposition du DAP et du HAP dans l'eau et le méthanol a été suivie en fonction du temps sur des solutions contenant 10 μg ml^{-1} (Fig. 3). Les courbes montrent que les deux phénazines sont plus stables dans le méthanol et que, dans l'eau, la demi-vie du DAP n'est que de 80 min, celle du HAP de 3 h 35 min. Par contre, les solutions de phénazines conservées à l'abri de la lumière sont stables pendant plus de 2 h et après 6 h, la concentration en DAP dans le méthanol était encore égale à 95% de la concentration initiale. Ces deux phénazines sont stables en milieu acide pendant au moins 15 jours.
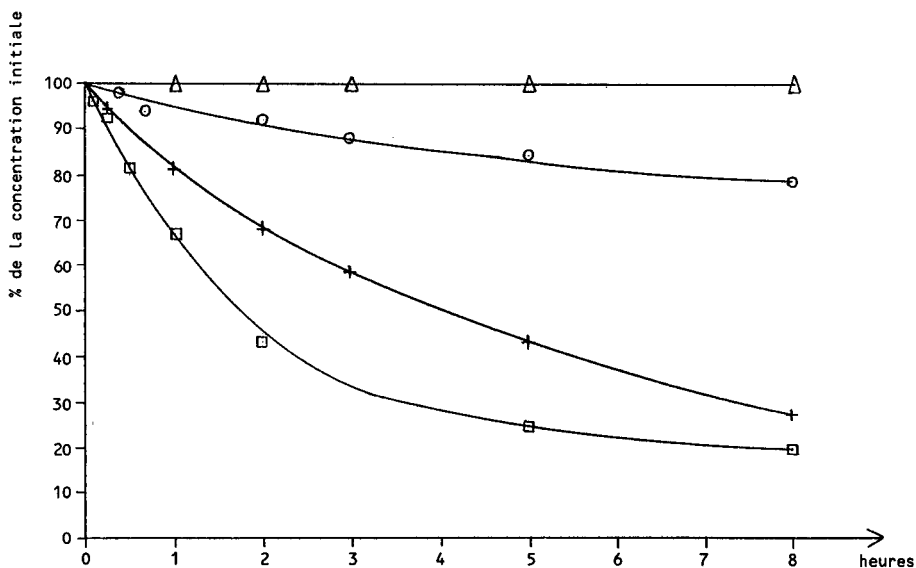
Fig. 3. Courbes de décomposition des phénazines. DAP dans l'eau (□) et dans le méthanol (○); HAP dans l'eau (+) et dans le méthanol (△).

Comme ces molécules sont solubles dans l'eau et stables en milieu acide, les premiers essais d'extraction ont été effectués avec de l'acide chlorhydrique 1 M, comme préconisé dans la méthode BASF, mais en milieu fortement acide, le HAP et le DAP s'adsorbent sur de nombreux substrats: le kaolin (matière de charge de certaines poudres mouillables), les particules de carbendazime non dissoutes, les filtres en polyéthylène des colonnes d'extraction en phase solide, qui ont été essayées comme moyen de concentration. Sur base de ces essais, il a été jugé préférable d'utiliser comme

solvant d'extraction le méthanol et, pour éviter au maximum la décomposition, d'opérer à l'abri de la lumière, d'acidifier le surnageant obtenu après centrifugation et d'injecter les solutions sans étape de concentration.

Chromatographie et détection

Pour améliorer la symétrie des pics, la phase mobile doit contenir une petite quantité d'acide fort ainsi que du méthanol dont le pourcentage permet de contrôler la séparation. Le mélange acétonitrile–méthanol à 0,1% H_2SO_4 (85:15 v/v) a été retenu, ainsi qu'une colonne contenant de la silice non modifiée. Dans ces conditions la réponse chromatographique est linéaire dans une gamme de concentrations allant de 30 à 4000 ng ml^{-1} avec un coefficient de corrélation de 0,99998 pour les deux phénazines; le DAP est séparé du carbendazime et des autres composés extraits, mais le HAP ne l'est pas (Fig. 6). Ce dernier peut cependant être analysé spécifiquement, car ces molécules ont des spectres d'absorption caractéristiques (Fig. 4) et la détection dans le visible à 453 (ou 409 nm) permet de mesurer le HAP (Figs. 5 et 6).

Au début de l'étude, une colonne de phase inverse à activité réduite (HS-3 CR C18, Perkin-Elmer, réf. 0258-0194) a également été utilisée avec la même phase mobile. Sur cette colonne, le DAP et le HAP sont séparés des autres composés, mais les temps de rétention sont relativement longs (de l'ordre de 3,4 min pour le HAP et de 4,6 min pour le DAP pour un débit de 1,25 ml min^{-1}). La colonne de silice a été finalement retenue, car la colonne de phase inverse s'est rapidement détériorée. Elle permet d'analyser le DAP en un temps plus court et le HAP qui n'est pas séparé peut être mesuré grâce à son absorption en lumière visible.

Les essais, la mise au point de la méthode et les chromatogrammes des Figs. 5 et 6, ont été réalisés avec un détecteur à barette de diodes qui offre l'avantage de mesurer simultanément à plusieurs longueurs d'onde et permet d'enregistrer l'ensemble du
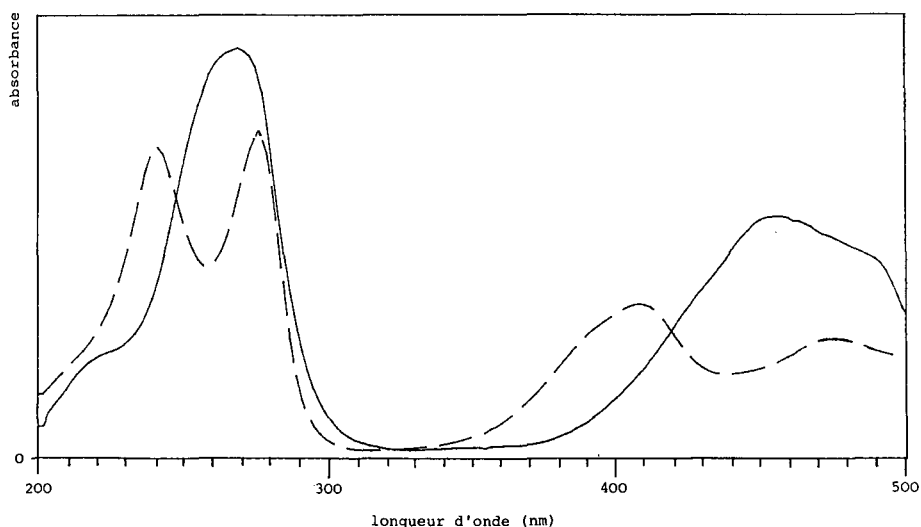
Fig. 4. Spectres d'absorption du DAP (————) et du HAP (– – –) dans le phase mobile.
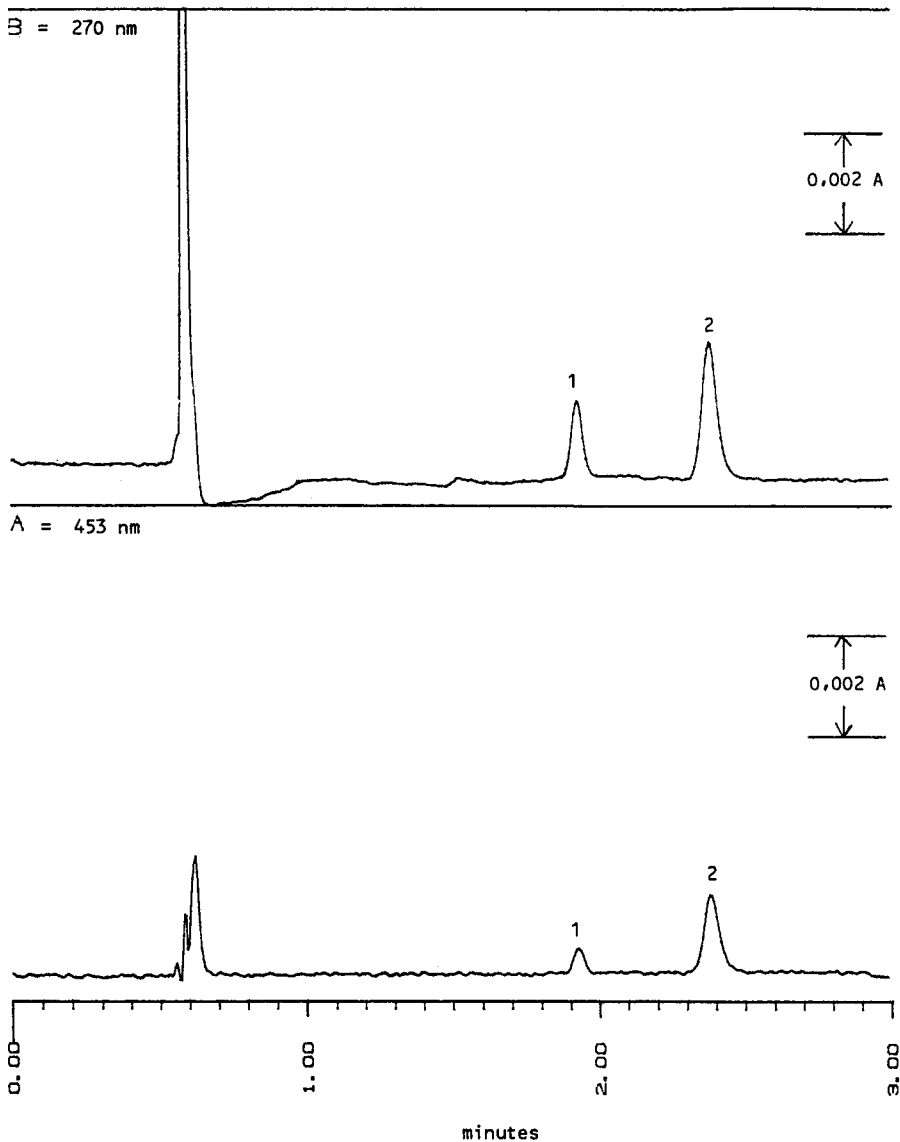
Fig. 5. Chromatogrammes à 270 et 453 nm d'une solution étalon contenant du DAP (0,16 μg ml^{-1}) et du HAP (0,08 μg ml^{-1}). Pics: 1 = HAP; 2 = DAP.

spectre du composé élué. Ce détecteur est cependant moins stable que le détecteur à longueur d'onde variable avec lequel ont été effectuées les analyses des échantillons et dont le seuil de détection dans le visible a été estimé à 0,2 mg kg^{-1} pour le DAP et 0,4 mg kg^{-1} pour le HAP. Si nécessaire, cette limite de détection peut encore être améliorée en augmentant la prise d'essai puisque les deux phénazines sont très solubles dans le méthanol.
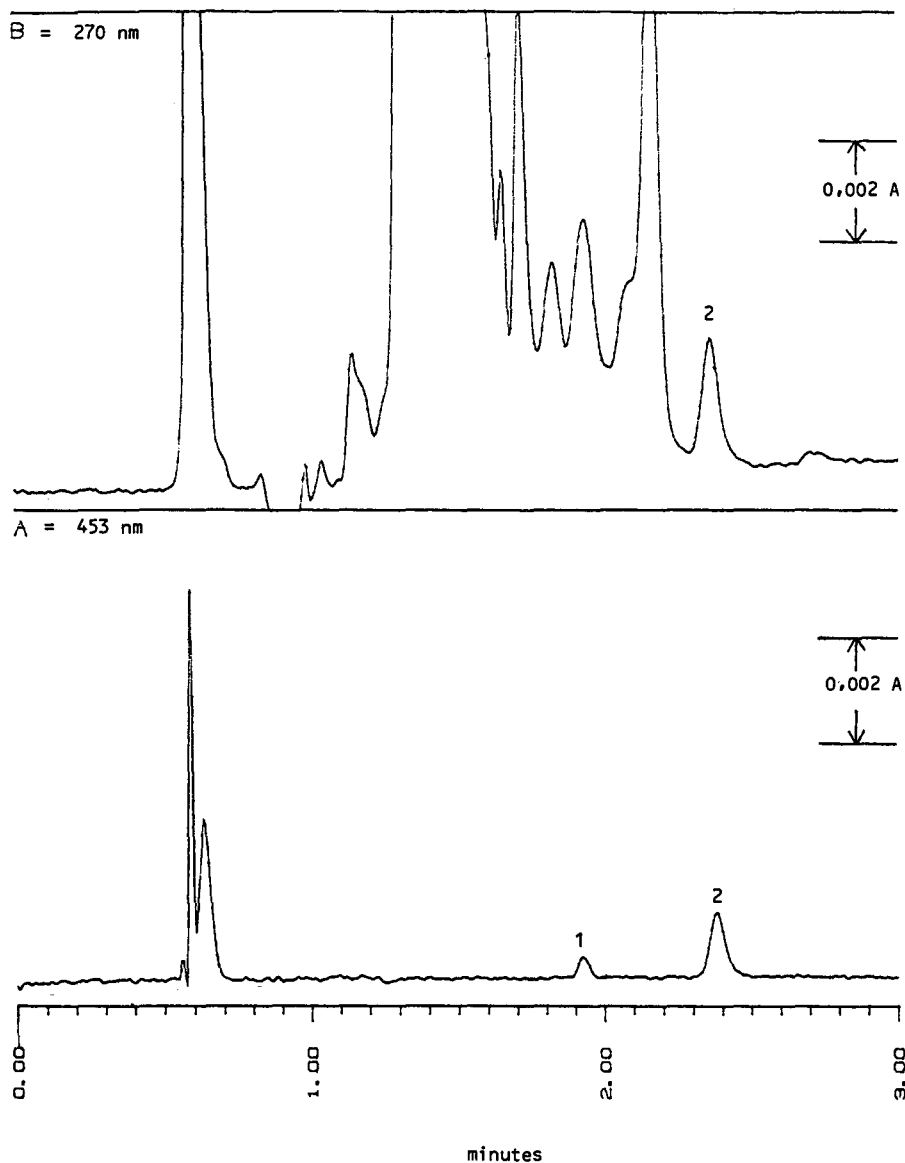
Fig. 6. Chromatogrammes à 270 et 453 nm du carbendazime technique TC 3 contenant du DAP (6,5 mg kg^{-1}) et dopé par du HAP (4 mg kg^{-1}). Pics: 1 = HAP; 2 = DAP.

Reproductibilité et rendement analytique de la méthode

La reproductibilité de la méthode est illustrée au Tableau I. Pour le produit technique TC 10 et la poudre mouillable WP 4 dont les teneurs en DAP sont de l'ordre de 20 et 200 mg kg^{-1}, les coefficients de variation pour six répétitions sont inférieurs à 1%. Pour les échantillons TC 6 et WP 3 contenant entre 1 et 2 mg kg^{-1}, ils sont compris entre 5 et 10%.

TABLEAU I

REPRODUCTIBILITÉ DE LA MÉTHODE, MESURÉE SUR DEUX PRODUITS TECHNIQUES (TC) ET DEUX POUDRES MOUILLABLES (WP)

TC 6		TC 10		WP 3		WP 4	
Prise d'essai (g)	DAP (mg kg^{-1})	Prise d'essai (g)	DAP (mg kg^{-1})	Prise d'essai (g)	DAP (mg kg^{-1})	Prise d'essai (g)	DAP (mg kg^{-1})
1,0591	1,77	0,9901	20,03	0,9920	1,54	0,1176	226,3
1,0283	1,70	1,0076	20,40	0,9899	1,53	0,1055	228,3
1,0000	1,78	0,9367	20,37	1,0322	1,83	0,1217	224,8
1,0212	1,92	1,0178	20,23	1,0200	1,61	0,1043	226,8
		2,4620[a]	19,96			0,9918	225,3
		5,0098[a]	20,20			1,0071	227,1
Moyenne	1,79		20,19		1,63		226,4
Ecart-type	0.09		0,18		0,14		1,28
Coefficient de variation (%)	5,1		0.9		8,6		0,6

[a] Extraction par 200 ml de méthanol.

Le rendement analytique a été déterminé en mélangeant 2 ml de méthanol contenant entre 1 et 20 μg de DAP à 1 g de technique TC 5 et à 1 g de poudre mouillable WP 1. Le méthanol est évaporé sous courant d'azote le plus rapidement possible et l'extraction est effectuée suivant la méthode décrite. Dans le cas de la suspension concentrée SC 1, peser 10 g de la formulation dans des tubes à centrifuger contenant des quantités croissantes de DAP, obtenues par évaporation de solutions méthanoliques, préalablement resolubilisées dans 0,5 ml d'eau pour faciliter le mélange avec la suspension aqueuse. Peser 1 g de suspension dopée et effectuer l'extraction en suivant le mode opératoire. Les résultats (Tableau II) sont compris entre 94 et 100% pour les 3 types d'échantillons. Les pourcentages moyens sont de 96 (± 2) pour la suspension concentrée, de 97 (± 3) pour le carbendazime technique et de 98 (± 1) pour la poudre mouillable.

TABLEAU II

RENDEMENT ANALYTIQUE

Résultats en % de DAP ajouté.

Référence	Quantité de DAP ajoutée (mg kg^{-1})				Moyenne	Coeffcient de variation (%)
	20	8	4	1,6		
TC 5	95,7	97,9	100,4	94,4	97,1	2,7
WP 1	99.2	98.0	96.7	98,3	98,1	1.1
SC 1	97,9	96,7	94,2	93,7	95,6	2.1

TABLEAU III

TENEURS[a] EN DAP ET EN HAP DANS LES PRODUITS TECHNIQUES

Référence	Année de fabrication	DAP (mg kg^{-1})	HAP (mg kg^{-1})
1	1988	74,4	n.d.[b]
2	1988	4,5	n.d.
3	1988	6,5	n.d.
4	1988	866	n.d.
5	1988	<0,5	n.d.
6	1988	1,8	n.d.
7	1988	4,8	n.d.
8	1987	137	n.d.
9	1988	23,7	n.d.
10	1988	20,2	n.d.
11	1989	3,1	n.d.
12	1989	3,1	n.d.
13	1989	26,0	n.d.
14	1989	8,5	n.d.

[a] Moyenne d'au moins trois déterminations.

[b] n.d. = Non détecté (limite de détection: voir discussion).

Résultats des analyses

Les résultats sont repris aux Tableaux III et IV. Les teneurs en DAP des échantillons de carbendazime technique (TC) vont de moins de 0,5 à près de 1000 mg kg^{-1}. En ce qui concerne les produits formulés (Tableau IV), seules trois poudres mouillables (WP) contiennent du DAP, parmi lesquelles l'échantillon WP 4, qui en contient 226 mg kg^{-1}.

Les deux types de formulations fabriquées en milieu aqueux: les suspensions concentrées (SC) et la formulation "granulés à disperser dans l'eau" (WG) ne

TABLEAU IV

TENEURS[a] EN DAP ET EN HAP DANS LES PRODUITS FORMULÉS

Référence	Année de fabrication	DAP (mg kg⁻1)	HAP (mg kg⁻1)
WP 1	1985	n.d.[b]	n.d.
WP 2	1985	<0,5	n.d.
WP 3	1988	1,6	n.d.
WP 4	1985	226	n.d.
WP 5	1985	n.d.	n.d.
WG 1	1988	n.d.	n.d.
SC 1	1985	n.d.	n.d.
SC 2	1988	n.d.	n.d.
SC 3	1985	n.d.	n.d.
SC 4	1985	n.d.	n.d.
SC 5	1985	n.d.	n.d.
SC 6	1989	n.d.	n.d.

[a] Moyenne d'au moins trois déterminations.

[b] n.d. = Non détecté (limite de détection: voir discussion).

contiennent pas de DAP. Ce qui s'explique par la décomposition rapide des phénazines dans l'eau. Le HAP n'a été détecté dans aucun des produits analysés. Cette méthode a également été appliquée à des formulations de bénomyl et de thiophanate-méthyl avec comme résultat pour les deux phénazines "non détecté".

CONCLUSION

La méthode décrite permet d'analyser rapidement, avec une bonne précision et une sensibilité suffisante, les teneurs en DAP et HAP dans les carbendazimes techniques et formulés. Tous les carbendazimes techniques analysés (14 échantillons) contiennent du DAP en quantité parfois importante. Le DAP a été détecté dans trois poudres mouillables mais pas dans les suspensions concentrées à base d'eau, ni dans la formulation "granulés à disperser dans l'eau" fabriquée en présence d'eau. Le HAP n'est pas formé, en quantité mesurable par cette méthode, ni lors de la synthèse du carbendazime ni lors de sa formulation.

RÉSUMÉ

Le diamino-2,3 phénazine (DAP) et l'hydroxy-2 amino-3 phénazine (HAP) sont des impuretés fortement mutagènes formées lors de la synthèse du carbendazime. Une méthode a été étudiée pour déterminer les teneurs en DAP en HAP dans les carbendazimes techniques et formulés. La méthode est simple, rapide (20 min) et évite la dégradation des phénazines en solution. Tous les produits techniques analysés (14) contiennent du DAP, mais seules trois poudres mouillables, sur les douze formulations analysées, ont donné un résultat supérieur à la limite de détection. Le HAP n'a été détecté dans aucun des échantillons.

BIBLIOGRAPHIE

1 RL S. Hammerschlag et H. D. Sisler, *Pestic. Biochem. Physiol.*, 3 (1972) 42–54.
2 J. P. Seier, *Mutat. Res.*, 32 (1975) 151–158.
3 I. M. Somlyay, *Meded. Fac. Landbouwwet. Rijksuniv. Gent*, 52 (2 b) (1987) 699–702.
4 F. Oesch, *Evaluation of the Genotoxicity Studies on Carbendazim (MBC), Benomyl and Thiophanate-methyl*, Department of Toxicology and Pharmacology, Université de Mainz, Mainz, 1982.
5 J. P. Seiler, *Mutat. Res.*, 15 (1972) 273–276.
6 G. Ficsor, S. Bordas et S. J. Stewart, *Mutat. Res.*, 51 (1978) 151–164.
7 V. Grignard, G. Dupont et R. Locquin, *Traité de Chimie Organique,* Tome XXI, Masson, Paris, 1953, pp. 195–196.
8 V. V. Richter, R. Anschütz et H. Meerwein, *Traité de Chimie Organique,* Tome II, série cyclique, Librairie Polytechnique Ch. Béranger, Paris, Liège, 1910, pp. 130–134, 1076–1083.
9 R. C. Gupta et S. P. Srivastava, *Indian J. Chem.* 9 1971, 1303–1304.
10 *Merck Index*, Merck & Co., Rahway, NJ, 9th, ed., 1976, pp. 391, 948.

Note

Derivatization–liquid chromatographic assay of chloroacetaldehyde in biological samples

JAN A. RUZICKA and PETER C. RUENITZ*

College of Pharmacy, University of Georgia, Athens, GA 30602 (U.S.A.)

(First received January 17th, 1990; revised manuscript received June 29th, 1990)

In connection with ongoing work in our laboratory, we desired a quantitative method for assaying chloroacetaldehyde (CA), a metabolite of drugs containing NCH_2CH_2Cl moieties. While several techniques have been employed to detect chloroacetaldehyde in biologic media, only three provide a means of quantitative assay. One of these, in which CA was derivatized with 2,4-dinitrophenylhydrazine followed by thin-layer chromatographic analysis of the resulting hydrazone, has served in the case of radio-labelled CA [1]. Alternatively, fluorimetric detection of $1,N^6$-ethenoadenine, an adduct formed from CA and cyclic AMP, has been used to measure CA [2]. Finally, gas-liquid chromatographic techniques have been used, coupled with both flame ionization [3] and electron-capture [4,5] detection to quantify CA in biological samples [3–5].

While these methods constitute sensitive and useful approaches our aim was to develop a convenient yet reliable high-performance liquid chromatographic (HPLC) assay requiring only standard UV detection while providing good sensitivity and linearity in the low nmol/mL concentration range. We also hoped to circumvent the need for liquid–liquid extractions, which become cumbersome in the case of multiple samples, and the need for synthesizing standards. This paper describes a novel assay for CA, utilizing the well-established cyclization reaction of CA with thiourea [6,7] to "trap" CA as 2-aminothiazole (2AT; Fig. 1). By virtue of its primary amino group, 2-AT may be readily concentrated by sorption on cation-exchange resins. It also exhibits an absorption max at 255 nm, enabling UV detection following HPLC. The application of our procedure to CA contained in water and in rat liver microsomal (RLM) suspensions is discussed.
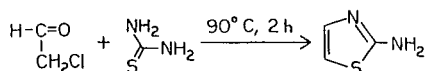
Fig. 1. Reaction of chloroacetaldehyde with thiourea to form 2-aminothiazole.

EXPERIMENTAL

All solvents used were of HPLC grade (J. T. Baker, Phillipsburg, NJ, U.S.A.). Water was distilled and deionized using a Continental Water Systems Type 1 purification system. Prepared mobile phase was passed through a 0.45-μm nylon 66 filter and degassed by sonication. 2-AT (97%, Aldrich, Milwaukee, WI, U.S.A.) was recrystallized from, benzene–light petroleum (b.p. 35–60°C) prior to use. Chloroacetaldehyde (50%, w/w, solution in water, Aldrich) was verified for CA content (by titration [8]) and used as received. All other chemicals were of reagent grade.

Preparation of stock solutions

Aqueous stock solutions of CA and thiourea were prepared by dilution of the 50% CA solution to a final concentration of 200 μM and by dissolving thiourea (with sonication) to a concentration of 100 mM. 2AT was dissolved in mobile phase and diluted to appropriate final concentrations.

Derivatization reaction

Derivatization of CA was carried out in 75 × 12 mm capped polypropylene tubes containing 10 to 200 μl stock CA solution (2–40 nmol) and 30 μl of stock thiourea (3 μmol) in a final volume of 0.5 ml. The tubes were heated at 90°C for 2 h and cooled to room temperature prior to solid phase extraction. 2-AT constitutes a stable product and reaction mixtures were stored at 8°C for up to 1 week without apparent detriment.

Solid-phase extraction and concentration of 2AT

Solid-phase extraction was performed using Bond Elut SCX cation-exchange columns (100 mg benzenesulfonic acid sorbent, 1 ml column volume; Analytichem, Harbor City, CA, U.S.A.). Columns were prepared by eluting, in order, methanol (1 ml), acetonitrile (1 ml), water (2 × 1 ml) and 1% glacial acetic acid (2 × 1 ml) prior to sample application. All solvents were eluted by gravity and were introduced sequentially when the previous volume level had reached the top of the sorbent; the sorbent was not allowed to dry.

Samples were adjusted to a pH of about 3 with 2 M hydrochloric acid (typically 5–6 μl) prior to application of the entire sample volume to a prewashed column. The columns were then washed with 1% acetic acid (4 × 1 ml) followed by 1% acetic acid–methanol (50:50, 3 × 1 ml). Finally, 2-AT was eluted using methanol–14.5 M NH$_4$OH (96:4, 1 ml).

Basic column fractions containing 2-AT were adjusted to a pH of about 6 using approximately 100 μl of 3.2 M hydrochloric acid and were concentrated to dryness under a stream of nitrogen with gentle (35°C) warming. The acid serves to convert 2-AT to its hydrochloride salt, eliminating the loss of free 2-AT which is slightly volatile. The residues were reconstituted in 200 μl of mobile phase with vortexing and injected directly.

HPLC

HPLC was performed using a Hitachi Model L-6200 pump, Model L-4000 UV detector and Model D-2000 integrator/recorder. Chromatography was effected on an

Alltech Econosil C_{18} column (250 mm × 4.6 mm I.D.; 10 μm particle size). The mobile phase was acetonitrile–0.05 M K_2HPO_4 pH 7 (20:80) which was pumped at a flow-rate of 1 ml/min. Injections were made using a 20-μl Rheodyne loop and the wavelength of detection was 255 nm.

Microsomal incubations

Washed hepatic microsomes from male Sprague-Dawley rats (225–275 g), pre-treated with phenobarbital, were prepared according to a published method [9]. Incubation mixtures contained hepatic microsomal protein (0.5 mg), $MgCl_2$ (5 mM), CA (2–40 nmol) and 0.04 M potassium phosphate buffer, pH 7.4, in a final volume of 0.5 ml and were incubated in open 75 × 12 mm polypropylene tubes for 10 min at 37°C with shaking. Protein was precipitated by addition of, sequentially, 5% $ZnSO_4$ (200 μl) and 2.5% $Ba(OH)_2$ (200 μl). Tubes were centrifuged at 450 g for 10 min and supernatant (600 μl) was withdrawn. Stock thiourea solution (30 μl) was added and the derivatization reaction was carried out as described for the samples run in water.

RESULTS AND DISCUSSION

We have developed a novel method to permit quantification of chloroacetalde-hyde from microsomal preparations, in which conversion of CA to 2-AT is followed by concentration via a solid-phase cation-exchange column and HPLC. Typical chro-
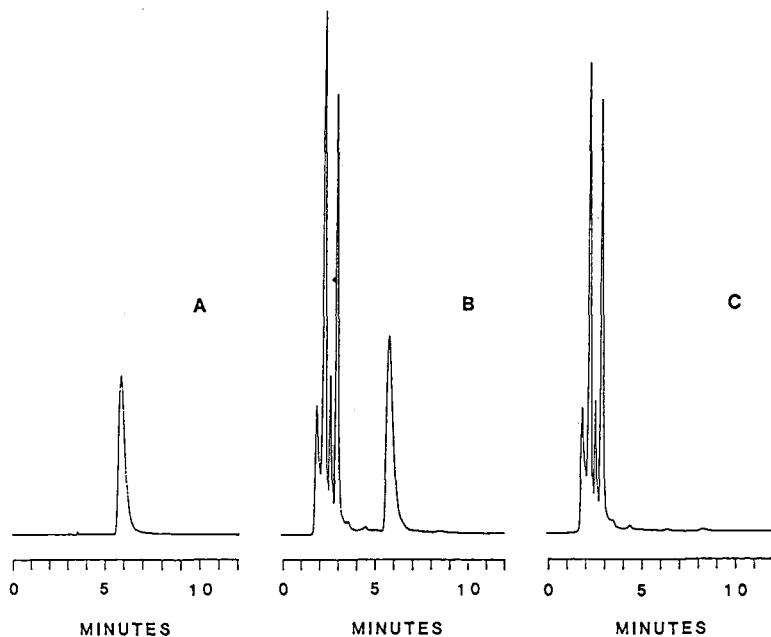
Fig. 2. High-performance liquid chromatograms of (A) authentic 2AT, (B) rat liver microsomal suspension spiked with CA and (C) "blank" rat liver microsomal suspension. Protein-free aliquots (0.5 ml) of B and C, containing, in turn, 16 nmol and 0 nmol of CA, were derivatized with thiourea. Then these and an aliquot of A (5 nmol/0.5 ml) were each subjected to solid-phase extraction. Chromatograms were recorded at 0.01 a.u.f.s. using conditions specified in the Experimental section.

matograms obtained from the work-up of CA spiked RLM incubations are presented in Fig. 2. 2-Aminothiazole exhibited a retention time of 5.9 min and blank test mixtures confirmed the absence of interfering peaks. Chromatograms obtained from aqueous test reactions were virtually identical, revealing the fact that several peaks eluting prior to 2-AT are artifacts of the use of methanol–NH_4OH on the sorbent in SCX columns. These peaks were not eliminated by pre-rinsing SCX columns with methanol–NH_4OH. However, its use was acceptable due to the efficiency of this solvent system in eluting 2-AT, the ease with which it may be concentrated, and the noninterferring nature of the "extra" peaks.

Amounts of 2-AT detected were correlated linearly with amounts of CA initially present. In aqueous samples containing 2-40 nmol of CA, the calibration parameters for the function $y = mx + b$ (where m = nmol/a.u., determined using 6–8 concentrations of CA in 3–4 separate experiments), were as follows: $m = 108 \pm 6$, $b = 0.4 \pm 0.5$ ($r \geqslant 0.998$). In microsomal suspensions analyzed in the same way, $m = 114 \pm 19$, $b = 2.6 \pm 1.1$ ($r \geqslant 0.989$).

The *extent* of derivatization of CA was independent of the *amount* of CA added to aqueous samples (Table I). Yields were calculated from a standard curve constructed from HPLC analysis of 2AT solutions of known concentrations. Comparison of data in Table I indicated that no loss of CA occurred in the presence of liver microsomal protein. The detection limit under these conditions was found to be reached at an initial CA concentration of roughly 2 nmol/0.5 ml. This may be improved marginally by lengthening the heating period of the derivatization, which results in an increase in % conversion of CA to 2-AT (data not shown). This marginal increase was deemed unnecessary for our applications.

CA has been identified as a metabolite of oxazaphosphorine antitumor agents. [1,2,5,10,11]. While its toxicity has not been fully explored, it has been implicated as a source of urotoxicity [10] and neurotoxicity [5] and identified as an alkylating agent [3]. We believe our assay procedure may prove useful to researchers exploring these and other areas in which a straightforward assay of nmol/ml levels of CA may be desired.

TABLE I

CALCULATED YIELDS OF 2-AT FOLLOWING DERIVATIZATION OF CA IN WATER AND IN MICROSOMAL PREPARATIONS

CA concentration (nmol/0.5 ml)	Yield (%, average $\pm$ S.E.M.)	
	In water	In microsomal preparation[a]
2.0	22.90 $\pm$ 2.42	18.24 $\pm$ 5.49
4.0	25.51 $\pm$ 1.53	23.01 $\pm$ 3.75
8.0	30.26 $\pm$ 2.00	27.21 $\pm$ 0.36
16.0	26.81 $\pm$ 4.28	26.98 $\pm$ 2.60
32.0	31.90 $\pm$ 1.29	25.26 $\pm$ 1.60
40.0	32.30 $\pm$ 0.62	25.53 $\pm$ 3.41

[a] Yields are adjusted to accomodate the fact that HPLC integration values reflect an aliquot of incubation mixtures removed after protein precipitation.

REFERENCES

1 I. C. Shaw, M. I. Graham and A. E. M. McLean, *Xenobiotica,* 13 (1983) 433–437.
2 S. J. Rinkus and M. S. Legator, *Anal. Biochem.,* 150 (1985) 379–393.
3 F. P. Guengerich, W. M. Crawford, Jr. and P. G. Watanabe, *Biochemistry,* 18 (1979) 5177–5182.
4 S. N. McCall, P. Jurgens and K. M. Ivanetich, *Biochem. Pharmacol.,* 32 (1983) 207–213.
5 M. P. Goren, R. K. Wright, C. B. Pratt and F. E. Pell, *Lancet,* ii (1986) 1219–1220.
6 M. N. Schukina, *Zh. Obshchei Khim.,* 18 (1948) 1653–1662.
7 H. Taniyama, B. Yasui and K. Ko, *Jpn. J. Pharm. Chem.,* 25 (1953) 678–681.
8 *National Formulary XVII,* U.S. Pharmacopeial Convention, Inc., Rockville, MD, 1989, p. 1904.
9 P. C. Ruenitz, J. R. Bagley and C. W. Pape, *Drug Metab. Dispos.,* 12 (1984) 478–483.
10 J. Pohl, J. Stekar and P. Hilgard, *Drug Res.,* 39 (1989) 704–705.
11 K. Norpoth, *Cancer Treat. Rep.,* 60 (1976) 437–443.

Book Review

Detection-oriented derivatization techniques in liquid chromatography, edited by H.
Lingeman and W. J. M. Underberg, Marcel Dekker, New York, Basel, 1990, XVI
+ 492 pp., price US$ 99.75 (U.S.A. and Canada), US$ 119.50 (rest of the world),
ISBN 0-8247-8287-9.

Although I found this book, in general, an excellent contribution, it was some-
what disturbing to me that the editors and authors of this book were all European or
Japanese, with 73% of the contributions coming from The Netherlands. Some very
relevant work in this field has been done in the U.S.A. From a cursory examination it
would seem that the majority of the references cited were non-American. Apart from
the English which was, at times, somewhat stilted and difficult to follow, there were no
other significant deficiencies in the entire book. However, any book or review should
contain an even-handed overview for *all* scientists who have contributed to the areas
of discussion, no matter where the work was done. The ten chapters are each written
by (a) different author/authors, and devoted to a different aspect or area of detection-
oriented derivatizations for high-performance liquid chromatography (HPLC). The
last four chapters describe different approaches for the most popular detectors avail-
able in HPLC today, such as ultraviolet, electrochemical, fluorescence and chemi-
luminescence. The specific chemical reactions described were thus designed to impart
that type of specific, enhanced detection property to the final analyte's derivative(s).
Though most of the chapters discuss solution derivatization approaches, one covers
enzymatic reagents, solution or immobilized, with a large number of specific enzymes,
conditions, substrates, and final detection methods employed in the literature. The
biochemical kinetics of enzymatic reactions, theory, equation, plots and other aspects
are all adequately covered for this particular approach to improved derivatizations
for better detection.

Another chapter deals with specific derivatization approaches for improved
enantiomeric recognition in HPLC, and covered virtually all methods, requirements,
conditions, approaches, with a large number of successful examples. It even covered
achiral derivatizations for improved chiral separations, a somewhat newer area/ap-
proach in HPLC. Chapter 4 covers postchromatographic reaction detection areas,
with both theory and practical aspects detailed, including reactor design, mixing
types, segmented stream reactors, membrane phase separators, solid state reactors,
photochemical, photolysis–electrochemical, photoconductivity, and specific derivati-
zations for electrochemical/chemiluminescence detections. This outstanding chapter
covers all important approaches and aspects of solution or solid-phase postcolumn
reaction detection as applied in HPLC. Chapter 3 discusses sample pretreatment
procedures, such as direct analysis of protein-containing samples, chemical mod-
ification techniques, solid-phase or liquid–liquid extractions, selective solid adsor-

bents (boronic acid gels), robotic approaches, sample processors, and other automated techniques. It is a very up-to-date review of all areas involving sample pretreatment prior to HPLC injection, with an obvious emphasis towards the newer automated techniques.

In the two remaining chapters, the first of these, written by the two editors, dealt with an introduction to derivatization in LC, covering basic concepts, theory, fundamentals, equations and overall approaches possible and described. Thus, it deals with both pre- and postchromatographic derivatizations, labelling *vs.* non-labelling reactions, physicochemical properties of analyte and matrix, possible chromatographic systems used in combination with derivatization reactions, mobile phase *vs.* derivatization requirements, application of multicolumn technology, and finally the basic equipment and procedures used in derivatization studies. A final section of this chapter deals with optimization of derivatization procedures, in a univariate approach, rather than describing computer generated optimization techniques such as simplex/optiplex/multiplex and so forth. There are no discussions at all, in the entire book, regarding computer optimization of any derivatization approaches, computer programs available, and the relative merits and demerits of univariate *vs.* computer generated optimizations. This was perhaps an oversight on the part of all authors, but especially in this very chapter.

In the second chapter of the book, the fundamental organic chemistry of derivatization reactions and kinetics for HPLC are reviewed. This chapter is really a miniature version of any text discussing structure and mechanism in organic chemistry. The authors have attempted to cover most of the popular derivatization methods for electrophiles and nucleophiles, discussing the fundamental reaction conditions, mechanisms, solvents, pH, dielectric constant and other aspects of how the overall reaction conditions can affect the final reaction efficiency. It even covered esoteric areas, at least for a book dealing with HPLC, such as substituent effects, reaction constants, substituent constants, deviations from Hammett equation, the Taft equation, and so forth. It could be argued that this chapter might have been better placed in a book on mechanistic organic chemistry. However, it was very well written, instructive, lucid, and completely relevant to the rest of the text and chemistry considered.

In conclusion, this is an excellent overview of reaction detection in HPLC, covering the more important and exciting areas, with a very up-to-date coverage of the literature. It is clearly an advanced text for the graduate student, post-graduate fellow, or practicing analytical chemist interested in how to employ derivatizations for enhanced detection in HPLC. For researchers involved in these areas, it is an essential text for the library bookshelf. This very practical and useful text is a worthy contribution to the literature of HPLC derivatizations.

Boston, MA (U.S.A.)   IRA KRULL

Author Index

Errata

J. Chromatogr., 477 (1989) 235–248
> Page 238, eqn. 12, "$j = 1$" should read "$j = i$".

J. Chromatogr., 511 (1990) 115–121
> Page 115, 4th line of Abstract, "CF" should read "CF_3".
> Page 119, 4th textline, "and α-CF_3 ASP" should be deleted.
> Page 120, Tabel I, "$\Delta(\Delta G)$" should read "$-\Delta(\Delta G)$".

PUBLICATION SCHEDULE FOR 1990

Journal of Chromatography and Journal of Chromatography, Biomedical Applications

MONTH	J	F	M	A	M	J	J	A	S	O	N	Dª
Journal of Chromatography	498/1 498/2 499	500 502/1	502/2 503/1 503/2 504/1	504/2 505/1	505/2 506 507 508/1	508/2 509/1 509/2 510	511 512 513	514/1 514/2 515	516/1 516/2 517 518/1	518/2 519/1	519/2 520 521/1 521/2	
Cumulative Indexes, Vols. 451–500		501										
Bibliography Section		524/1		524/2		524/3		524/4		524/5		
Biomedical Applications	525/1	525/2	526/1	526/2 527/1	527/2	528/1 528/2	529/1	529/2 530/1	530/2	531 532/1	532/2 533/1	

ª The publication schedule for further issues will be published later.

INFORMATION FOR AUTHORS

(Detailed *Instructions to Authors* were published in Vol. 513, pp. 413–416. A free reprint can be obtained by application to the publisher, Elsevier Science Publishers B.V., P.O. Box 330, 1000 AH Amsterdam, The Netherlands.)

Types of Contributions. The following types of papers are published in the *Journal of Chromatography* and the section on *Biomedical Applications:* Regular research papers (Full-length papers), Notes, Review articles and Letters to the Editor. Notes are usually descriptions of short investigations and reflect the same quality of research as Full-length papers, but should preferably not exceed six printed pages. Letters to the Editor can comment on (parts of) previously published articles, or they can report minor technical improvements of previously published procedures; they should preferably not exceed two printed pages. For review articles, see inside front cover under Submission of Papers.

Submission. Every paper must be accompanied by a letter from the senior author, stating that he is submitting the paper for publication in the *Journal of Chromatography*. Please do not send a letter signed by the director of the institute or the professor unless he is one of the authors.

Manuscripts. Manuscripts should be typed in double spacing on consecutively numbered pages of uniform size. The manuscript should be preceded by a sheet of manuscript paper carrying the title of the paper and the name and full postal address of the person to whom the proofs are to be sent. As a rule, papers should be divided into sections, headed by a caption (*e.g.*, Abstract, Introduction, Experimental, Results, Discussion, etc.). All illustrations, photographs, tables, etc., should be on separate sheets.

Introduction. Every paper must have a concise introduction mentioning what has been done before on the topic described, and stating clearly what is new in the paper now submitted.

Abstract. Full-length papers and Review articles should have an abstract of 50–100 words which clearly and briefly indicates what is new, different and significant. (Notes and Letters to the Editor are published without an abstract.)

Illustrations. The figures should be submitted in a form suitable for reproduction, drawn in Indian ink on drawing or tracing paper. Each illustration should have a legend, all the *legends* being typed (with double spacing) together on a *separate sheet*. If structures are given in the text, the original drawings should be supplied. Coloured illustrations are reproduced at the author's expense, the cost being determined by the number of pages and by the number of colours needed. The written permission of the author and publisher must be obtained for the use of any figure already published. Its source must be indicated in the legend.

References. References should be numbered in the order in which they are cited in the text, and listed in numerical sequence on a separate sheet at the end of the article. Please check a recent issue for the layout of the reference list. Abbreviations for the titles of journals should follow the system used by *Chemical Abstracts*. Articles not yet published should be given as "in press" (journal should be specified), "submitted for publication" (journal should be specified), "in preparation" or "personal communication".

Dispatch. Before sending the manuscript to the Editor please check that the envelope contains four copies of the paper complete with references, legends and figures. One of the sets of figures must be the originals suitable for direct reproduction. Please also ensure that permission to publish has been obtained from your institute.

Proofs. One set of proofs will be sent to the author to be carefully checked for printer's errors. Corrections must be restricted to instances in which the proof is at variance with the manuscript. "Extra corrections" will be inserted at the author's expense.
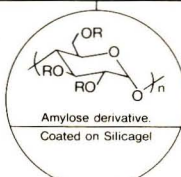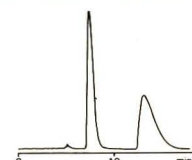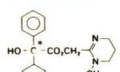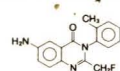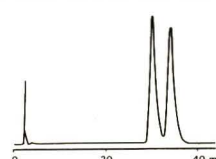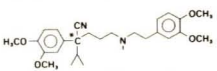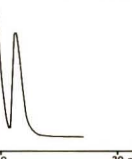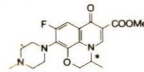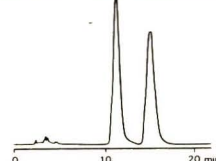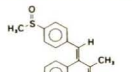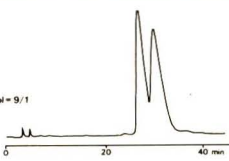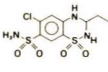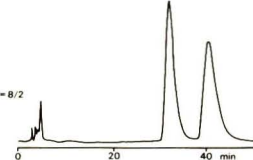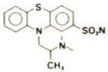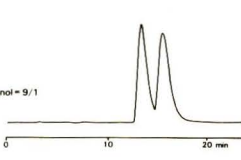
Reprints. Fifty reprints of Full-length papers, Notes and Letters to the Editor will be supplied free of charge. Additional reprints can be ordered by the authors. An order form containing price quotations will be sent to the authors together with the proofs of their article.

Advertisements. Advertisement rates are available from the publisher on request. The Editors of the journal accept no responsibility for the contents of the advertisements.